ATMOSPHERIC TRANSPORT OF ACIDITY IN SOUTHERN CALIFORNIA BY WET AND DRY MECHANISMS

Thesis by

Howard Michael Liljestrand

In Partial Fulfillment of the Requirements

for the degree of

Doctor of Philosophy

California Institute of Technology

Pasadena, California

1980

(Submitted August 27, 1979)

ACKNOWLEDGMENTS

The author would like to thank Professor James J. Morgan as the research advisor for this project. His chemical insight and ability to formulate excellent questions guided this effort. His humor and view of the world made the work enjoyable.

Special thanks go to Dr. Michael Barcelona, Dr. Thomas Holm and Dr. James Pankow for critical help and discussions. Among the many other people I owe thanks for useful discussions are Dr. John Brock, Dr. Norman Brooks, Dr. Glen Cass, Dr. Cliff Davidson, Dr. Richard Flagan, Dr. Sheldon Friedlander, Jim Hunt, Dr. George Jackson, Dr. I. R. Kaplan, Greg MacRae, Dr. Antonio Miguel, Dr. Robert Reynolds, Art Stelson, and Dr. Werner Stumm.

Technical assistance from the following people is also greatly appreciated: Sylvia Garcia for analytical assistance; Elton Daly, Joe Fontana and Rich Eastveldt for manufacturing sampling and analysis equipment; Dave Byrum for drafting; Larry McClellan for instrument repair; and Vere Snell for the excellent typing and cryptographic analysis.

My deepest thanks go to those who aided in sampler placement and operation. All of those who cut through or overlooked bureaucratic barriers will go unnamed at their request.

Support for my education and research at Caltech came from a

variety of sources including N.I.E.H.S., E. I. du Pont de Nemours and Company, Inc., Ford/Exxon Energy Research Program, Department of Energy and State of California Air Resources Board. Some of this support was administered by the Environmental Quality Laboratory.

ABSTRACT

Acid precipitation samples collected at Pasadena, California, from February 1976 to April 1979 and at eight other southern California sites for shorter periods were analyzed to determine acid and base composition. The concentrations of major cations (H^+, NH_4^+, Na^+, K^+, Ca^{2+}, Mg^{2+}) and anions (Cl^-, NO_2^-, Br^-, NO_3^-, SO_4^{2-}) as well as trace weak acids (Fe, Al, Mn, $Si(OH)_4$, RCOOH) were determined. Titrations with base showed acidity predominantly to be due to strong acids (nitric and sulfuric) and weak acids (ammonium ion and carbonic acid). The pH was controlled by strong acidity at the urban sites in the Los Angeles Basin.

The chemical composition of precipitation samples collected in $\sim$0.25 in increments is modeled in several ways. Chemical balances are used to determine the contributions of sea salt, soil dust, stationary sources, mobile sources and non-point sources of ammonia. Multiple regression analysis is used to relate ground-level measurements of air quality and atmospheric conditions with rainwater nitrite plus nitrate and sulfate concentrations. Precipitation intensity, ozone, nitric oxide and nitrogen dioxide concentrations are most strongly correlated with rainwater nitrite plus nitrate. Precipitation intensity, ozone, and nitric oxide are most strongly correlated with rainwater sulfate.

Gas-liquid equilibrium models yield the following predictions: Low partial pressures of ammonia (average of 0.001 - 0.006 ppbv

within the basin) during precipitation scavenging; total sulfite amounting to less than 25% of the non-sea salt sulfur; and nitrite concentrations from NO and NO_2 dissolution which are slightly larger than observed values. Kinetic models of the formation of nitrate and sulfate underestimate the observed concentrations. Spatial distributions of acids and base correspond with local sources. The mountain sites and the more rural eastern sites have significantly less net acidity than the western urban sites.

Estimates of the dry deposition of atmospheric acids indicate the dry flux is ∿6600 equivalents/HA-YR in the Los Angeles Basin compared to ∿380 equivalents/HA-YR for the wet flux of strong acidity. The semi-arid climate and high ambient pollutant concentrations cause the large dry flux. Advection of pollutants is the most important mechanism for the removal of acidity from the Los Angeles airshed.

TABLE OF CONTENTS

LIST OF FIGURES

LIST OF TABLES

Chapter 1

INTRODUCTION

1.1 General Comments

The impact of anthropogenic releases of chemical substances into the environment depends upon many physical, chemical and biological factors. When estimating the potential impact of trace metal and refractory hydrocarbon emissions, Jernelöv (1974) considered the following environmental characteristics:

1) anthropogenic emissions in relation to natural releases,
2) residence time in each compartment of the environment,
3) chemical speciation,
4) biological transformations of species,
5) bio-accumulation, and
6) acute and chronic toxicity.

The same considerations apply to the release of not only trace species but also nontrace constitutents as exemplified by the impact of carbon dioxide release from fossil fuel consumption on the global carbon cycle (Ekdahl and Keeling, 1973).

Acidity in the form of halide, sulfur, nitrogen and organic acids may also be considered an entity being released by man. While the global acid-base balance is controlled by weathering of soils and sediments, local inbalances of acid and base fluxes have been documented. The historical increase of acidity of precipitation in Scandanavia resulted in decreased pH of surface waters in areas of slowly weathering soil, decreased productivity of aquatic ecosystems

and mortality of acid sensitive fauna (Dickson, 1975). The spread of acid rain and increased intensity of rainfall acidity in northern Europe is attributed to increased anthropogenic emissions of NO_x and SO_2 upwind (Odén, 1968). Chemical analysis of precipitation and measurements of pH and acidity by titration determined that sulfuric acid was the dominant acid (Granat, 1972; Odén, 1976) with the nitric to sulfuric acid equivalent ratio being about 1 to 3 (Söderlund, 1977).

A similar increase in precipitation acidity over time has been determined by Cogbill and Likens (1974) for the northeastern United States. Again the acidity was predominantly due to sulfuric acid (60%) and to a lesser degree nitric acid (30%) and hydrochloric acid (5%). Unfortunately, the historical record of acidity measurements in the United States is sporadic. The more complete records of major cation and anion concentrations have been used with chemical relationships to calculate pH values. Figure 1.1 shows the results of measured and calculated precipitation weighted mean pH [1] for the Eastern United States.

The calculated pH values are sensitive to errors due to small differences in relatively large numbers around pH 5.65. The charge balance for major ion concentrations (Equation 1.1) in addition to equilibrium relationships for carbonic acid species and water (Equations 1.2-1.5) can be used to calculate $[H^+]$ from the known major ion concentrations (Equation 1.6). Activity coefficient corrections have been omitted for these dilute solutions.

---

1 Precipitation weighted means are discussed in Section 2.7. The precipitation weighted acidity/alkalinity determines the mean pH for a given CO_2.

Figure 1.1 pH of Precipitation in Eastern United States

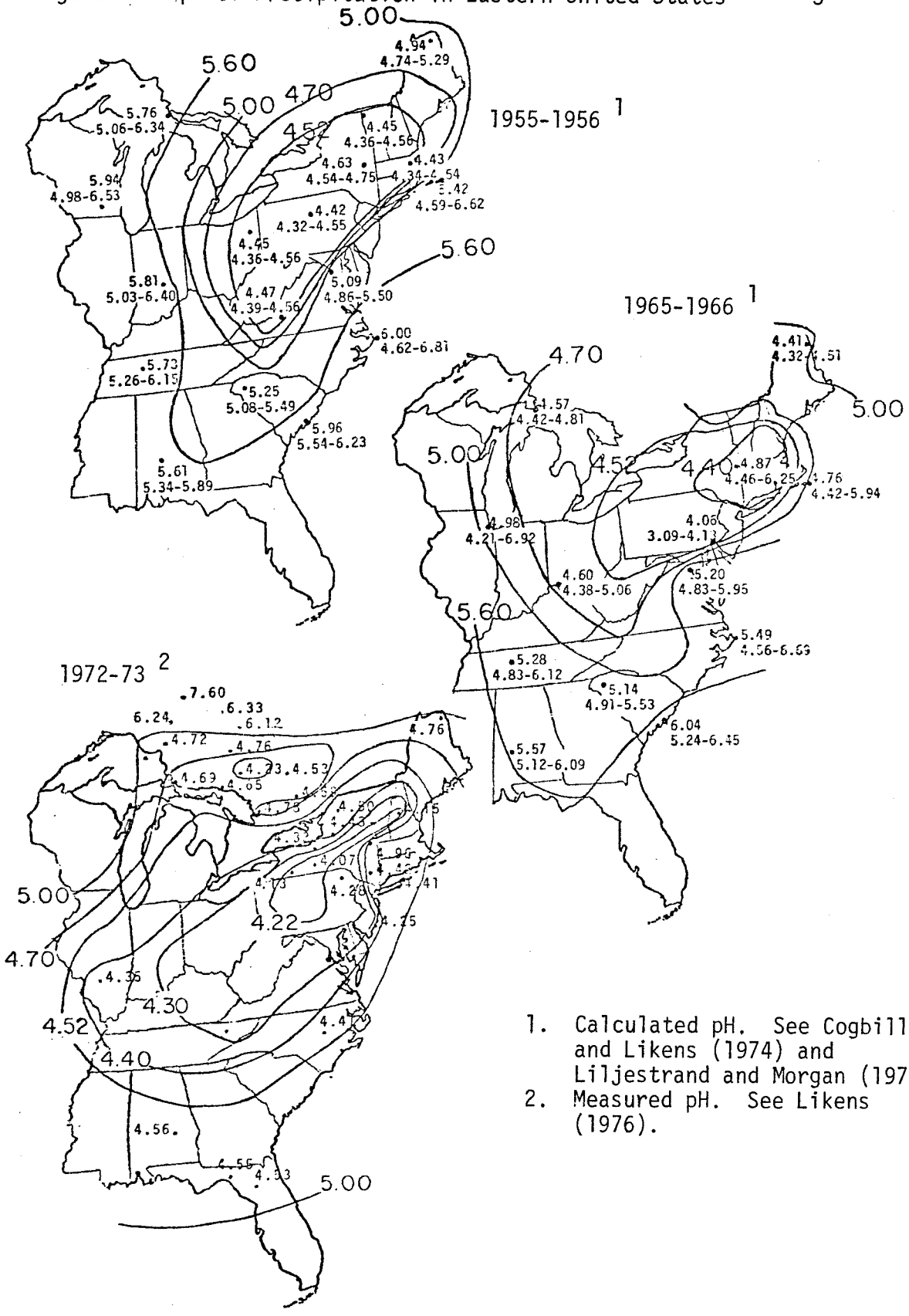

1. Calculated pH. See Cogbill and Likens (1974) and Liljestrand and Morgan (1979).
2. Measured pH. See Likens (1976).

$$[H^+] + [NH_4^+] + [Na^+] + [K^+] + 2[Ca^{2+}] + 2[Mg^{2+}] = \quad (1.1)$$
$$[Cl^-] + [NO_3] + 2[SO_4^{2-}] + [OH^-] + [HCO_3^-] + 2[CO_3^{2-}]$$

$$K_{H_{H_2CO_3^*}} = \frac{[H_2CO_3^*]}{P_{CO_2}} \quad (1.2)$$

$$K_{1_{H_2CO_3^*}} = \frac{[H^+]\,[HCO_3^-]}{[H_2CO_3^*]} \quad (1.3)$$

$$K_{2_{H_2CO_3^*}} = \frac{[H^+]\,[CO_3^{2-}]}{[HCO_3^-]} \quad (1.4)$$

$$K_W = [H^+]\,[OH^-] \quad (1.5)$$

$$[H^+] - \frac{K_W}{[H^+]} - \frac{K_H K_1 P_{CO_2}}{[H^+]} - \frac{2K_H K_1 K_2 P_{CO_2}}{[H^+]^2} = \quad (1.6)$$

$$[Cl^-] + [NO_3^-] + 2[SO_4^{2-}]$$

$$-[NH_4^+] - [Na^+] - [K+] - 2[Ca^{2+}] - 2[Mg^{2+}]$$

The uncertainty in the calculated pH depends upon the uncertainty in the known ion concentrations, the validity of the assumptions of equilibrium with a known partial pressure of carbon dioxide, and insignificant net charge contribution from the undetermined trace ion concentrations. In areas with precipitation of relatively high ionic

strength and low acidity/alkalinity, the uncertainty in the calculated pH is large (Liljestrand and Morgan, 1979).

Figure 1.2 shows calculated mean pH values for precipitation in the West in the 1950's and 1960's. While the uncertainties can be large, most of the Western precipitation probably had a net alkalinity due to soil dust although local areas could have shown net acidity. The calculated values for 1960-1966 agree with measured values from a number of short term studies (Carroll, 1962; Feth et al, 1964; Whitehead and Feth, 1964; Likens, 1976). Measured values in the 1970's showed more acidity (Miller, 1977; Kennedy et al, 1976; McColl and Bush, 1978; Kennedy et al, 1979; Seymour et al, 1978; Knudson et al, 1977; Commission on Natural Resources, 1975) although trends in pH changes in the western United States to the present are hard to determine due to limitations of the indirect calculations of acidity/alkalinity. Southern California may have been one of the areas where acidic anthropogenic emissions are sufficiently intense to neutralize natural alkalinity fluxes and cause locally acidic precipitation.

1.2 Acidity Definitions

Since the historical data base of direct measurements of acidity/alkalinity in precipitation is so sparse, acidity and pH have been estimated from a variety of chemical measurements including major ion concentration as in the charge balance relationship (Equation 1.6), $[HCO_3^-]$ with equilibrium relationships (Equations 1.2-1.3), and various

Figure 1.2 Calculated pH of Precipitation in Western United States (Liljestrand and Morgan, 1979)

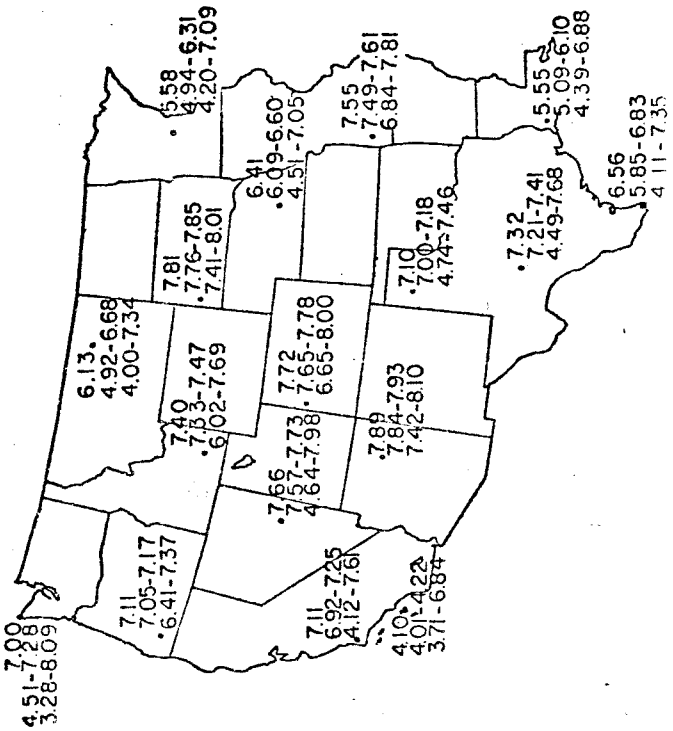

1960-1966

Based on data of Lodge et al (1968).

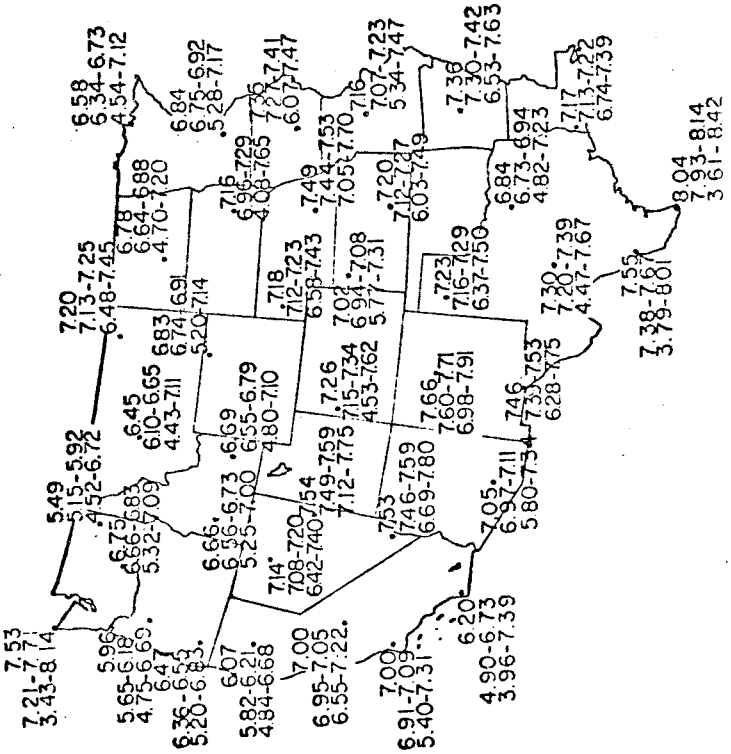

1955-1956

Based on data of Junge (1958) and Junge and Werby (1958)

methods of titration with base. Chapter 2 lays the theoretical framework for acidity in the rainwater system so that results from operationally defined acidity measurements can be compared. (Analytical and sampling techniques used in this study are discussed in Chapter 3.) Conventions used in studies of precipitation chemistry differ slightly from traditional chemical definitions for closed aqueous solutions. For example, equilibrium with atmospheric carbon dioxide is often used as the reference point for precipitation chemistry. Pure water in equilibrium with P_{CO_2} = 315 ppm has a pH of 5.65 at 25°C due to dissolved carbonic acid species (Stumm and Morgan, 1970). While pH 7 is the closed system neutral pH, it represents the presence of 50 μN of excess alkalinity in an open aqueous phase in equilibrium with P_{CO_2} = 315 ppm.

Besides defining the conventions used for rainwater, Chapter 3 outlines the concept of atmospheric acidity which recognizes all acids and bases, whatever their speciation, in rainwater, in aerosol or as gas. This approach is useful in the understanding of acidity/base balances and source/receptor impact relationships. For arid regions such as southern California, the dry flux of acidic pollutants may be more important than the wet flux (precipitation). Estimates of removal of SO_2 and sulfates from the atmosphere by wet and dry mechanisms indicate the dry deposition flux may be 2.1 times the wet flux in California (Fox, 1976). By extending such calculations to all acids and bases from anthropogenic and natural sources, environmental impact can be better predicted.

1.3 Wet Flux

Since the wet flux of acids and bases is poorly characterized in southern California, sampling of precipitation for chemical analysis is the first step in describing the acid precipitation phenomenon. The wet acid/base flux must be quantified. The chemical speciation should identify the important acids and bases. If possible, the sources of the acids and bases should also be identified. Temporal and spatial distributions of acidity should be noted to determine how widespread the phenomenon is and, if possible, trends.

From a control strategy point of view, predictive models of precipitation acidity are desirable. Relationships between air and water quality should be identified. Statistical models may have adequate predictive capabilities for engineering decisions. More fundamental and complex mechanistic models of precipitation scavenging are both more satisfying from a scientific point of view and better predictors for new environmental conditions. Both types of models will be applied to available data. The wet flux is discussed in Chapter 4.

1.4 Dry Flux

While wet deposition is an important but intermittent process for the scavenging and transport of atmospheric aerosols and gases to the earth's surface, the dry flux is a constant input of acidity/alkalinity to the terrestrial ecosystem. The dry flux of acidity/alkalinity has been examined by a number of approaches including the erosion of

calcareous stone exposed to the atmosphere but not precipitation (Gauri, 1978), comparisons of wet deposition only samples with bulk or wet plus dry deposition collected before precipitation (Whitehead and Feth, 1964), collection of dry fallout in buckets (Gatz, 1975), comparisons of wet precipitation with throughfall or leaf-wash samples (McColl and Bush, 1978; Brosset, 1976) and pH changes of leaf surfaces near roadways compared with control leaf surfaces (Flückiber-Keller et al, 1979). Depending upon the surface conditions, air contaminants can be involved in air-base reactions with the surface upon removal from the atmosphere or can accumulate on the surface to be washed into the soil by the next rainfall.

Since the dry flux depends upon the surface and a variety of atmospheric conditions, estimates of the dry deposition of acidity/alkalinity for southern California discussed in Chapter 5 are based on two approaches. First, field studies with controlled surfaces provide measurements of the dry flux. Since the field experiments are limited temporally and spatially, models of the dry flux employing available data on air quality and environmental conditions will also be used. Annual and seasonal calculations of the dry flux will then be compared with the measured wet flux of acidity.

Thus the intent of this thesis is to describe the acidity flux from the atmosphere to the terrestrial ecosystem in southern California. Both wet and dry transport mechanisms are considered to account for the deposition of the major acid and base species in the form of

gases or aqueous components of precipitation or aerosol. Spatial and temporal distributions and source characterization of acids and bases are modeled to help describe the physical-chemical conditions that may lead to ecological changes, material erosion, trace metal mobility in the soil and other environmental impacts.

Chapter 2

ACIDITY - DEFINITIONS AND CONCEPTS

2.1 Introduction

In describing the acid-base characteristics of a system, three parameters are of interest. First is the pH = $-\log_{10}\{H^+\}$ as an intensive quantity describing the present state of the system. Second is the buffer intensity (β) as a measure of the resistance to change in pH upon addition of strong base (C_B) or strong acid (C_A in units equivalents/liter).

$$\beta = \frac{dC_B}{dpH} = \frac{-dC_A}{dpH} \tag{2.1}$$

Third is a measure of how much base or acid is needed to reach a desired or reference pH as operationally defined by a titration. The more general quantities are the acid and base neutralizing capacities ([ANC] and [BNC] in equivalents/liter) defined as the amount of acid and base, respectively, needed to change acid speciation from an initial condition of protolysis (degree of ionization), f_0, to an end point degree of ionization, f_1.

$$[ANC] = \int_{f_0}^{f_1} \beta dpH \tag{2.2}$$

$$[BNC] = -\int_{f_0}^{f_1} \beta dpH = \int_{f_1}^{f_0} \beta dpH \tag{2.3}$$

With proper choice of reference levels, the acid and base neutralizing capacities are conservative quantities.

2.2 Reference States

Carbon Dioxide - Water System

Pure water in equilibrium with atmospheric partial pressure of carbon dioxide (333 ppm in 1979) (Council on Environmental Quality, 1979) has the following charge balance

$$[H^+] = [OH^-] + [HCO_3^-] + 2[CO_3^{2-}] \qquad (2.4)$$

From the equilibrium relationships given in chapter 1, the $[H^+]$ is fixed by P_{CO_2} as given in Equation (2.5)

$$[H^+] = \frac{K_W}{[H^+]} + \frac{K_1 K_H P_{CO_2}}{[H^{+-}]} + \frac{2K_2 K_1 K_H P_{CO_2}}{[H^+]^2} \qquad (2.5)$$

At 25°C, the pH for the pure water-carbon dioxide system is 5.65 for P_{CO_2} = 315 ppm, 5.64 for P_{CO_2} = 330 ppm and 5.63 for P_{CO_2} = 345 ppm. With atmospheric P_{CO_2} increasing at a rate of 1.5 ppm/year (Council on Environmental Quality, 1979), there is a slight decrease in rainwater pH over time attributable to carbonic acid.

The presence of other acids and bases changes the charge balance equation. In general for additional species X_i of charge z_i (z_i can

be either positive, negative or zero),

(2.6)

$$-\sum_i z_i [X_i] = [H^+] - [OH^-] - [HCO_3^-] - 2[CO_3^{2-}]$$

For $-\sum_i z_i [X_i]$ a positive number, the pH of the solution is less than that of the pure water-carbon dioxide system - the solution has a net excess acidity. Likewise for $-\sum_i z_i [X_i]$ a negative number, the solution has a net excess alkalinity. Stumm and Morgan (1970) provide an extensive description of this system for strong acids and strong bases.

The corresponding acid and base neutralizing capacities require consideration of undissociated acids of zero charge and therefore of no contribution to the lefthand side of Equation (2.6). Titration to a higher pH will cause a shift in the weak acid speciation and a dissociation of bound hydrogen ions. In general for acids of the form H_nA[1] where

(2.7)

$$\alpha_o = \frac{[H_nA]}{TOTA} = \frac{[H_nA]}{[H_nA] + [H_{n-1}A^-] + ... + [H_1A^{(n-1)-}] + [A^{n-}]}$$

(2.8)

$$\alpha_1 = [H_{n-1}A^-]/TOTA$$

---

1 In concordance with the Brønsted-Lowry definition of acids and bases, consider weak acid metal ions as in the form $Me(H_2O)_n^{z+} \rightarrow H^+ + Me(H_2O)_{n-1}(OH)_1^{(z-1)+}$.

$$\alpha_{n-1} = [H_1A^{(n-1)-}]/TOTA \tag{2.9}$$

$$\alpha_n = [A^{n-}]/TOTA \tag{2.10}$$

The base and acid neutralizing capacities are given in Equations 2.11 and 2.12, respectively.

$$[BNC] = [H^+] - [OH^-]\Big/_{pH_o}^{pH_f} + \sum_i \left([TOTA_i] \left(\sum_{j=0}^{n} (n-j)\alpha_j \right)_i \Big/_{pH_o}^{pH_f} \right) \tag{2.11}$$

$$[ANC] = [OH^-] - [H^+]\Big/_{pH_o}^{pH_f} + \sum_i [TOTA_i] \left(\sum_{j=0}^{n} (j)\alpha_j \right)_i \Big/_{pH_o}^{pH_f} \tag{2.12}$$

The limits of integration are defined in terms of initial and final pH values which in turn fix the speciation $(\alpha_j)_i$'s. For mixing of solutions of different initial pH and weak acid concentrations, the limits of integration must be defined in the more general terms of degree of protolysis (f).

Odén proposed acidities of the type outlined in Equation 2.11. While only strong acids and base were considered in the carbon dioxide-water system, he calculated the base neutralizing capacity of precipitation in Europe with respect to several reference pH_f's. One datum was $pH_f \sim 5.65$, discussed above, as the neutral pH for water. A second

datum was the pH of rain before anthropogenic emissions of acidic air pollutions. This pH was estimated to be ∿7.2 for Scandanavia. A third datum was the measured pH of precipitation in Northern Europe in the 1950's. Even though acidification of Scandanavian lakes had begun prior to the 1950's, a baseline could be set at the first direct measurements of precipitation acidity.

Equations 2.11-12 are an accounting procedure for hydrogen ions both bound to acids and released from acids. It is in principle similar to the TOTH convention used in the REDEQL2 equilibrium program (Morel and Morgan, 1972) although TOTH uses separate data for metals and anionic-ligand species. The choice of datum is largely a matter of convenience. The acid and base neutralizing capacities can also be defined as the change in TOTH between initial and reference speciations. See Morel, McDuff and Morgan (1976) for an extensive discussion of alkalinity, buffer intensity and TOTH in seawater.

For precipitation chemistry characterized by strong acids and bases, Equations 2.11 and 2.12 simplify to the form of Equation 2.6. For the reference pH of 5.65 and strong acids and bases (i.e., no complexation of metals including hydrogen ion and ligands other than carbonic acid and bicarbonate), base neutralizing capacity reduces to Equation 2.13, a convenient calculation.

(2.13)

$$[BNC] = [H^+] - [OH^-] + \sum_i z_i[x_i] = -[ANC]$$

2.3 Atmospheric Acidity

The previous discussion of acidity in the context of aqueous chemistry does not address atmospheric chemistry or gas-liquid equilibria other than that of carbon dixoide-carbonic acid. By considering gases and aerosols in terms of their dissolution products in dilute aqueous systems (e.g., raindrops), the previous framework for acid and base neutralizing capacities can be extended to atmospheric species. Table 2.1 shows gas-liquid equilibria for typical atmospheric species. For a volume of pure water V_L in equilibrium with the reference state partial pressure of carbon dioxide, there is a change in acid and base neutralizing capacities of the water upon dissolution of all of the acid and base species from a volume of air V_A. Equations 2.11 and 2.12 are applicable when the following substitution is made where R is the ideal gas law constant ($0.08205 \frac{\text{L-ATM.}}{\text{gm-mole}^{\circ}\text{K}}$) T is absolute temperature ($^{\circ}$K), V_A is volume of air (L), V_L is volume of liquid (L), and P_{A_i} is partial pressure of A_i (ATM.):

$$[TOTA_i] = \frac{P_{A_i} V_A}{\frac{RT}{V_L}} \tag{2.14}$$

Equation 2.14 assumes the ideal gas law ($PV=nRT$) to describe the number of moles of acid/base scavenged into the volume V_L to form to total concentration of species A_i. Aerosol concentrations are often given in micrograms/cubic meter and can be converted to partial pressure units by Equation 2.15 (Seinfeld, 1974).

TABLE 2.1

Gas-Liquid Equilibria

$$SO_{3(g)} + H_2O \rightleftharpoons H^+ + HSO_4^- \rightleftharpoons 2H^+ + SO_4^{2-}$$

$$SO_{2(g)} + H_2O_{(g)} \rightleftharpoons SO_2\ H_2O_{(aq)} \rightleftharpoons H^+ + HSO_3^- \rightleftharpoons 2H^+ + SO_3^{2-}$$

$$N_2O_{5(g)} + H_2O_{(aq)} \rightleftharpoons 2H^+ + 2NO_3^-$$

$$HNO_{3(g)} \rightleftharpoons H^+ + NO_3^-$$

$$2NO_{2_{(g)}} \rightleftharpoons N_2O_{4(g)} + H_2O_{(aq)} \rightleftharpoons 2H^+ + NO_3^- + NO_2^-$$

$$HNO_{2_{(g)}} \rightleftharpoons HNO_{2(aq)} \rightleftharpoons H^+ + NO_2^-$$

$$NO_{(g)} + NO_{2(g)} \rightleftharpoons N_2O_3 + H_2O_{(aq)} \rightleftharpoons 2HNO_{2(aq)} \rightleftharpoons 2H^+ + 2NO_2^-$$

$$NH_{3(g)} + H_2O_{(aq)} \rightleftharpoons NH_4OH \rightleftharpoons NH_4^+ + OH^-$$

$$HCl \rightleftharpoons H^+ + Cl^-$$

$$RCOOH_{(g)} \rightleftharpoons RCOOH_{(aq)} \rightleftharpoons RCOO^- + H^+$$

$$H_2S_{(g)} \rightleftharpoons H_2S_{(aq)} \rightleftharpoons H^+ + HS^- \rightleftharpoons 2H^+ + S^{2-}$$

(2.15)

$$\frac{\mu g}{m^3} \quad \frac{P^2 \times 10^{-9}}{RT \text{ Molecular Weight}} = P_i$$

2.4 Oxidation-Reduction

Implicit in the acid-base equilibrium models above (Equations 2.6-2.15) is the absence of redox reactions which can transform basic and neutral species to acidic species or convert acids to basic or neutral species. Biological catalysis of redox reactions that can mitigate or intensify acidity in aqueous systems has been reviewed by Reuss (1977) and Odén (1976). A few important examples are given in Table 2.2.

Oxidative processes can be important in the atmosphere and photochemically catalyzed. For example, one of the products of oxidation of reactive olefins by ozone is organic acid (O'Neal and Blumstein, 1973).

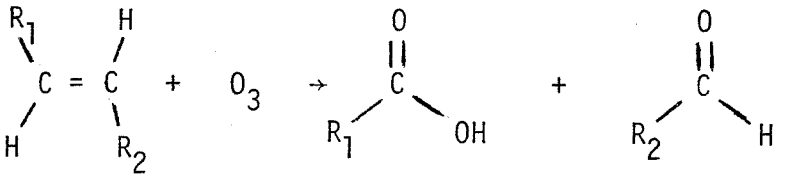

Further oxidation of organics to carbon dioxide reduces the acid impact to that of raising the partial pressure of carbon dioxide. The conversion of nitrogen and oxygen gases, neutral species, to acidic NO_X species during electrical discharge can be a natural cause of acidic precipitation (Bass-Becking et al, 1960).

TABLE 2.2

Oxidation-Reduction Reactions

$$NH_4^+ + 3/2O_2 \rightarrow H^+ + HNO_2 + H_2O$$

$$HNO_2 + 1/2O_2 \rightarrow H^+ + NO_3^-$$

$$6NO_2^- + 3CH_3OH \rightarrow 3N_2 + 3CO_2 + 3H_2O + 6OH^-$$

$$2H^+ + SO_4^{2-} + 2CH_2O \rightarrow H_2S + 2CO_2 + 2H_2O$$

$$RCH_3 + O_2 \rightarrow RC(=O)-O-H$$

$$H_2S + 2O_2 \rightarrow 2H^+ + SO_4^{2-}$$

To describe source-sink relationships for acidity/alkalinity, the extent of oxidation/reduction for each redox couple must be known. Redox reactions are at best in steady state and seldom in equilibrium in the terrestrial environment. Once the extent of oxidation-reduction is known, corrections can be made to the mass balance equations (i.e., $[TOTA_i]$ is no longer constant between source and sink). The speciation f_o is determined by the mass balance, charge balance and equilibrium relationships. Acid and base neutralizing capacities can be calculated by Equations 2.11-2.12 for any extent of oxidation-reduction for each redox couple.

2.5 Primary Source-Receptor Models

Since the acid and base neutralizing capacity calculation require mass balances on a number of species, the primary sources of acidity/alkalinity can to some extent be traced. Mass balance relationships to calculate aerosol sources have been used by Miller, Friedlander and Hidy (1972), Andren and Lindberg (1977), Gartrell and Friedlander (1975) and Gatz (1975) and are especially useful when elements which are of high abundance in one source but not the other sources are used as tracers. Liljestrand and Morgan (1978) estimated the mass source contributions to Pasadena rainwater with the same model developed by Miller, Friedlander and Hidy (1972) by excluding water from the mass balance. The percentage of the ith element in the dry sample, P_i, is given by

$$P_i = \sum_j \alpha_{ij} P_{ij} C_j \qquad (2.16)$$

where α_{ij} is the fractionation factor for the ith element from the jth source, P_{ij} is the percentage of the ith element from the jth source and C_j is the mass fraction from the jth source to the sample. Fractionation factors are assumed to be unity when specific data are lacking. Knowing the alkalinity/acidity of each source and extent of redox reactions, a net acidity for the sample can be calculated from the source contributions.

Granat (1972) and Cogbill and Likens (1974) developed similar source relationships to characterize the strong acid and base sources for precipitation in Europe and the Northeast. Granat (1972) assumed the following sources and acidities/alkalinities: sulfuric acid from air pollutants with two equivalents of acidity per mole, nitric acid from air pollutants with one equivalent of acidity per mole, ammonia from air pollutants with one equivalent of alkalinity per mole, sea salt of negligible alkalinity, calcium soil dust with two equivalents of alkalinity per mole, magnesium soil dust with two equivalents of alkalinity per mole and potassium soil dust with one equivalent of alkalinity per mole. In addition, Cogbill (1974) used hydrochloric acid air pollutants with one equivalent per mole or sodium soil dust with one equivalent alkalinity per mole. When the sodium to chloride ratio in precipitation was greater than that of seawater, chloride was used as the sea salt tracer instead of sodium.

By using secondary pollutant sources, Cogbill and Likens (1972) and Granat (1974) avoided considerations of extent of oxidation of

sulfur and nitrogen species. There is no distinction as to which air pollutant sources contributed the nitric acid, sulfuric acid and ammonia. Wind trajectory analysis has been used to determine probable source locations (Wolff et al 1979; Miller et al 1978, Odén 1976; Cogbill and Likens 1976), but there is still no distinction between types of sources as in stationary vs mobile sources. By restricting the number of sources, these models risk improper identification of sources. For example, if gypsum is a source of calcium and sulfate in precipitation, the pH will be correctly calculated but the calcium soil dust and sulfuric acid contributions will be overestimated.

It should be noted that while the Granat (1972) and Cogbill and Likens (1974) models have limitations, they gave the best interpretation for the available data and worked well for precipitation having strong acidity. Extending the models to include more chemical species and stable isotope balances provide possibilities for more accurate interpretations (Liljestrand and Morgan, 1979). If weak acids are present in precipitation, the more complex model outlined in Sections 2.2-2.4 is the accurate approach.

2.6 Operational Definitions of Acidity

Direct measures of acidity take several forms. Measurement of pH with glass and reference electrodes gives $-\log_{10}[H^+]\ \gamma_{H^+} + E_j$, a small junction potential assumed constant in electrode calibration. $[H^+]$ is sometimes referred to as the free acidity as opposed to protons bound to weak acid species. In the absence of weak acids other than

carbonic acids, an accurate pH measurement can be used with equilibrium relationships (Equations 1.2-1.5) to calculate acid and base neutralizing capacities with Equations 2.6 and 2.13 and buffer intensities (see Stumm and Morgan, 1970).

Acid and base neutralizing capacities can be directly measured by potentiometric titration or titration to a colorimetric endpoint. A titration curve also yields the buffer intensity (β) as a function of pH from the slope of the titration curve. The presence of weak acids can be determined by comparing measured and calculated base neutralizing capacities where the calculated value assumes no weak acids. The strength of the acids as measured by the pK_a's can also be calculated from the titration data.

$$K_a = \frac{[A^+]\,[A^-]}{[HA]} \tag{2.17}$$

$$pK_a = pH - \log_{10} \frac{[A^-]}{[HA]} \tag{2.18}$$

Under the Brønsted-Lowry definition of acidity, acid strength is determined by the ability to ionize or transfer a proton to a water molecule.

$$HA + H_2O \rightarrow A^- + H_3O^+ \tag{2.19}$$

Acids that are essentially fully dissociated are defined as strong acids; in fact $pK_a \leq 0$:$pK_a=0$ is the only thermodynamically defined value for water as a solvent. In dilute solutions such as rainwater of $pH=pH_o$, any acid of $pK_a<pH_o-2$ is effectively a strong acid since the acid is more than 99% dissociated. Thus for a sample of $pH_o=4$, any acid of $pK_a<2$ in Table 2.3 would be considered a strong acid. The rest would be weak acids.

Strong and weak acid concentrations can be quantified with the use of Gran functions (Gran, 1952). The Gran function $F_1=(v+v_o)10^{-pH}$ (see Section 3.5 for an example) where v_o is the initial volume and v is the volume of base added represents the total free acidity in the sample. A plot of F_1 vs v has negative slope of the normality of the base (N) in the region of titration of strong acids. Each equivalent of strong base added neutralizes an equivalent of free acidity.

(2.20)

$$H_3O^+ + OH^- \rightarrow H_2O$$

In the region where the titration of weak acidity is important, the slope of F_1 vs v is less than the normality of the base since base is also being consumed by reactions of the form

(2.21)

$$HA + OH^- \rightarrow H_2O + A^-$$

The intercept of the linear region of F_1 vs v gives the total equivalents of strong acid in the sample.

Table 2.3 pK_a of Acids

acid	$pK_a = -\log_{10}\frac{[H^+][A^-]}{[HA]}$	acid	$pK_a = -\log_{10}\frac{[H^+][A^-]}{[HA]}$
$HClO_4$	-7[1]	H_2S	7.1
HCl	-3[1]	HSO_3^-	7.2
H_2SO_4	-3[1]	$H_2PO_4^-$	7.2
HNO_3	-1	Pb^{2+}	7.5
H_3O^+	0	Fe^{2+}	9.2
$HOCCOH$ (O, O)	1.1	HCN	9.2
		H_3BO_3	9.3
$SO_2 \cdot H_2O$	1.8	NH_4^+	9.3
HSO_4^-	2.0	$Si(OH)_4$	9.5
H_3PO_4	2.1		9.6
Fe^{3+}	2.2	HCO_3^-	10.3
HF	3.2	Mg^{2+}	12
HNO_2	3.3	HPO_4^{2-}	12.4
$HCOH$ (O)	3.8	$Si(OH)_3^-$	12.6
		Ca^{2+}	12.6
CH_3COH (O)	4.7	HS^-	14
Al^{3+}	4.9	H_2O	14
H_2CO_3*	6.3		

[1] from nonaqueous solvents
Representative Values of Acidity Constants at Infinite Dilution in Aqueous Solutions (25°C) (Sillén and Martell, 1964, 1971).

The Gran function $F_2 = (v+v_o)10^{+pH}$ is used to determine the total amount of strong plus weak acids in the sample. A plot of F_2 vs v gives a line of slope N/K_W once the weak acids have been titrated. Any further addition of base represents base dilution and the intercept of F_2 vs v determines the total equivalents of acid in the sample. For dilute solutions, the titration of weak acids of $pK_a > 11$ is hard to resolve from the base dilution effect. Thus "strong" acids are those of $pK_a > pH_o - 2$ and "weak" acids are those of $pH_o - 2 < pK_a < 11$ as operationally defined by potentiometric titration and the use of Gran functions to determine endpoints.

Acidity as operationally defined by the amount of base to reach an indicator endpoint (pH = 8.3 for the endpoint as given in Standard Methods (1975)) represents the strong acidity plus some fraction of the weak acidity. Again, weak acids of $pK_a < pH_{endpoint} - 2$ will be essentially completely titrated. Acids of $pK_a > pH_{endpoint} - 2$ will be partially neutralized by the titration. For example, for the Standard Method endpoint pH of 8.3 will titrate 93% of the bisulfite and $H_2PO_4^-$ acidity and 10% of the boric acid and ammonium acidity.

Titration procedures often vary as to how carbonic acid species are included or excluded. Since the atmospheric carbon dioxide-water system is the standard state, strong and weak acids in addition to the carbonic acid species are often the quantities measured. Dissolved carbonic acid species are stripped from solution by bubbling an inert gas through the sample. The change in hydrogen ion concentration

from gas stripping has been defined as the volatile weak acidity (Krupa, Coscio and Wood, 1976) and corresponds to dissolved carbonic acids and significant fraction of other acids of low solubility and high $pK_{a_{HA}}$ (i.e., hydrogen sulfide). Stripping out carbonic acid with $pK_{a_{H_2CO_3^*}}=6.3$, extends the linear region of F_1 vs v in the Gran plot and allows a sharper determination of strong acidity. The F_2 vs v intercept determines strong plus nonvolatile weak acid equivalents in the sample.

Alternatively, the sample can be titrated in the system closed to the atmosphere, and carbonic acid acidity is then determined. Seymour et al (1978) used Gran type functions to linearize titration curves and determine the best fit solution of acid concentrations and pK_a to describe the titration curve. Precipitation samples for Tucson, Arizona, were described by strong acid, weak acid of $pK_a \sim 6.06$ (probably $H_2CO_3^*$), weak acid of $pK_a \sim 9.25$ (probably NH_4^+) and a weak acid of $pK_a \sim 9.76$ (probably total carbonate in the HCO_3^- form). These pK_a values differ from those given in Table 2.3 due to the ionic strength effect. Samples were titrated at 0.1 ionic strength.

A third approach is to titrate the sample open to the atmosphere. As base is added, carbon dioxide dissolves and neutralizes the base. The titration curve does not have sharp endpoints, which makes the determination of acids other than carbonic acids difficult (Galloway et al, 1976a; Jacobson et al, 1976; Galloway et al, 1976b). The measured base neutralizing capacity could be compared with the theoretical $[BNC]$ for the carbon-dioxide-water system for the endpoint

pH used. The difference would correspond to strong and weak acidity other than carbonic acid but such a determination would be very inaccurate being based on small differences in large numbers. While the titration of samples open to atmospheric carbon dioxide follows the definition of base neutralizing capacity given in Equation 2.11, it is not the method of choice. The carbonic acid contribution can be calculated separately with equilibrium relationships. The excess acidity due to strong and weak acids is the quantity that needs to be characterized.

2.7 Mean pH

The average pH of precipitation has unfortunately been defined several ways. One approach is the arithmetic mean of the measured pH values, since pH values tend to be normally distributed (Cogbill, 1976; Wolff et al, 1979) or, as will be discussed in Section 4.4, rainwater concentrations including $[H^+]$ tend to be log normally distributed. This mean pH ($p\bar{H}$) describes the geometric mean of $[H^+]$.

$$(p\bar{H})_1 = \sum_{i=1}^{n} pH_i/n = -\log_{10}{}^{\mu}{}_g[H^+] \tag{2.22}$$

$$\sigma_{(pH)_1} = \sqrt{\sum_{i=1}^{n} (pH_i - p\bar{H})^2/n} \tag{2.23}$$

If the amount of precipitation during the collection of each sample was constant, then $(p\bar{H})_1$ can be related to $(p\bar{H})_2$ discussed below. Most sampling is done by storm or by month, and precipitation amount varies. Then $(p\bar{H})_1$ has statistical meaning, but cannot be directly related to

the physical quantity of wet acid flux. For constant precipitation amount, the geometric mean and geometric standard deviations can be related to sample mean and standard deviation for $[H^+]$.

A second approach is to weigh free acidity ($[H^+]$) by the precipitation amount (P_i in mm) during the collection of the ith sample.

$$(p\bar{H})_2 = \sum_i^n P_i [H^+] / \sum_i^n P_i \qquad (2.24)$$

This approach ignores the alkalinity of samples of pH > 5.65. For aqueous solutions of strong acids or bases in equilibrium with P_{CO_2}=333 ppm, mixing of one part pH 4.5 with one part pH 6.8 will give $(p\bar{H})_2$ of 4.8 when the equilibrium pH is 5.8. For samples of pH $\leq$ 4.99 and strong acidity, $[H^+] \simeq [BNC]$ and error in this approach is $\leq$5%.

The third approach, the one used in this study, is to define the mean pH as the equilibrium pH of the solution made by mixing the precipitation that fell at the sampling site and allowing the liquid to come to equilibrium with atmospheric carbon dioxide. Thus the precipitation weighted base neutralizing capacity fixes the mean pH. The base neutralizing capacity flux divided by the water flux, given in Equation 2.25, defines the precipitation weighted mean $[\overline{BNC}]$.

$$[\overline{BNC}] = \sum_{i=1}^n P_i [BNC] / \sum_{i=1}^n P_i \qquad (2.25)$$

In general, the precipitation weighted mean of a species or conservative quantity X is given by

$$[\overline{X}] = \sum_{i=1}^{n} P_i [X]_i / \sum_{i=1}^{n} P_i \tag{2.26}$$

The corresponding standard deviation of the mean as defined by Miller (1977) is given by

$$s^2_{pwm} = \frac{1}{n} \frac{1}{\sum_{i=1}^{n} P_i} \sum_{i=1}^{n} P_i([X]_i - [\overline{X}])^2 \tag{2.27}$$

Chapter 3

SAMPLING AND ANALYTICAL TECHNIQUES

3.1 Introduction

The chemical characterization of acids and bases in precipitation samples often requires the determination of inorganic anion and cation as well as organic species at trace concentrations. Ideally all species would be determined from the same aliquot. In practice, samples for organic and inorganic analysis are collected and analyzed separately to avoid contamination from sampler materials. The procedures for preserving the integrity of inorganic samples are largely based on those outlined for trace metal analysis (Patterson and Settle, 1976) although additional steps to avoid anion contamination are necessary.

3.2 Sampling Procedures

Based on the recommendations of Galloway and Likens (1976) and Smith (1976) the precipitation sampler III shown in Figure 3.1 was designed and used. The sampler consists of one sampling train of all glass and metal for organic analysis and one sampling train of all conventional polyethylene plastic (CPE) for inorganic species. Plexiglass lids cover the collecting funnels with pressure provided by two opposing 1.9-lb. 5-in. springs (Lane Spring Co. #108, 1910 Santa Anita, South El Monte, California). At the onset of rainfall, the central polyvinyl alcohol strip (Dissolvo Paper, D. Robbins Inc., 127 W. 17th Street, New York City, N.Y.) dissolves and the springs flip

Figure 3.1 Precipitation Sampler III

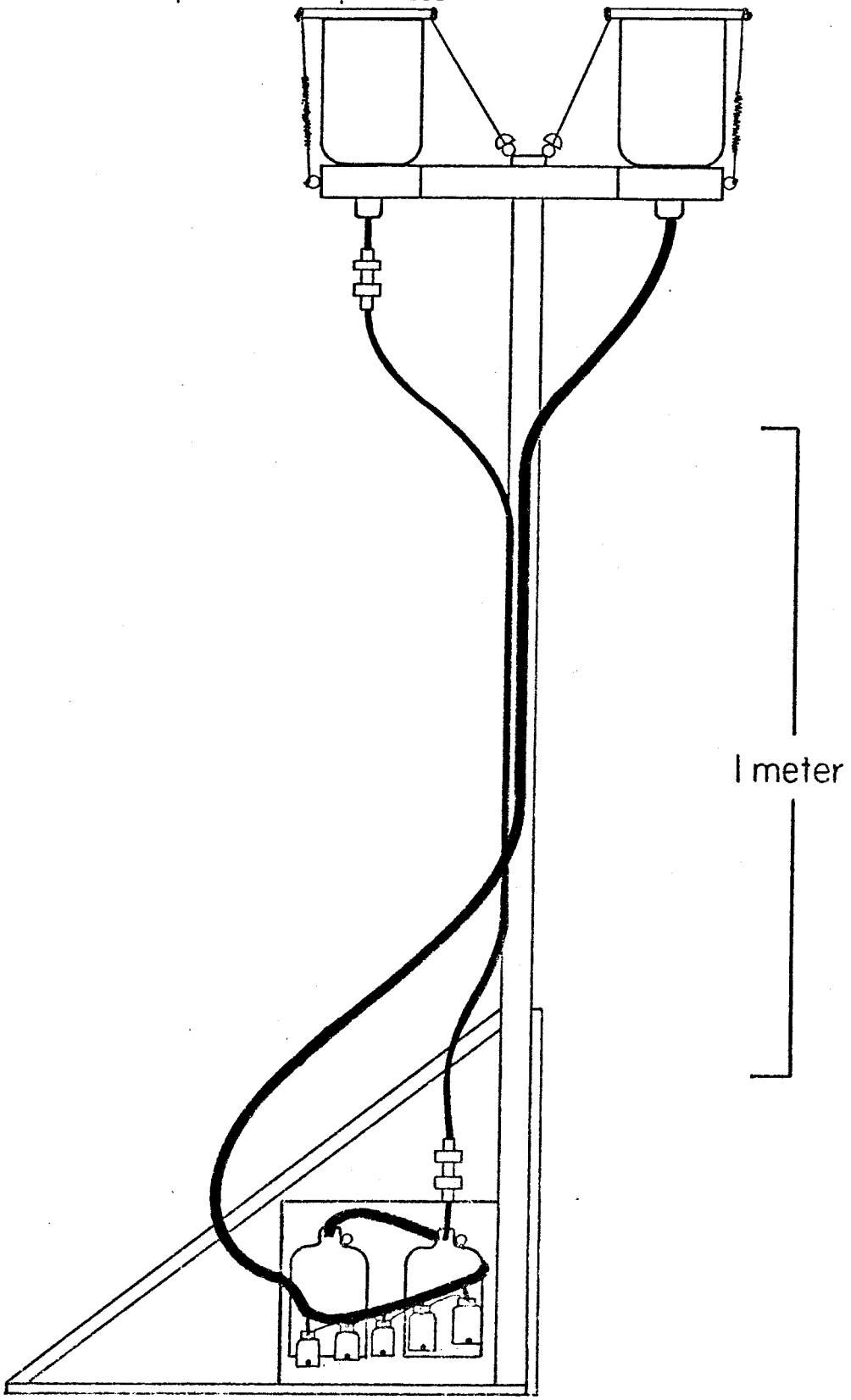

the lids off the funnels. The use of inverted bottles with bottoms removed as funnels approximates the height to width ratio and collection efficiency of the standard rain gauge. A comparison of precipitation collected by the precipitation samplers used in this study and by standard rain gauges operated by the L. A. County Flood Control District shown in Figure 3.2 demonstrates the samplers take representative samples, with the possible exception of light storms (precipitation < 0.05 in).

Samples flow by gravity to containers, total precipitation is collected for organic samples (only one container) and sequential increments of precipitation are collected for inorganic samples. Water siphons into the first bottle until a CPE float ball seals against the lid. The next drop seals the air line from that bottle and additional precipitation flows up the incline until it flows into the next bottle. The process is repeated until the first 3 to 7 100 mL bottles, corresponding to 0.25 in of precipitation, the next 2 500 mL bottles corresponding to 1.25 in of rainfall and the final 1 gallon overflow bottle corresponding to 8.17 in of precipitation are filled. The inverted siphon remains after precipitation stops and serves as a barrier against contamination of collected sample by dry deposition. In practice, filled collection bottles were replaced during extended storms to keep incremental samples at 0.25 in (or less for partially filled last bottles). Collection bottles are housed in an insulated styrofoam shipping container to protect sample from sun-

Figure 3.2 Precipitation Collected by Samplers vs Precipitation Collected by Standard Rain Guage

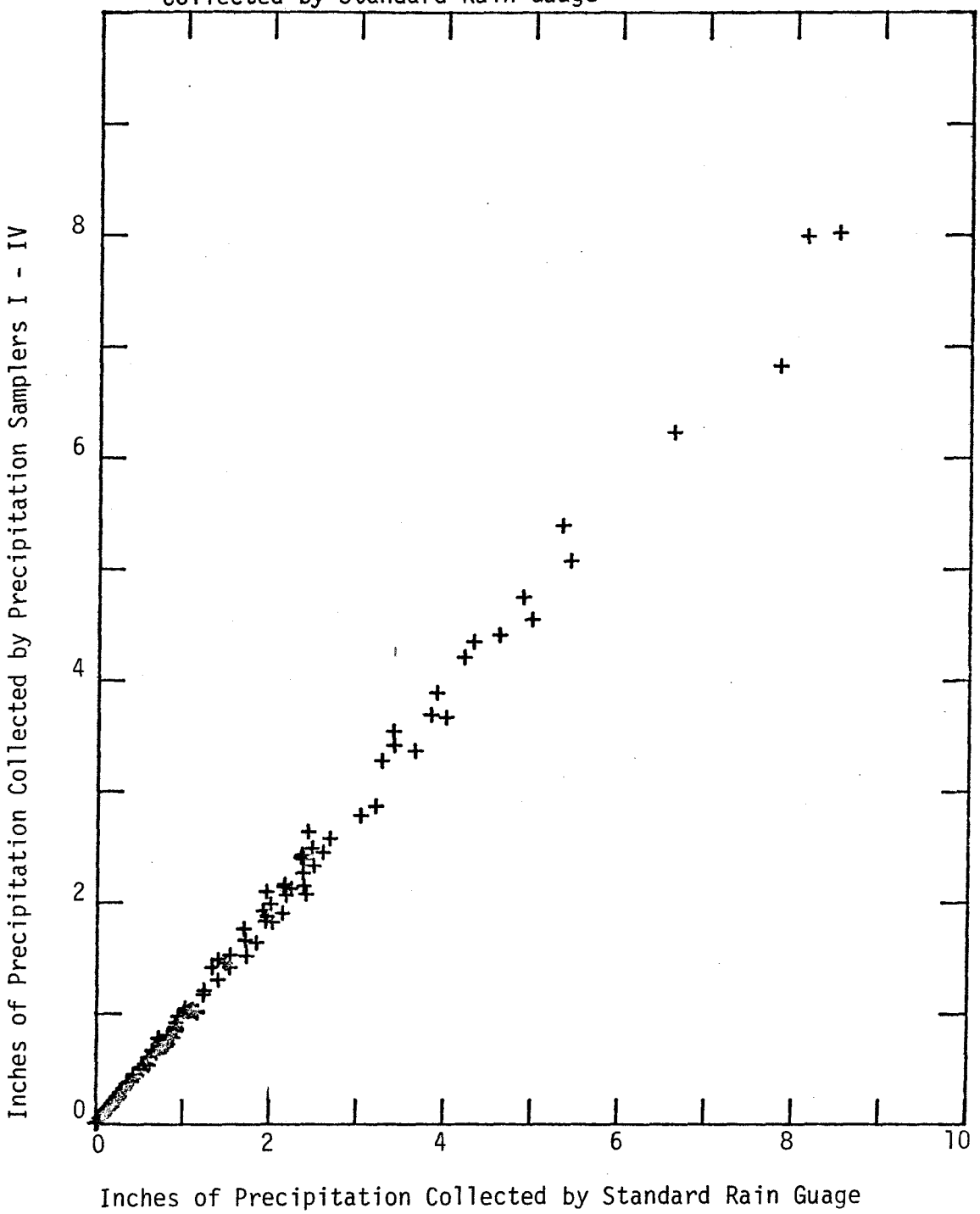

light and concurrent evaporation and algal growth.

The advantages of Sampler III include low cost, ease of disassembly and cleaning, no power requirements and high funnel height from ground to prevent contamination by material splashed up by raindrops. Unfortunately, it is unsuitable for frozen precipitation and requires manual resetting of the lids between periods of precipitation with a storm. Table 3.1 describes the prototype Models I and II and their period of use as well as Model IV designed for collecting snow at the mountain sites.

The locations of the samplers, summarized in Table 3.2, were chosen according to several criteria. First, the site must be representative of the area and free of local sources (overhanging vegetation, heavy travelled roads, stationary source plumes). Second, the site should have convenient access but low visibility to avoid vandalism, intentional or not. Roof top locations seemed best in this regard. Finally,samplers were placed near air monitoring and/or rain gauge sites which were representative of the area.

Dry deposition sampling techniques were similar to those of Huntzicker, Friedlander and Davidson (1975) and Forland and Giessing (1975). A lower limit of the dry flux of aerosol was estimated by the accumulation of material on roughened sticky FEP teflon plates mounted 2.25 meters above ground or roof level. Two FEP teflon disks of 71 cm^2 exposed surface area were secured to the top and bottom of a stainless steel disk by TFE teflon rings which were bolted to the steel disk. Teflon surface was made sticky by the application of 1 mL

Table 3.1 Description of Samplers

SAMPLER MODEL	CHARACTERISTICS DIFFERENT FROM SAMPLER III SHOWN IN FIGURE 3.1
I	One meter height Funnels of "V" cross section manually uncovered One plastic and one glass collection bottle manually replaced
II	Only one plastic collection bottle
III	Same as shown in Figure 3.1
IV	Plastic garbage can with cleaned plastic liner Manual lid removal

Table 3.2 Locations of Samplers

SITE	MODEL	DATES
Azusa - C.I.T. Azusa Hydraulics Lab Roof	III	9/78 - 4/79
Big Bear - Big Bear Solar Observatory	IV	1/79 - 4/79
Central Los Angeles - U.S.C. Biegler Hall Roof	III	9/78 - 4/79
Long Beach - C.S.U.L.B. Science Building I Roof	III	2/79 - 4/79
Mt. Wilson - Mt. Wilson Observatory	III	9/78 - 4/79
	I	2/76 - 1/77
Pasadena - CIT Keck Lab Roof	II	1/77 - 3/77
	III	3/77 - 4/79
CIT Spaulding Roof	III	7/78 - 9/78
Wilson-Del Mar Apartment Roof	IV	9/77 - 5/78
Riverside - UCR Pierce Hall Roof	III	9/78 - 4/79
Westwood - UCLA Geology Building Roof	III	9/78 - 4/79
	IV	1/78 - 9/79
Wrightwood - Grassy Hollow Campground	IV	1/78 - 4/79

of 7.5% by weight vaseline in 'Photrex' benzene (J. T. Baker) which had been extracted with double distilled water three times. Sample was removed from the FEP teflon disk by ultrasonic extraction with double distilled water, followed by 'Photrex' benzene, and finally double distilled water. Extracts were combined and benzene allowed to evaporate. Sample volume was adjusted to 20 mL and analyzed by the methods for precipitation samples.

The dry flux of aerosol and gases to snow surface was estimated by the accumulation of chemical species in snow. Since precipitation concentrations were low for snow, accumulation could be detected. Snow pack sampling techniques were modifications of those described by Patterson and Settle (1976). A trench is dug in the snow pack with a clean CPE shovel. Discarded snow is placed downwind. Polyethylene gloves were changed and the upwind vertical trench face is scraped clean with a cleaned scraper. Vertical cores of snow pack were taken with a clean scoop made by cutting the bottom off of a 1 L CPE bottle. Samples of known snow volume were transferred to clean CPE bottles. Samples were taken at successive 3 or 6 inch depths (depending on snow pack depth) with the top and bottom samples being 3 inches thick. Samples were taken every seven days or less. Mass balances on water were checked to ensure no loss of accumulated acids and base by runoff of melted snow. Since the first snow melt is higher in ionic composition than the average of the snowpack, a mass balance on water is essential (Odén, 1976).

3.3 Cleaning Procedures

Materials used in organic analysis were first washed with warm Alconox soap and rinsed with double distilled water. Glassware was soaked in hot HCl (60°C) for 24 hours, and soaked in hot HNO_3 (60%) for 24 hours. Glassware was rinsed with double distilled water, wrapped in aluminum foil and baked at 450°C for pyrex and 160°C for more fragile glassware for at least 24 hours. Metal-ware was soaked in hot (60°C) double distilled water for two days, autoclaved for 15 minutes at 15 psi and 121°C, rinsed with double distilled water and dried at 160°C. Organic free water used for rinsing and analytical procedures was distilled in a quartz still and collected in glass.

Teflon and conventional polyethylene plastic was washed with warm Alconox soap, rinsed with double distilled water and soaked in hot 60°C in HCL for 24 hours to remove metal ions and ammonia in the plastic. The plasticware was soaked in hot (60°C) double distilled water for a week with the bath water changed daily. Plasticware was not considered clean until the double distilled bath water did not change in pH or chloride concentration over 24 hours. Bottles were filled with double distilled water and stored. Plasticware was emptied and dried one day prior to use.

3.4 Analytical Procedures

Samples were retrieved from the field as soon as possible and were stored at 4°C in the dark until analyzed. Sample weight, pH,

conductivity and ammonium concentrations were first determined. Aliquots for trace metal and calcium and magnesium analysis were placed in acid cleaned CPE vials. The fraction for trace metal analysis was spiked with 20 mL sub-boiling distilled nitric acid per 5 mL of aliquot volume. The subsample for calcium and magnesium analysis was spiked with lanthanum and HCl as recommended by Standard Methods (1975). A third subsample, 5% of the original volume, was combined with other subsamples for that site to give a precipitation weighted mean sample.

pH was determined with an Orion 801A digital pH/mv meter, Beckman glass electrode (Model A6U 39099) and Orion double junction reference electrode (Model 90-02-00). Electrodes were calibrated with dilute nitric and sulfuric acid standard solutions as primary standards and Beckman pH 4.01 and 7.00 buffers as secondary standards. The difference in primary standards calibration curve and calibration curve due to standard buffers was 2 mv, possibly due to junction potential difference. The secondary standard buffers were used to calibrate the pH meter prior, during and after each day of pH measurements.

Titrations with base were performed with the apparatus shown in Figure 3.3. To allow a sharp endpoint for the strong acidity determination and to quantify the weak acid concentrations other than those of carbonic acid species, 20 ml samples in the CPE lined 50 ml jacketed beaker were stripped with high purity N_2 or Ar for thirty minutes. The pH values after stripping and addition of aliquots of

Figure 3.3 Titration Apparatus

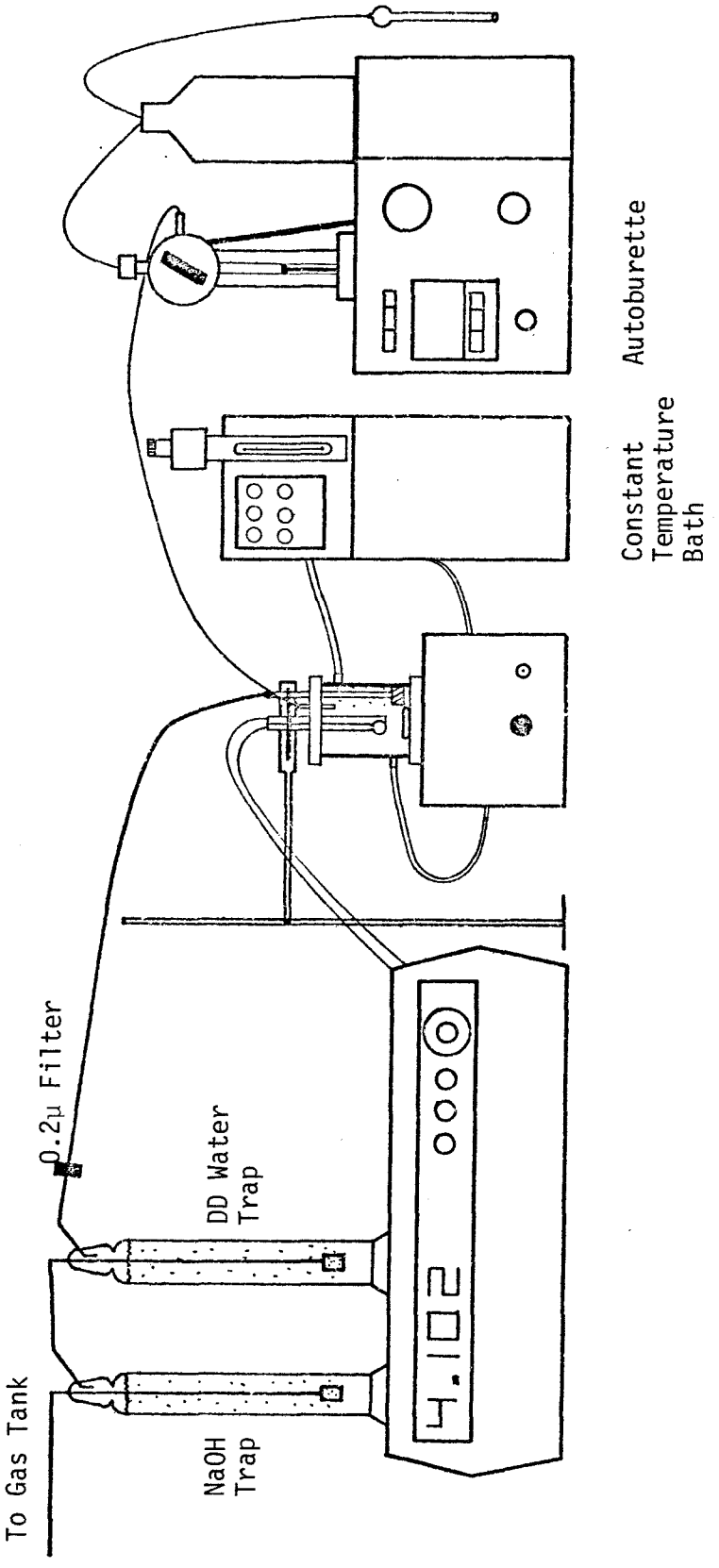

standard base (Dilut-it NaOH) were recorded. The base normality used was 0.001N although known volumes of 0.01N were used to start the titration of samples of initial pH $\leq$ 3.7.

Tables 3.3 and 3.4 reference the analytical procedures and instruments used. Most of the methods are described in Standard Methods for the Examination of Water and Wastewater Treatment (1975). Primary standard solutions were as follows: Harleco 1000 ppm Metal Ion Standards (Harleco 60th and Woodland Avenue, Philadelphia, PA 19143), Orion 0.1M Standardizing Solutions (F^- #94-09-06, CL #94-17-06 NO_2^- #95-46-06, NO_3^- #92-07-06, SO_4^{2-} #92-84-07, Br^- #94-35-06).

A Dionex Model 10 ion chromatograph was used for the determining anion concentrations. A 100 mL sample loop was used with 0.003M $NaHCO_3$ 0.0024M Na_2CO_3 eluent, anion precolumn (#002106), anion separatory column (#002176) and suppressor or H^+ form cation exchange column (#001802). The anions are separated by ion exchange chromatography and converted to their acid forms in the suppresser column. The conductivity detector is sensitive to the separated acid anion ions (H^+ and A^-). Anion peaks are identified by retention time, and anion concentrations are determined by the integrated area under the curve. Figure 3.4 shows typical chromatograms for standards and samples. Standard calibration curves were determined daily. Quantification of anion concentrations is difficult for anions of similar retention time, e.g., the bromide peak shoulders on the nitrate peak and the nitrite peak shoulders on the chloride peak. Cross

Table 3.3 Analytical Methods - Cationic Species

Species	Instrument/Technique	Minimum Detectable Limit (μg/L)[1]	
		Flame	Carbon Rod
H^+	pH meter (Orion 801A)		
NH_4^+	Orion Ammonia Electrode 95-10 Phenate Standard Method	20	
Na	AAS - 589.0 nm	5	0.02
K	AAS - 766.5 nm	10	0.2
CA	AAS - 422.7 nm	21	0.06
Mg	AAS - 285.2 nm	3	0.01
Fe	AAS - 248.3 nm		0.6
Al	AAS - 309.3 nm		6.0
Mn	AAS - 279.5 nm		0.1
Ni	AAS - 232.0 nm		2.0
Pb	AAS - 217.0 nm	110	1.0
Zn	AAS - 213.9 nm	9	0.02

1 Metal ion minimum detectable limits given by Varian.

Table 3.4 Analytical Methods - Anionic and Neutral Species

Species	Instrument/Technique	Minimum Detectable Limit (µg/L)
Conductivity	Conductivity Meter-Radiometer Model CDM2e	
F^-	Dionex Model 10 - I.C. [1] SPADNS Standard Method 570 nm Beckman ACTA CIII	0.48
Cl^-	Dionex Model 10 - I.C. 460 nm (Florence, 1971)	0.96
NO_2^-	Dionex Model 10 - I.C.	
$o\text{-}PO_4^{3-}$	Dionex Model 10 - I.C.	4.8
Br^-	Dionex Model 10 - I.C.	4.8
NO_3^-	Dionex Model 10 - I.C.	4.8
SO_4^{2-}	Dionex Model 10 - I.C.	4.8
Total P	Persulfate Digestion - Ascorbic Acid Standard Method - 880 nm	
$Si(OH)_4$	(Strickland and Parsons, 1968)	
Total Organic Carbon	Dohrmann Envirotech DC-50 Carbon Analyzer	500

1 Ion Chromatograph

Figure 3.4 Chromatograms from Ion Chromatography

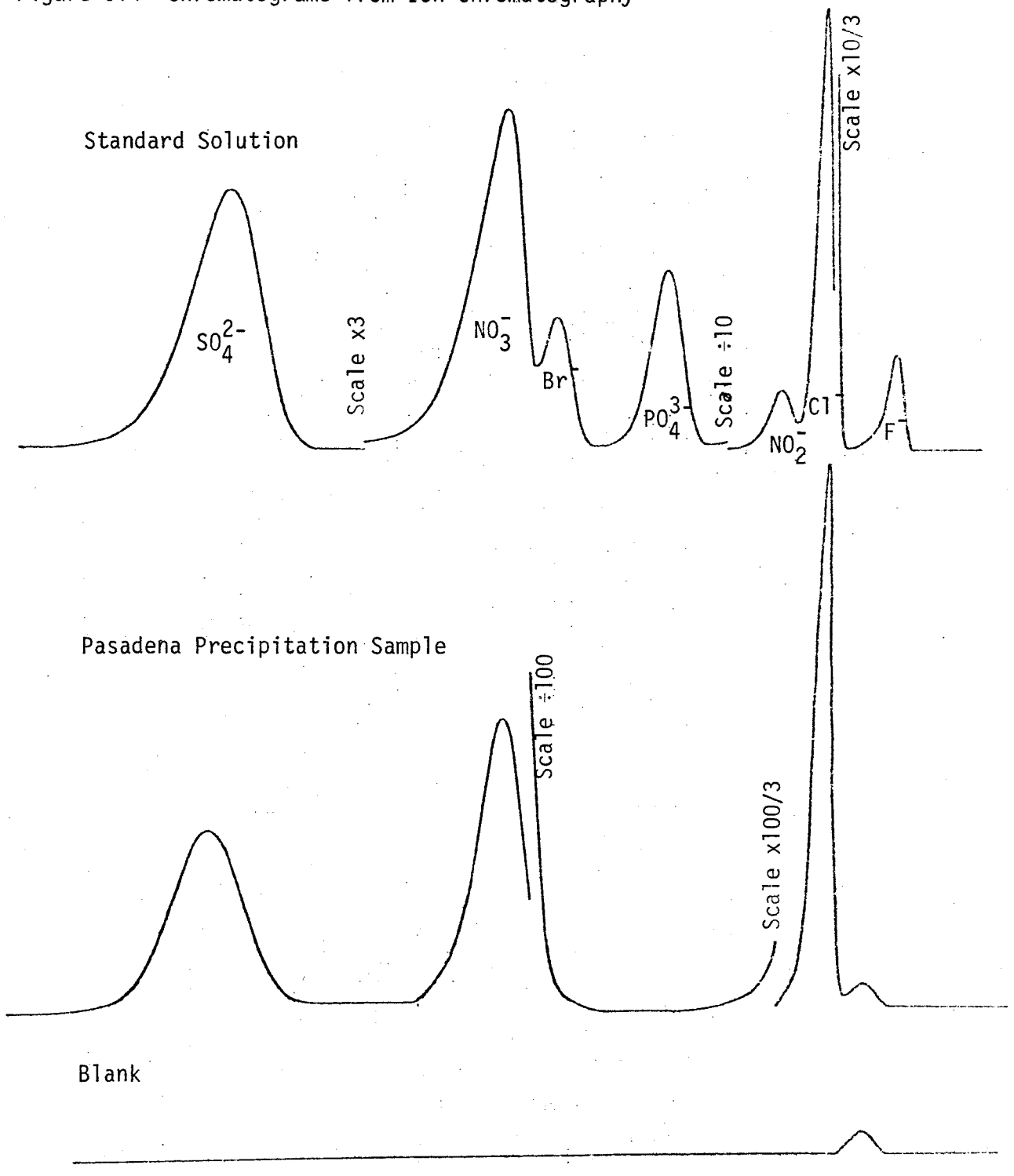

calibration of Dionex ion chromatographic results with standard methods has shown excellent correlations (Lathouse and Coutant, 1978; Butler et al, 1978). Precision and accuracy of fluoride and chloride determinations were improved by spiking a 5 mL subsample with 60 mL of 0.2M Na_2CO_3 + 0.25M $NaHCO_3$ to raise the total carbonate concentration and baseline conductivity of sample solution to that of the eluent.

The procedure for the determination of organic acid concentrations is outlined in Figure 3.5 and is a modification of the procedures used by Bethge and Lindström (1974) and Umeh (1971). The pH of the sample from the glass and metal collector was raised to greater than 9 with 1N NaOH to reduce the volatility of the organic acids. (In retrospect, KOH would have been preferable to NaOH. The sample was spiked with n-heptanoic acid as an internal standard, filtered with a cleaned Millipore GF/C filter (see below), lyophilized at 100 millitorr and redissolved in 2 mL of water. One milliliter was adjusted to pH 7-8 with 1N HCl and loaded on a potassium form strong cation exchange microcolumn (Biorad H^+ form AG® 50W-X12 100-200 MESH).

The ion exchange resin had been cleaned by mascerating overnight in 1N KOH and washing with three BED volumes double distilled water, two bed volumes 1N HCl and three BED volumes of double distilled water and two bed volumes of 1N KCl.

Sample was eluted from the microcolumn with two BED volumes of double distilled water and lyophilized. The dry salt was mixed with 5 mL acetonitrile, 0.01 millimole dicyclohexyl-18-crown-6 ether and

Figure 3.5 Organic Acid Preparative Procedure

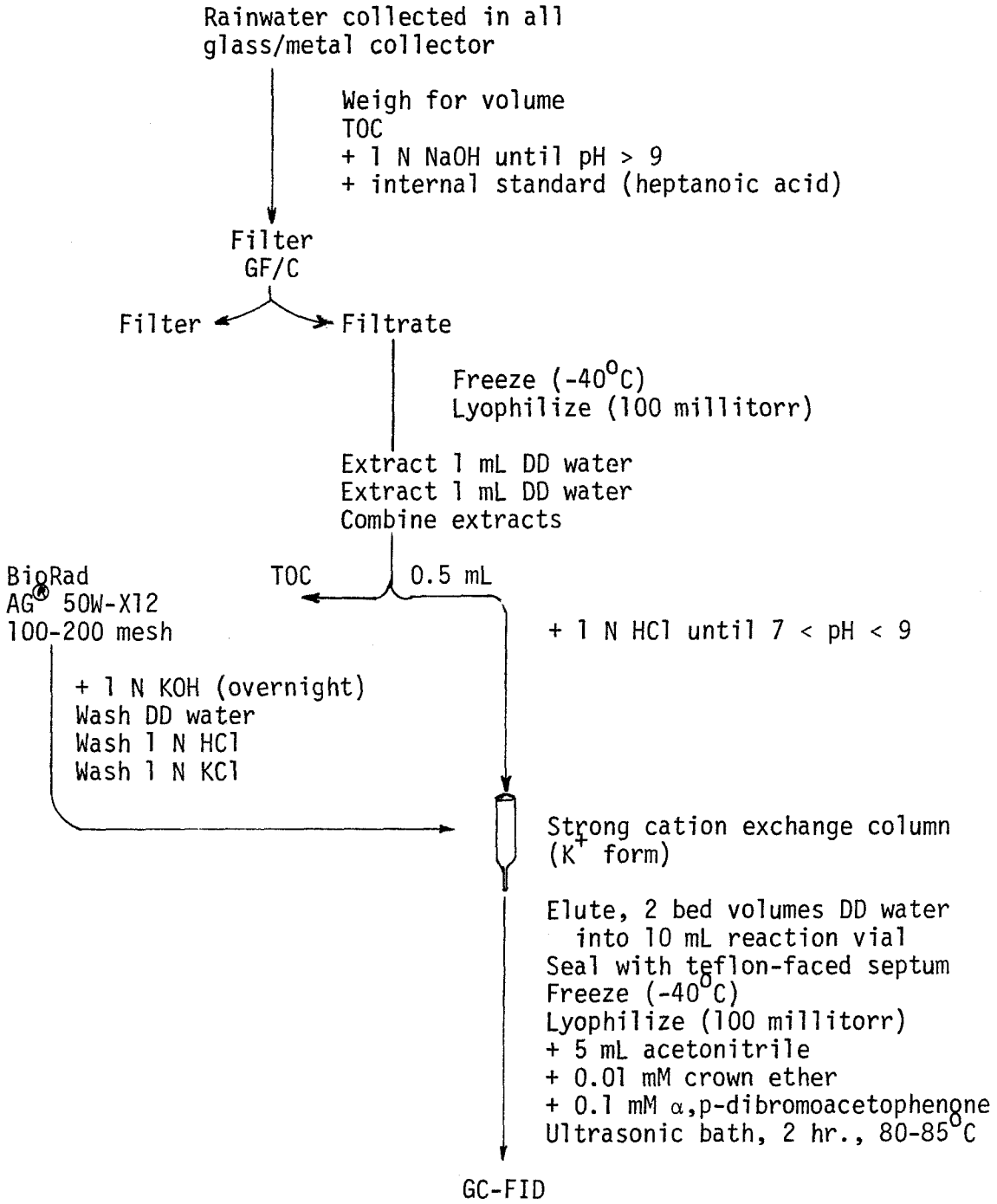

0.1 millimole α,p-dibromoacetophenone (Applied Science Laboratories, State College, Penn. 16801). The p-bromophenacyl ester derivatives of the organic acids were formed by heating the mixture at 80-85°C for 2 hours in an ultrasonic bath. The derivative concentrations were determined with a Hewlett-Packard Model 5830A gas chromatograph using a flame ionization detector 4' long, 1/4" diameter column of 3% H1-EFF 4BP on 120/140 CW-AW (Custom Packing 39 Applied Science Laboratories). The GC was run isothermally at 170°C for 8 minutes, temperature programmed to 190°C at 5°C/min and run at 190°C for 15 minutes. Figure 3.6 shows typical chromatograms of samples, procedural blanks and standards.

Filterable residue was measured with Millipore GF/C glass fiber filters. Filters were mascerated in double distilled water for three days with water changed daily. Filters were baked at 450°C for at least twenty-four hours to remove organic contaminants. Filters were weighed and stored in a dessicator. After the organic sample was filtered, the filter was dried to constant weight at 103-105°C. Total residue was measured by adding 5 mL aliquots to test tubes of total weight < 10g. Subboiling evaporation at 60°C until liquid was no longer visible preceded the standard 103-5°C drying to constant weight. For samples of total residue $\leq$ 1 mg/L, the procedure was repeated with 5 mL samples until residue weight was at least twice the accuracy of the Mettler M5SA balance (5 μg).

Raindrop size distributions were determined by measuring raindrop stains on filter paper (Anderson, 1948). Whatman filter paper was

Figure 3.6 Chromatograms from Gas Chromatography

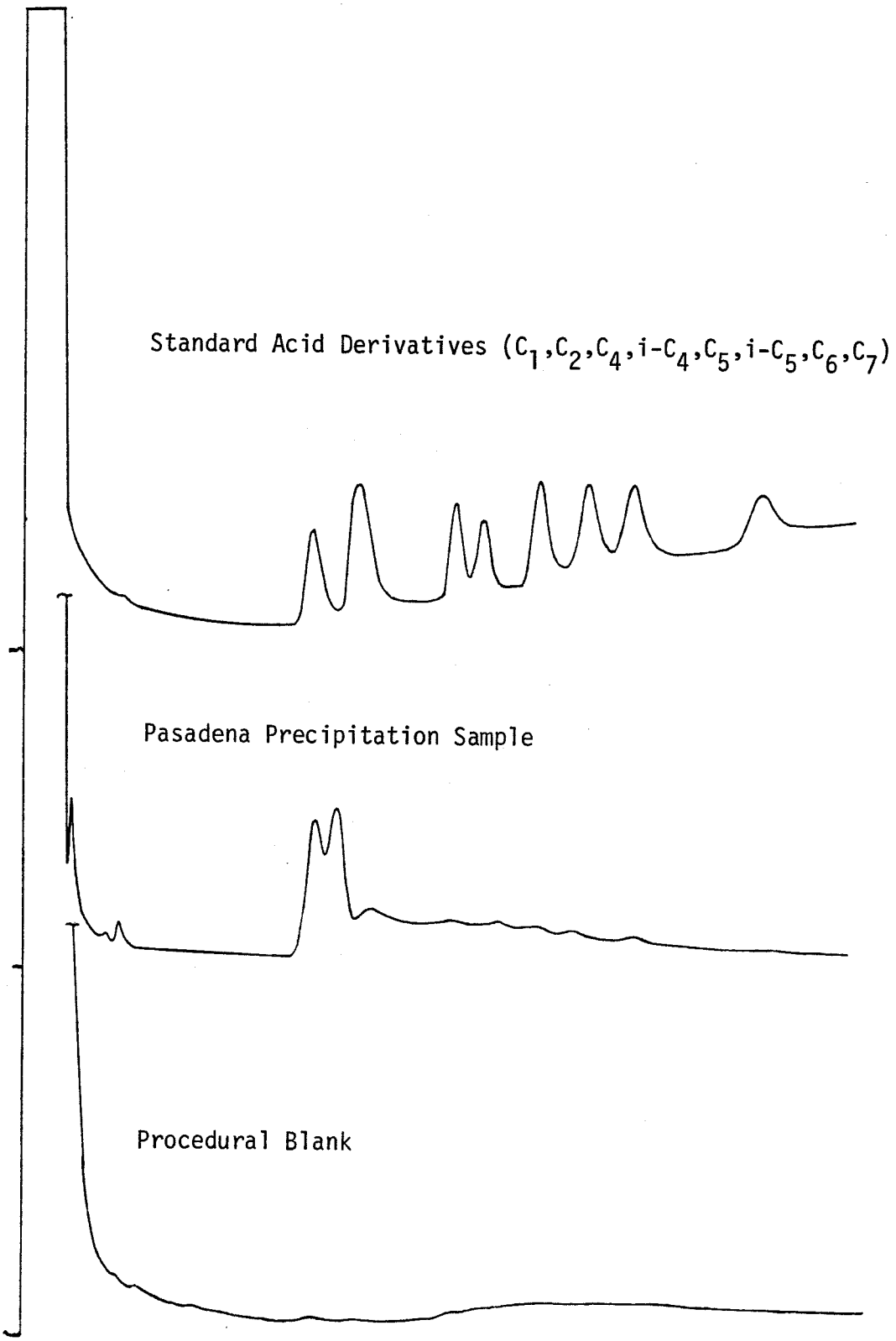

dusted with methylene blue and exposed to rain for a measured time (5 seconds for the heaviest rain to 120 seconds for the lightest rain). The raindrop spreads and darkens the dye and soaks into the filter paper. Cheng (1977) has shown the drop diameter can be theoretically predicted from the stain diameter to within 16% for a wide range of drop sizes and to within 2% for large drops moving at their terminal velocity .

3.5 Quality of the Data

The results from the many sample analyses must be evaluated from two points of view. First, the data must be complete and internally consistent for each sample. Checks of the charge, conductivity, and mass balances and comparisons of titration results with species concentrations provide assurances that the major species in the sample have been determined. Second, the samples themselves must be representative of concentrations in the environment. The sample must not be biased by contamination or sampling errors.

3.5.1 Consistency of Chemical Analyses

The charge balance is a necessary but not sufficient condition that all the major ionic species have been determined. A charge balance of known ion concentrations implies that unknown ion concentrations are low (trace ions) and/or unknown anion and cation equivalent concentrations are equal. The ratio of known cation and anion equivalent concentrations defined by Equation 3.1 should equal unity.

$$\frac{\sum_i z_i[Me_i^{z_i^+}]}{\sum_j |z_j|[A_j^{z_j^-}]} = \frac{[H^+]+[NH_4^+]+[Na^+]+[K^+]+2[Ca^{2+}]+2[Mg^{2+}]}{[Cl^-]+[NO_3^-]+2[SO_4^{2-}]+[HCO_3^-]+[OH^-]+[NO_2^-]+[HSO_4^-]}$$

Analytical uncertainty in each of the measured ion concentrations results in charge ratios that deviate slightly from 1. Galloway and Likens (1978) recommend re-analysis of samples with charge ratios outside the range 1±0.1. Equation 3.2 defines the uncertainty in the charge ratio ($V_{CHARGE\ RATIO}$) in terms of the molar analytical uncertainty of each measured ion concentration.

(3.2)

$$V_{CHARGE\ BALANCE} = \sqrt{\sum_i (\sigma_i |z_i|)^2} \Big/ \sum_i z_i[Me_i^{z_i^+}]$$

$$+ \sqrt{\sum_j (\sigma_j |z_j|)^2} \Big/ \sum_j |z_j|[A_j^{z_j^-}]$$

Figure 3.7 shows the charge balance of cation and anion concentrations with error limits for precipitation samples from all sites and shows good agreement with the expected slope of one.

The conductivity balance is a necessary and sufficient condition that all the major ion concentrations have been determined. The conductivity balance is given in Equation 3.3 where Λ is the specific conductance (μmho/cm) and λ_i is the ionic conductance of the ith ion (μmho/cm-N).

Figure 3.7 Charge Balance of Measured Concentrations

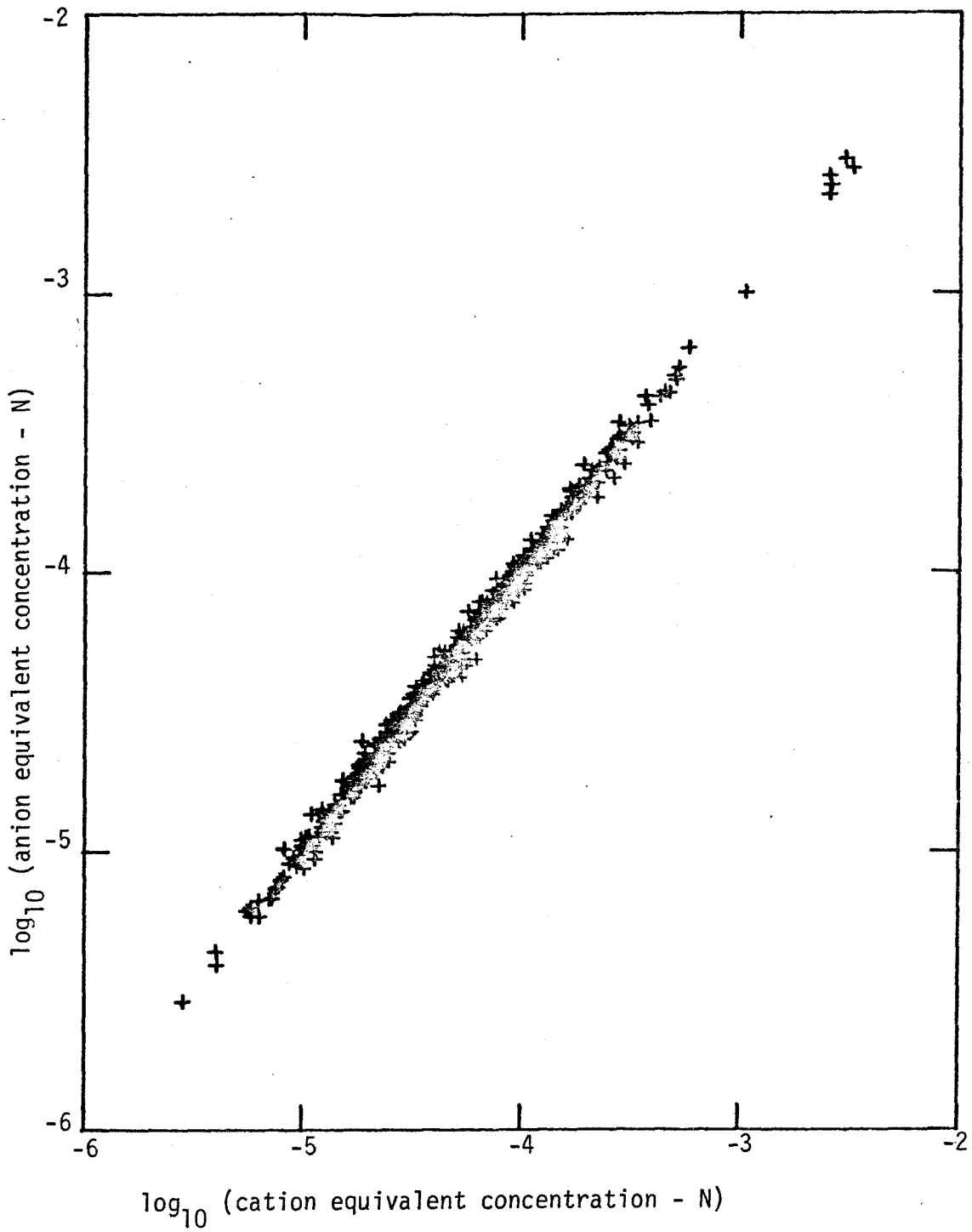

(3.3)

$$\Lambda = \sum_i \lambda_i [X_i^{z_i}]|z_i|$$

The ratio of conductivity calculated from known ion concentrations (R.H.S. equation) to measured specific conductance (L.H.S. equation) should also be 1±0.1 (Galloway and Likens, 1978). Equation 3.4 defines the uncertainty in calculated to measured conductivity ratio.

(3.4)

$$V_{\text{CONDUCTIVITY RATIO}} = \sqrt{\sum_i (V_i \lambda_i |z_i| [X_i^{z_i}])^2} \Big/ \sum_i \lambda_i |z_i| [X_i^{z_i}] + V_{\text{MEASURED SPECIFIC CONDUCTANCE}}$$

Figure 3.8 shows the balance of measured and calculated conductivities within error limits for precipitation samples from all sites and shows good agreement with the expected slope of one. The agreement implies that undetermined ion concentrations are within the uncertainty of the measured values.

Calculating undetermined ion concentrations from the difference in measured and calculated conductivities (Equation 3.5) yields imprecise values due to the problem of small differences in relatively large numbers (Liljestrand and Morgan, 1979).

(3.5)

$$\Lambda_{\text{MEASURED}} - \sum_i^{\text{MEASURED}} \lambda_i [X_i^{z_i}]|z_i| = \sum_j^{\text{UNKNOWN}} \lambda_j [X_j^{z_j}]|z_j|$$

Figure 3.8 Conductivity Balance of Measured Values

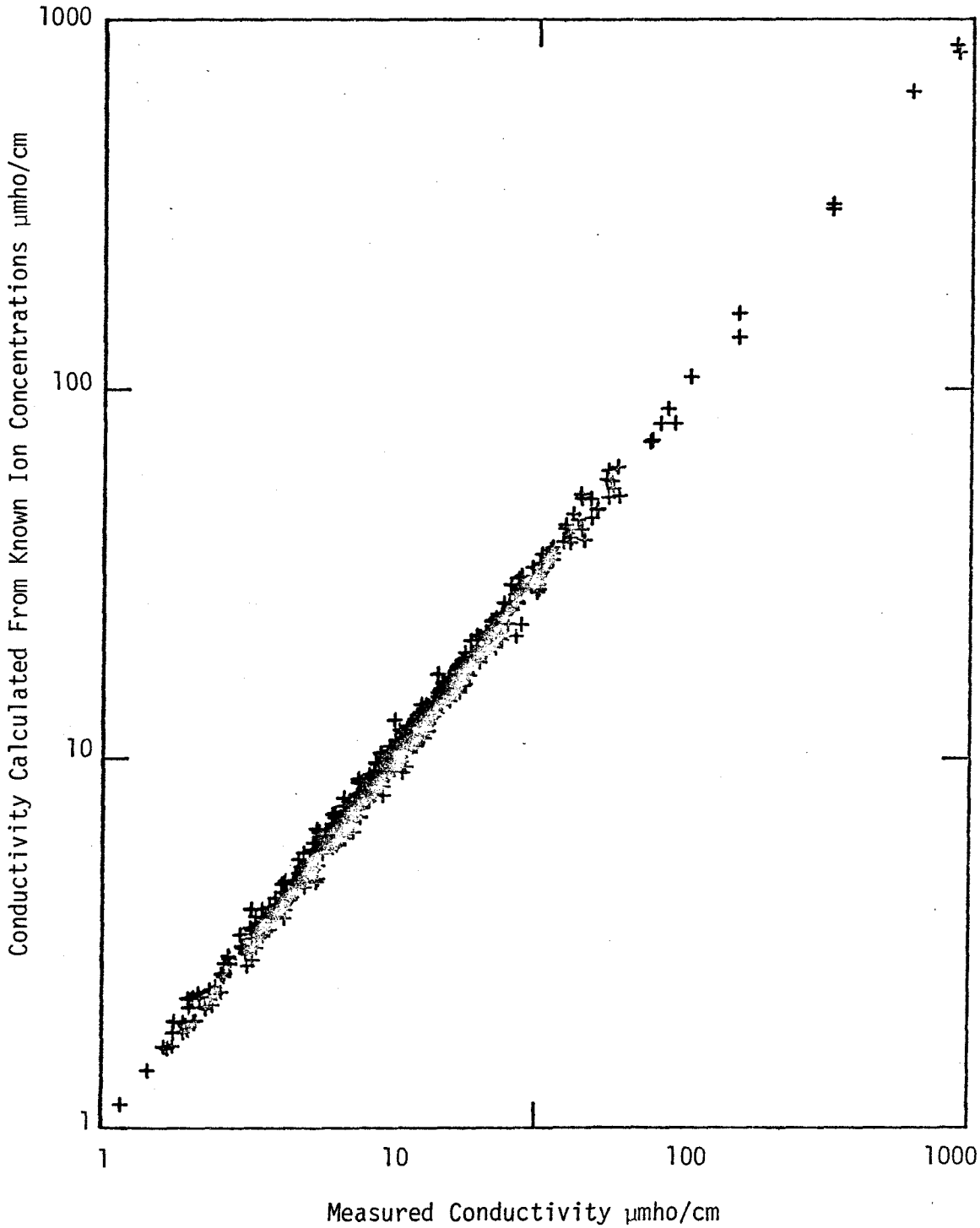

In addition, λ_j varies over a factor of three between trace organic ions of ion mobility and trace metal ions. A cross correlation of measured and calculated specific conductance gave a slope of 0.99 ± 0.01 and intercept - 0.2 ± 0.4 μmho. The difference between measured and calculated could be due to trace ion concentrations on the order of five per cent of the total ionic concentration.

The mass balance was checked for only a few samples since it requires large volumes of water to be precise. The problem of small differences in large numbers occurs in the measurements of total solids (residue on evaporation) and suspended solids (filterable residue) as well as the mass balance calculation (Equation 3.6).

(3.6)

$$\underset{g/L}{\text{TOTAL RESIDUE}} = \underset{g/L}{\text{FILTERABLE RESIDUE}} + \sum_i [X_i](\text{MOLECULAR WEIGHT})_i$$

Calculated total residue tended to be greater than measured total residue which may be due to the loss of volatile salts and acids during drying (Standard Method 1975).

The ion chromatograms also serve as a check that all the major anions have been determined. Table 3.5 shows retention times for various anions for the Dionex 10 under the conditions used. The hazard of ion chromatography is misidentifying peaks of similar or identical retention times. For example, sulfite elutes near the same time as sulfate. By changing eluent concentrations, sulfite and

Table 3.5 Retention Times for Ions with Ion Chromatography

Anion	τ_R(min) [1]
F^-	2
$HCOO^-$	3
Cl^-	3
NO_2^-	4
$H_2PO_4^-$	8
Br^-	9
NO_3^-	14
SO_3^{2-}	16
SO_4^{2-}	18
$HAsO_4^{2-}$	17

1. Retention time for standard eluent (3.0 mM $NaHCO_3$ - 2.4 mM Na_2CO_3 at 2.3 mL/min) and 500 mm column (Hansen et al, 1979)

sulfate peaks can be separated but some sulfite is oxidized to sulfate by oxygen in the alkaline eluent solution, especially in the presence of trace metal ion catalysts (Fe III and Cu II (Hansen et al 1979). The importance of sulfite vs sulfate species is discussed further in Section 4.

The results of titration with base were checked with some ion concentrations and were used to provide upper bounds for other species' concentrations. Gran functions as described by Gran (1952) were used to linearize titration data and provided sharp endpoints. Figure 3.9 gives an example of one titration curve and resulting Gran plots. A plot of the Gran function $F_1 = (v_o + v)10^{-(pH+\log\gamma_{H^+})}$ vs volume of base (v) gave a line of negative slope equal to the normality of the base (N). v_o is the volume of sample being titrated and γ_{H^+} is the activity coefficient of the hydrogen ion. Thus each equivalent of base neutralizes an equivalent of free acidity from strong acids. The intercept volume of F_1 vs v was multiplied by the normality of the base to give the equivalents of strong acid in v_o. Further additions of base titrated the weak acids to about pH 10.3, beyond which pH changes represented dilution of the base; each equivalent of base added causes an equivalent increase in $[OH^-]$. A plot of the Gran function $F_2=(v_o+v)10^{+(pH+\log\gamma_{H^+})}$ gave a straight line of slope N/K_w. The intercept volume of F_2 vs v was multiplied by the normality of the base (N) to give total equivalents of strong plus weak acid. Total weak acid concentration was determined by difference. The

Figure 3.9 Titration Curve with Gran Plots

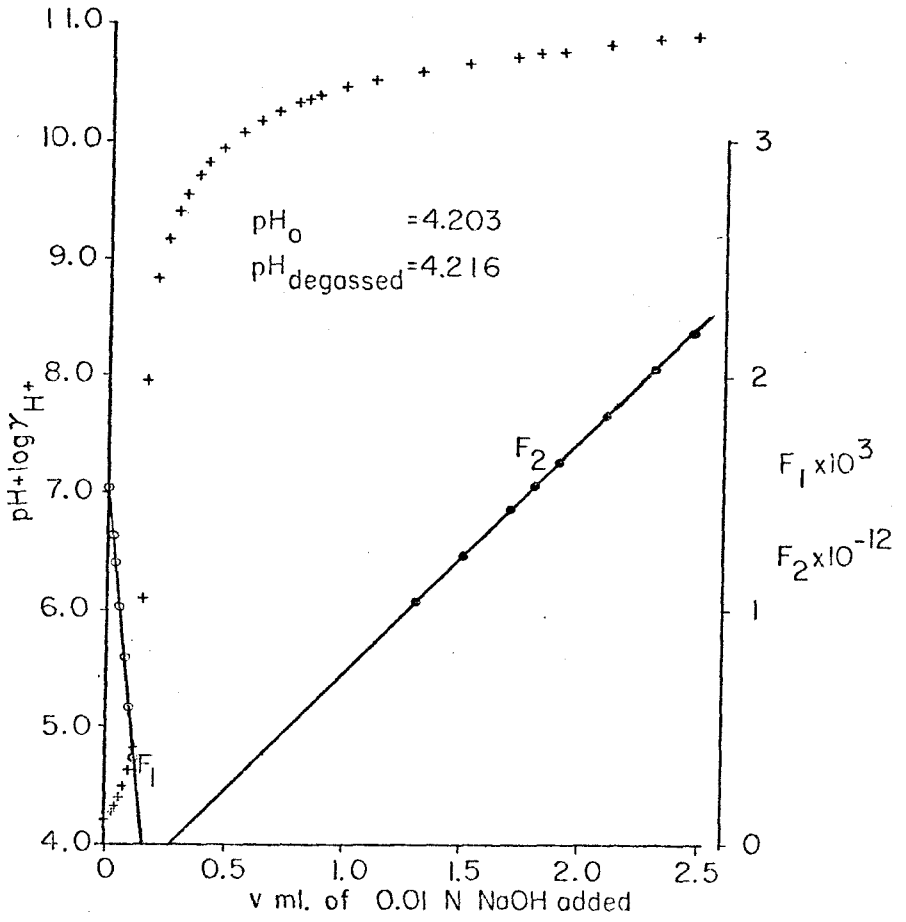

uncertainty in the intercept volumes was at least 3% (Burden and Euler,1975).

Figure 3.10 shows a comparison of initial pH and strong acidity determined by titration and a comparison of weak acidity and ammonium concentration. The titration results emphasize that precipitation chemistry consists predominantly of strong acids plus ammonium weak acid in addition to the carbonic acid. Any undetermined weak acids were present at an average concentration of less than 5 μN. In some samples, metal ion weak acid concentrations were not negligible.

3.5.2 Sample Representativeness

3.5.2.1 Contamination

Systematic errors from sample contamination are a great concern for the analysis of dilute solutions. The cleaning procedures and separate organic and inorganic sampling described earlier were the first precautions to avoid contamination. Quick analysis and/or rapid transfer to containers specially cleaned for that analysis as for trace metals were the second preventative measures. The final assurance that samples are not altered comes from the carrying of blanks through the sampling and analytical procedure (one blank for every twenty samples) and the reanalysis of samples over time. Samples that were noticeably contaminated in sampling by insects, pollen, leaves were analyzed but excluded from the results summarized in Chapters 4 and 5.

3.5.2.2 Sampling Uncertainty

The representativeness of sampling procedures was checked in

Figure 3.10 Strong Acid Concentration vs Free Acidity and Weak Acid Concentration vs Ammonium Concentration

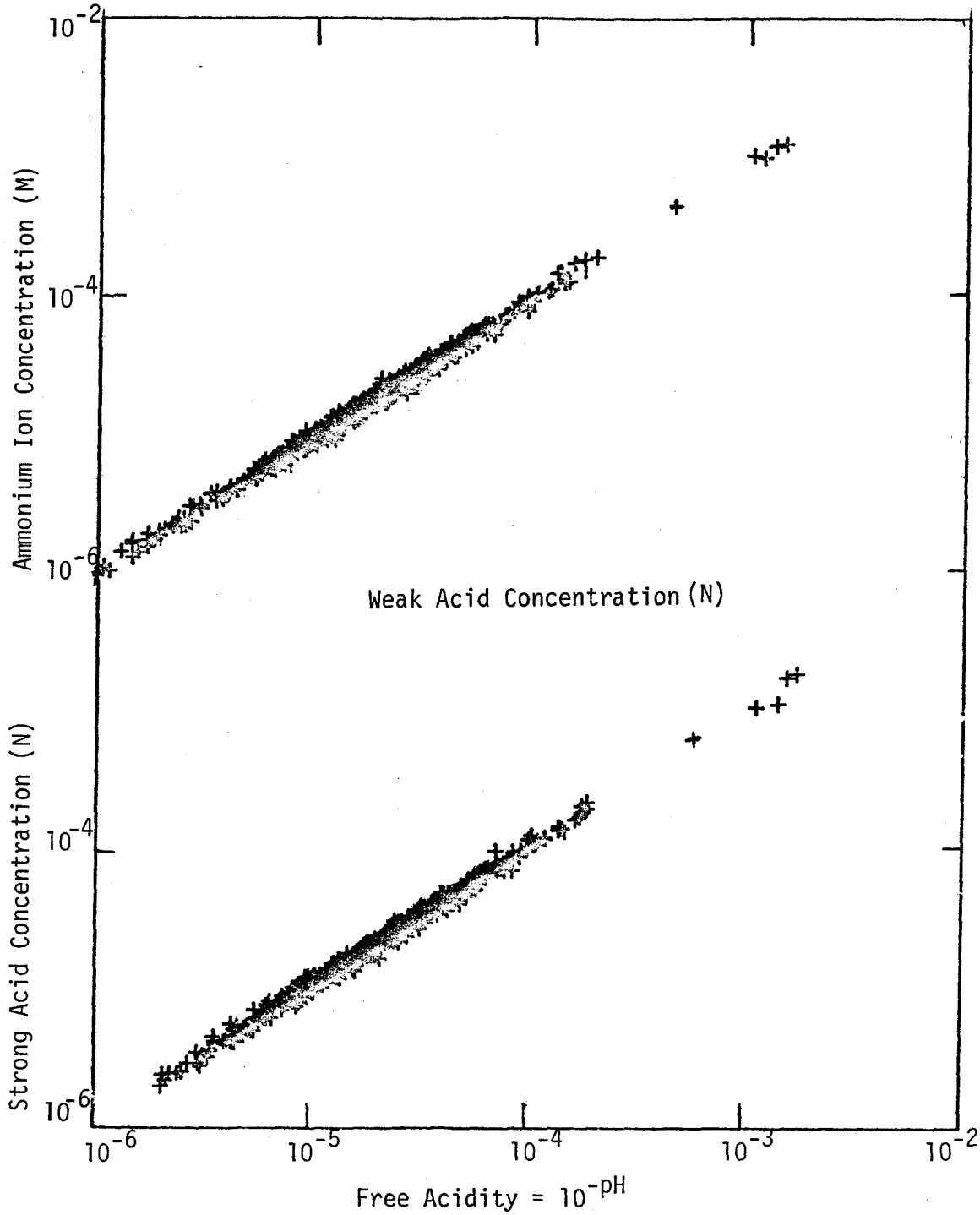

several ways. First, three samplers were operated side by side to look for variation. Second, two samplers were operated simultaneously in the Pasadena area to ensure the Keck Lab sampling site was representative. The results coincided with those of more extensive studies of sampling errors summarized in Table 3.6. Areal variation is much greater than sampling and analytical errors.

Table 3.6 Variation in Precipitation Concentrations

Source of Variation	Coefficient of Variation (σ/μ)	
Analytical Error (for concentrations greater than the minimum detectable limit)	0.04 - 0.10 ~0.06	(Semonin et al, 1978)
Analytical Precision	0.01 - 0.13	(Galloway and Likens, 1978)
Variation Between Samplers at the Same Site	0.05 - 0.35 ~0.18	(Galloway, 1976) (Galloway and Likens, 1978) (Granat, 1976) (Lewis and Grant, 1978)
Spatial Variation (directly related to distance between samplers and inversely related with averaging time)	0.33 - 0.87 >0.30	(Granat, 1976) (Granat, 1977) (Galloway and Likens, 1978) (Semonin et al, 1978)

Chapter 4

WET DEPOSITION OF ACIDITY/ALKALINITY

4.1 Introduction

The precipitation process can be highly variable. Sampling began at Pasadena during a period of drought in southern California, continued at three sites through the second wettest hydrologic year (1977-78) recorded in southern California and ended April 1979 at nine sites during a slightly wetter than normal winter. Results are presented for all samples collected at a site or for shorter periods (e.g., the last winter) to allow spatial comparisons. Raw data for all samples will be available as a technical report.

4.2 Quantification of Wet Acidity Flux

Since the titration results for southern California showed precipitation acidity can be approximated as strong acidity plus NH_4^+, $H_2CO_3^*$, and HCO_3^- weak acid acidities, Equation 2.11 is almost identical to Equation 2.13 for $pH_f \sim 5.65$; the amount of base neutralized by ammonium in titration from pH_o to 5.65 is on the average negligible compared to that neutralized by strong acids. To simplify calculations, Equation 2.13 was used in the computation of precipitation weighted mean acidity (base neutralizing capacity) and corresponding mean pH.

Figure 4.1 shows the measured mean acidity, pH and annual acidity wet flux in equivalents/hectare-year. In general, acidities

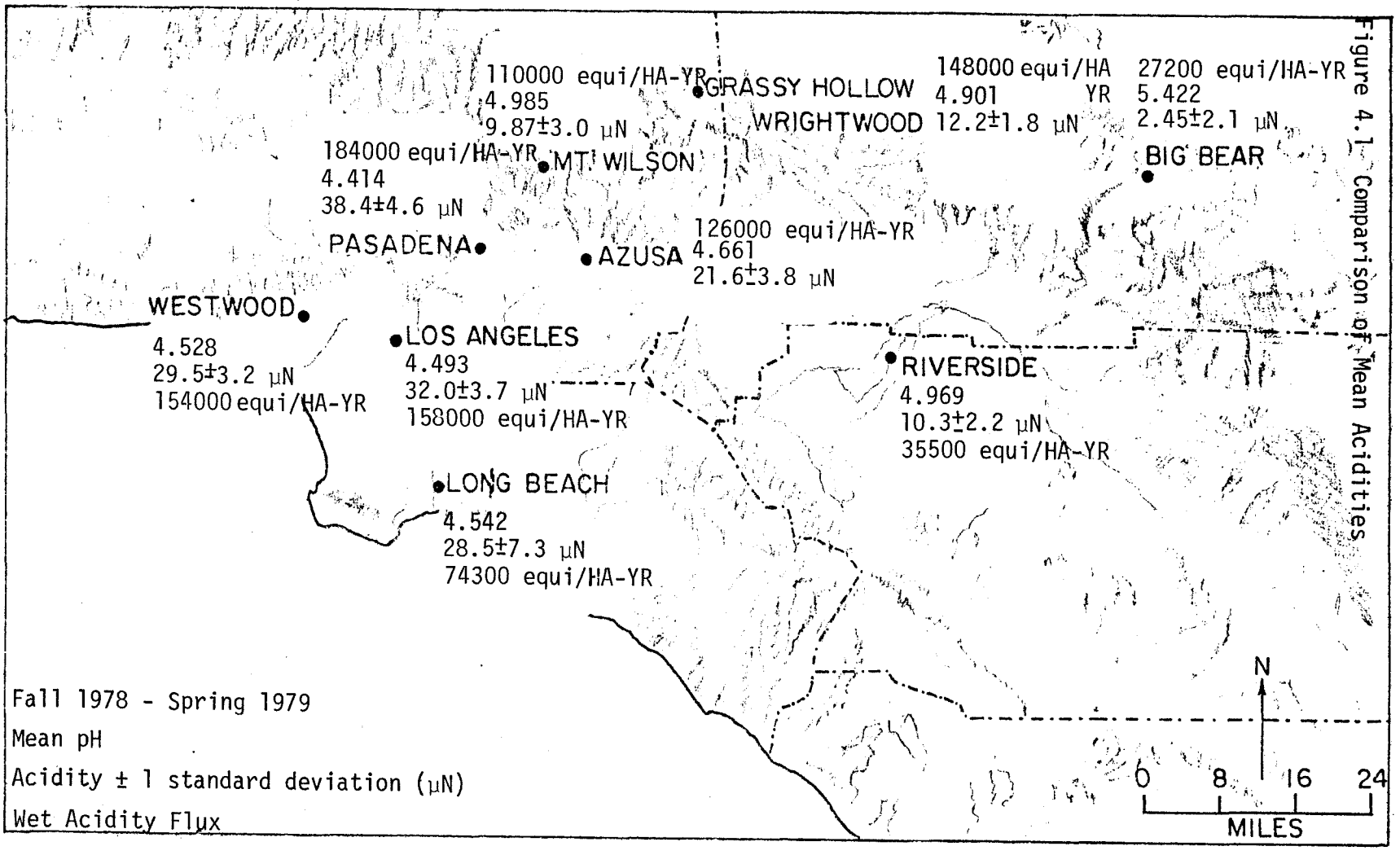

Figure 4.1 Comparison of Mean Acidities

are highest in the western and central Los Angeles basin urban areas and lowest in the mountains and eastern basin. In Table 4.1, the significance of areal variation in mean acidity for fall 1978 - spring 1979 is assessed by a pair-wise comparison (Cochran, 1964) of results for the nine sampling sites. Differences are characterized as not significant (less than the 95% confidence level), significant at greater than the 95% confidence level and significant at greater than the 99% confidence level. There is no significant difference in the acidities at Long Beach, Westwood, Central Los Angeles and Pasadena. Azusa's acidity is significantly different from Pasadena's but not from the other Los Angeles County urban sites. Riverside and the mountain sites have mean acidities which are significantly different from the west and central basin sites.

The wet flux is the annual mean acidity times annual precipitation. Since sites in and nearest the mountains receive the most precipitation, low mean acidities in the mountains do not necessarily mean low fluxes of acidity. Notice Mount Wilson and Long Beach have comparable depositions of wet acidity since Mount Wilson receives more than three times as much precipitation as does Long Beach. Likewise, wet fluxes at Riverside and Big Bear Lake are comparable because Big Bear receives more than four times as much precipitation as does Riverside.

While the relative acidity and acid flux is characterized by the fall 1978 - spring 1979 sampling, the absolute fluxes are known

Table 4.1 Significance of Spatial Distribution of Mean pH

SITE		SITE							
		Long Beach	Mt. Wilson	Pasadena (Caltech)	Westwood (UCLA)	Riverside (UCR)	Los Angeles (USC)	Wrightwood	Big Bear Lake
	Azusa	n.s.	>95%	>99%	n.s.	>95%	n.s.	>95%	>99%
	Long Beach		>95%	n.s.	n.s.	>95%	n.s.	>95%	>99%
	Mt. Wilson			>99%	>99%	n.s.	>99%	n.s.	>95%
	Pasadena				n.s.	>99%	n.s.	>99%	>99%
	Westwood (UCLA)					>99%	n.s.	>99%	>99%
	Riverside (UCR)						>99%	n.s.	>95%
	Central L.A. (USC)							>99%	>99%
	Wrightwood - Grassy Hollow								>99%

Significance of the Difference in Mean pH for Each Pair of Sampling Sites

only within a factor of two. The variability in mean acidity and annual precipitation both contribute to the uncertainty. A comparison of annual flux calculated from fall 1978 - spring 1979 samples and from all samples collected at Pasadena, Westwood and Wrightwood showes the flux can vary by a factor of two.

4.3 Chemical Characterization of Acidity

The wet deposition of acidity in Section 4.2 is based on measurements of net acidity. From ion concentration data, the acidic and to some extent extent basic and neutral components can be identified. Figure 4.2 shows precipitation weighted mean composition and probable acid and base components. The breakdown of components is based on the model of Cogbill and Likens (1974) and shows either neutralization of strong acids upon the reaction of acid and base sources or the scavenging of neutral emissions.

Several trends are evident from the acid-base characterization. First, the net acidity can be viewed as a neutralization of strong acids (nitric and sulfuric) by bases (ammonia, calcium, magnesium and potassium carbonates/oxides) at all the sampling sites. Second, the sea salt contribution with a small alkalinity is highest at the near coastal sites (Long Beach, Westwood and Central Los Angeles), intermediate farther inland (Pasadena, Mt. Wilson, Azusa and Riverside) and lowest at the eastern mountain sites. Third, non-sea salt sulfate, probably derived from SO_2 and SO_3, decreases from the western coastal stations to the inland and mountain stations.

Figure 4.2 Acid and Base Contributions to Mean Acidity

Ionic composition is grouped into four classifications.

1. Sea salt (Na, Cl, Mg, traces of SO_4, Ca, K)
2. Metal ion neutral salts (Ca, traces of Mg, K)
3. Ammonium salts
4. Free acids

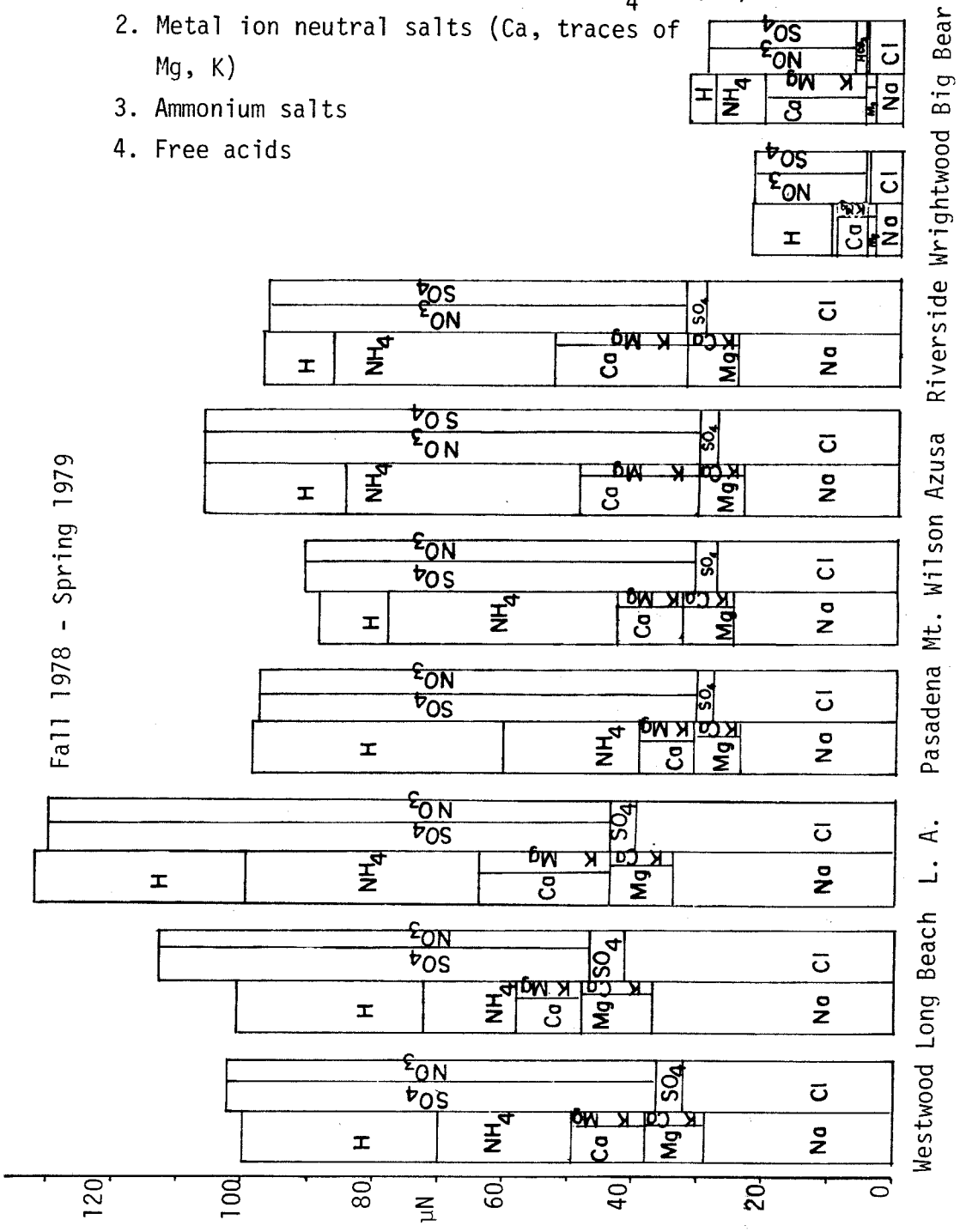

This trend coincides with the locations of major sources of sulfur oxide emissions (Cass, 1978). Fourth, nitrate to non-sea salt sulfate ratio increases from the coastal to inland sites.

The ammonium and non-sea salt metal ion equivalent concentration ($[K^+] + 2[Ca^{2+}] + 2[Mg^{2+}]$ in excess of the predicted from $[Na^+]$ and sea salt ratios) trends are less obvious. The excess metal ion normality is about 10 μN for Long Beach, Westwood, Pasadena, and Mt. Wilson. The higher concentrations at central Los Angeles and Azusa reflect construction and earth moving activity near the sample sites. The high ammonium concentration at Azusa is expected due to dairy cattle feedlots in the area. In general the concentrations reflect local sources and amount of precipitation. A further discussion of ammonia-ammonium gas-liquid phase equilibrium follows in Section 4.61.

The Azusa site provides an interesting example of net acidity. Table 4.1 shows that Azusa has significantly less acidity than Pasadena at the 95% confidence level. This difference is due to higher contributions of alkalinity from ammonia and metal carbonates/oxides. The mean nitrate concentration is higher at Azusa than Pasadena, while the nonseasalt sulfate concentrations are comparable. Thus, Azusa probably has a higher nitric acid input than Pasadena, but it is neutralized by higher alkalinity from local sources.

4.4 Primary Source Characterizations

4.4.1 Source Strength Model

Estimates of the primary source contributions (or strengths) can be calculated from the chemical compositions of source emissions and receptor (rainwater) by the model discussed in Section 2.5. Previous applications of this model have focused in the nonvolatile species or have only traced species involved in gas to particule conversion to airborne pollutants of unknown primary source. The practical reason for not tracing gaseous species to the primary sources is the uncertainty in the fractionation factor or relative efficiency of scavenging by precipitation. Fractionation factors for non-volatile elements are predictable from data on species' mass distribution within the aerosol particle size distribution and on raindrop size distributions. Fractionation of gaseous species with respect to particulate species depends on the extent of oxidation and pH controlled solubility. Overall, the fractionation may be small as evidenced by similar washout ratios for reactive gases (NO_2, SO_2, NH_3) and particulates (Slinn, 1979).

Figure 4.3 shows the results of applying the source strength to the precipitation weighted mean concentrations for the nine sites. Details of the calculation are given in Appendix A. The sources were assumed to be sea salt, soil dust, automotive exhaust, stationary emissions and unidentified ammonia sources. Since the number of chemical species used in the calculation exceeded the number of

Figure 4.3 Source Contributions to Mean Acidity

Ionic composition is described by five major sources.

1. Sea salt
2. Soil dust alkalinity shown by Ca and to a lesser degree, Mg and K
3. Stationary acid sources given by crosshatched area.
4. Mobile acid sources with no crosshatching
5. Ammonia

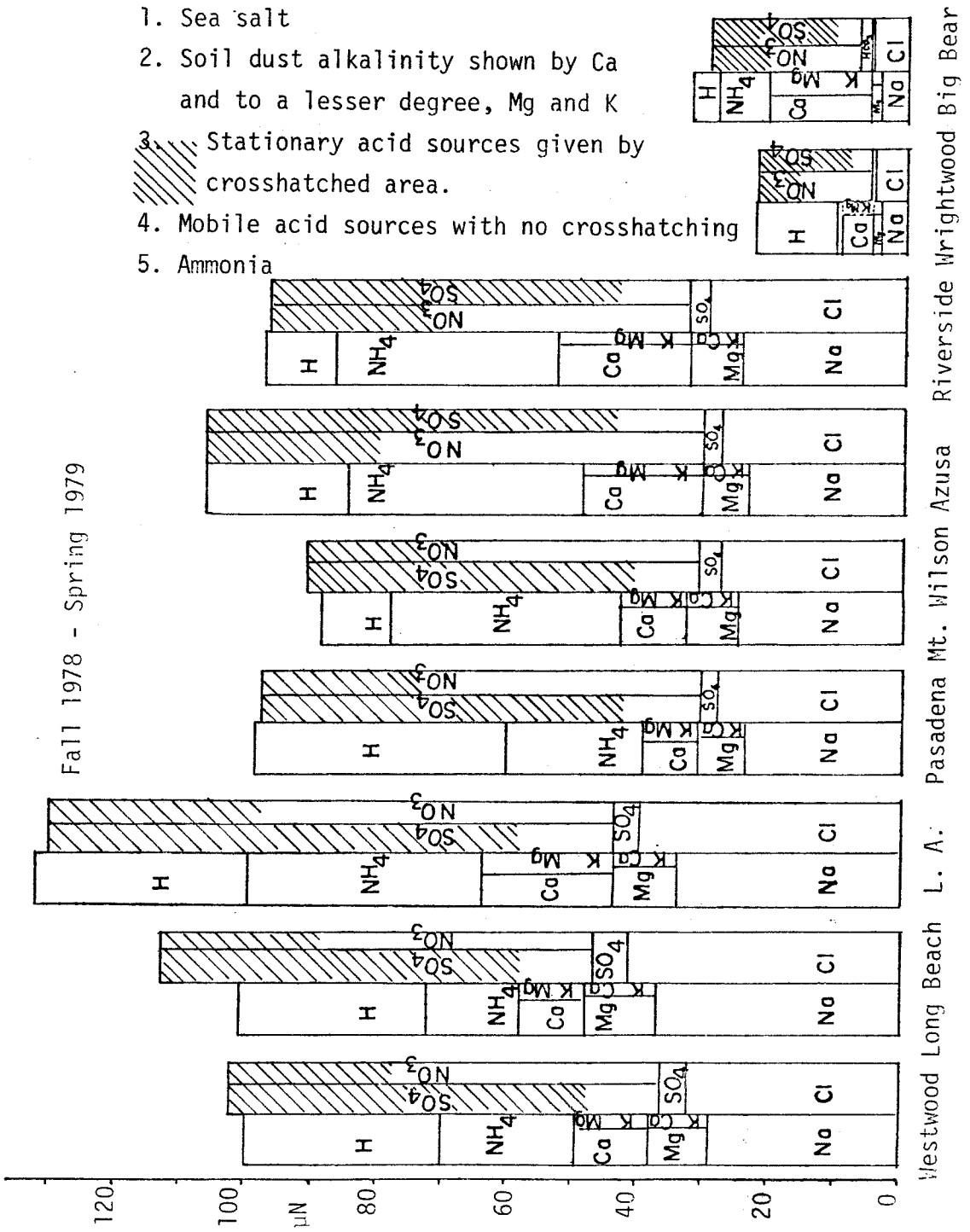

assumed sources, a least-squares solution of an overdetermined system of equations (Equation 2.4) was used to calculate the source strengths. Further research, including studies with stable isotopic ratios, is needed to confirm the relative importances of mobile and stationary sources in nitrate and sulfate production in rainwater.

4.4.2 Wind Trajectory Models

The source strength model gives the relative importance of types of sources of unknown locations. The model does not distinguish between long and short range transport or between two stationary sources of the same type. Some indication of source location comes from wind trajectory models. By determining the distribution of chemical species with respect to surface and upper atmosphere air trajectories, source location can be better characterized. Trajectories at 850 mb are estimated from semidaily upper air soundings at Vandenberg Air Force Base, San Diego, Los Angeles International Airport and El Monte Airport using the model of Pack et al (1978). Measured wind vectors are weighted by the inverse of the square of the distance between precipitation sampling site and wind sounding site. Similar air trajectory models have been used by Miller, Galloway and Likens (1978), Wolff et al (1979), Nordo (1976), Cogbill and Likens (1974) and Forland (1973). Errors in calculated trajectories can be quite high and would be as high as $\pm 30^{o}$ in these calculations.

Unfortunately, there was little variation in surface and frontal air mass trajectories for the fall 1978 - spring 1979 sampling. De Marrais et al (1965) describes these winter wind roses. Pasadena samples collected from February 1976 to April 1979 represented northern frontal systems, southern tropical storms as well as storms from the west. Figure 4.4 shows precipitation weighted concentration distributions with respect to air trajectory for sodium (see salt tracer), calcium (soil dust tracer), nitrate, and sulfate.

The sea salt tracer shows little variation with surface wind vector. The sodium variation with upper air trajectory reflects storm intensity. The calcium soil dust tracer shows little variation with upper air trajectory.

Nitrate and sulfate concentrations show little variation with upper air trajectory. Higher concentrations for the southeastern surface wind trajectories reflect the urban sources in that direction. Upper air trajectories from the southeast are dominated by tropical storms of high precipitation intensity. The concentrations are less than might be expected from urban sources in the wind trajectory and may be low due to dilution effects during the heavy rains. Concentrations for upper air from the north are higher than might be expected. While there are no major sources along this trajectory, surface and upper air mixing on the southern side of the mountains may input sulfur and nitrogen oxides into the upper atmosphere at the sampling site.

Figure 4.4 Concentration Distribution with Respect to Wind Trajectory

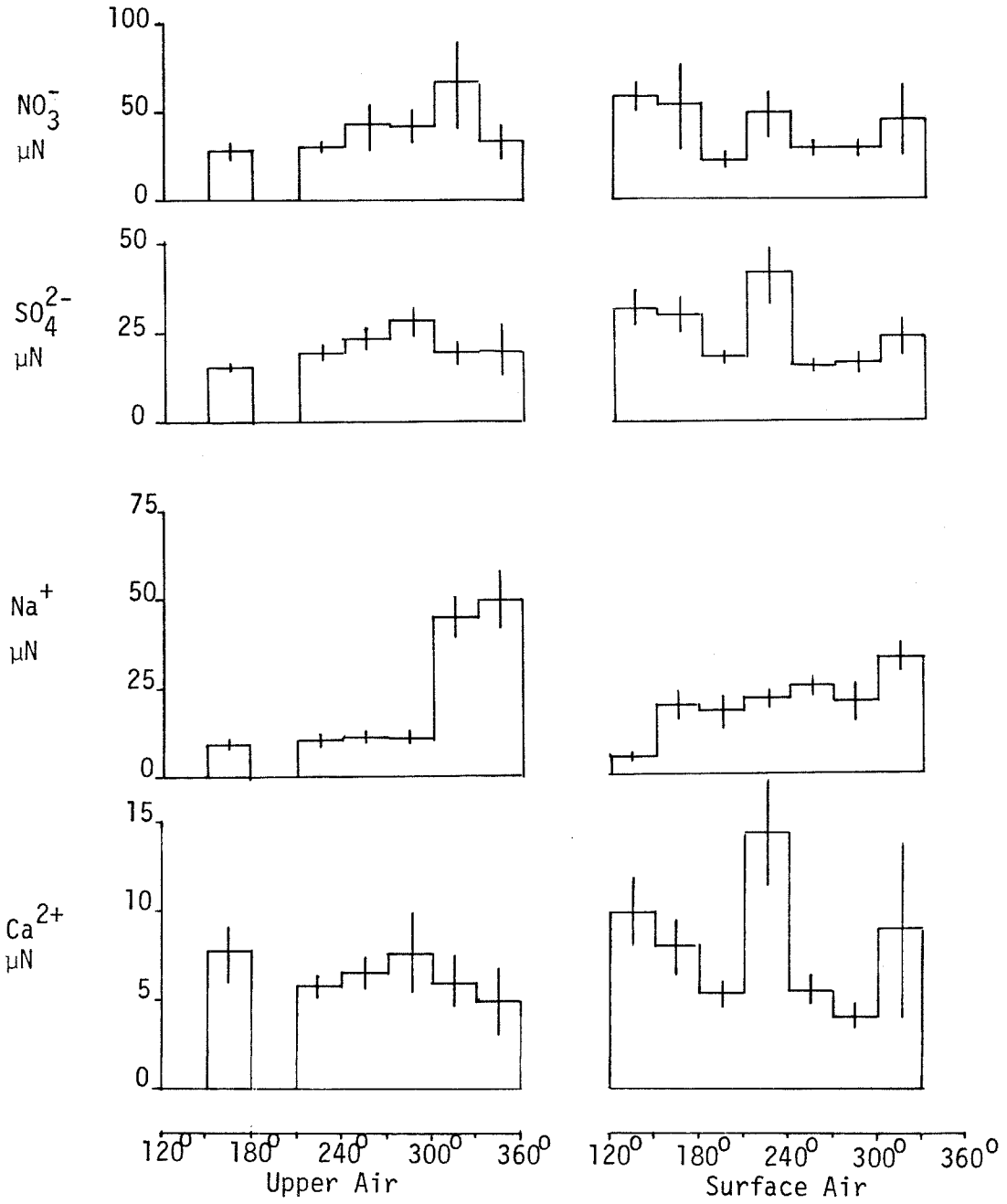

4.4.3 Temporal Distributions

Another approach to distinguish source contributions is to examine temporal distributions. Mobile sources and power plants have diurnal patterns of emissions corresponding to patterns of human activity. Other stationary sources, such as those related to petroleum refining, run continuously at full capacity and therefore cause constant emission of pollutants. Figures 4.6 and 4.7 show the average diurnal and seasonal patterns of emissions for the major stationary and mobile sources in southern California (Cass, 1978).

Figures 4.6 and 4.7 also show the temporal distribution patterns of precipitation for each 0.25 inch sample of precipitation as determined from recording rain gage data. Precipitation weighted means for each hour are determined for work days and non-work days. Grouping samples by the hour is somewhat arbitrary and the bar graphs should be smoothed between adjacent hours. Precipitation weighted standard deviations are also given to distinguish real differences between subsets, especially those of a few samples.

There are several factors contributing to diurnal, weekly and seasonal variations in precipitation concentrations. The largest variations may be in the scavenging processes. By averaging over enough storms, variations in the precipitation processes may average out. A check of total precipitation during each hour in Figure 4.6 shows this criterion is not met; either the sample population

Figure 4.5 Concentration Distribution with Respect to Day of Week

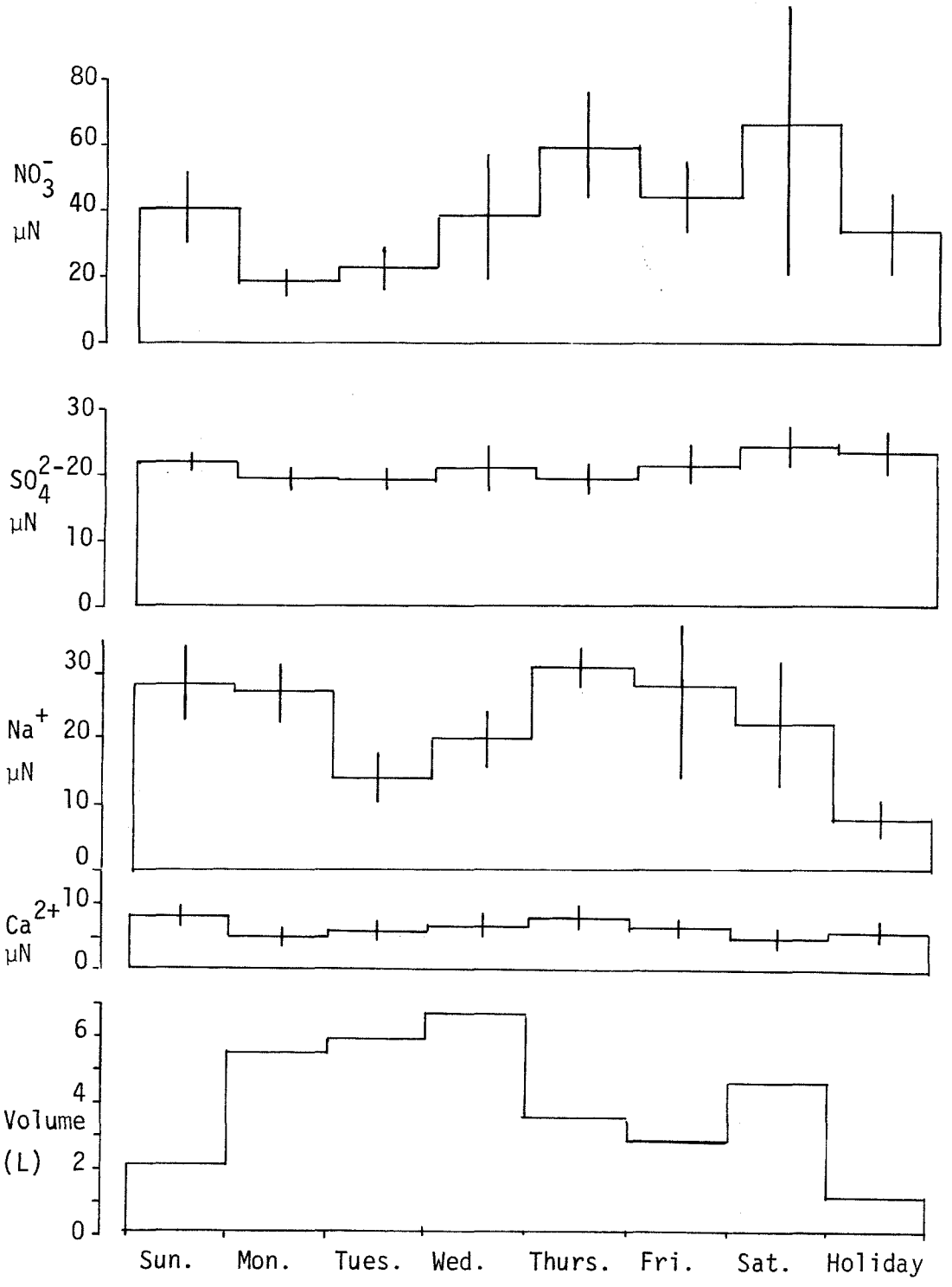

Figure 4.6 Concentration Distribution with Respect to Hour of Day

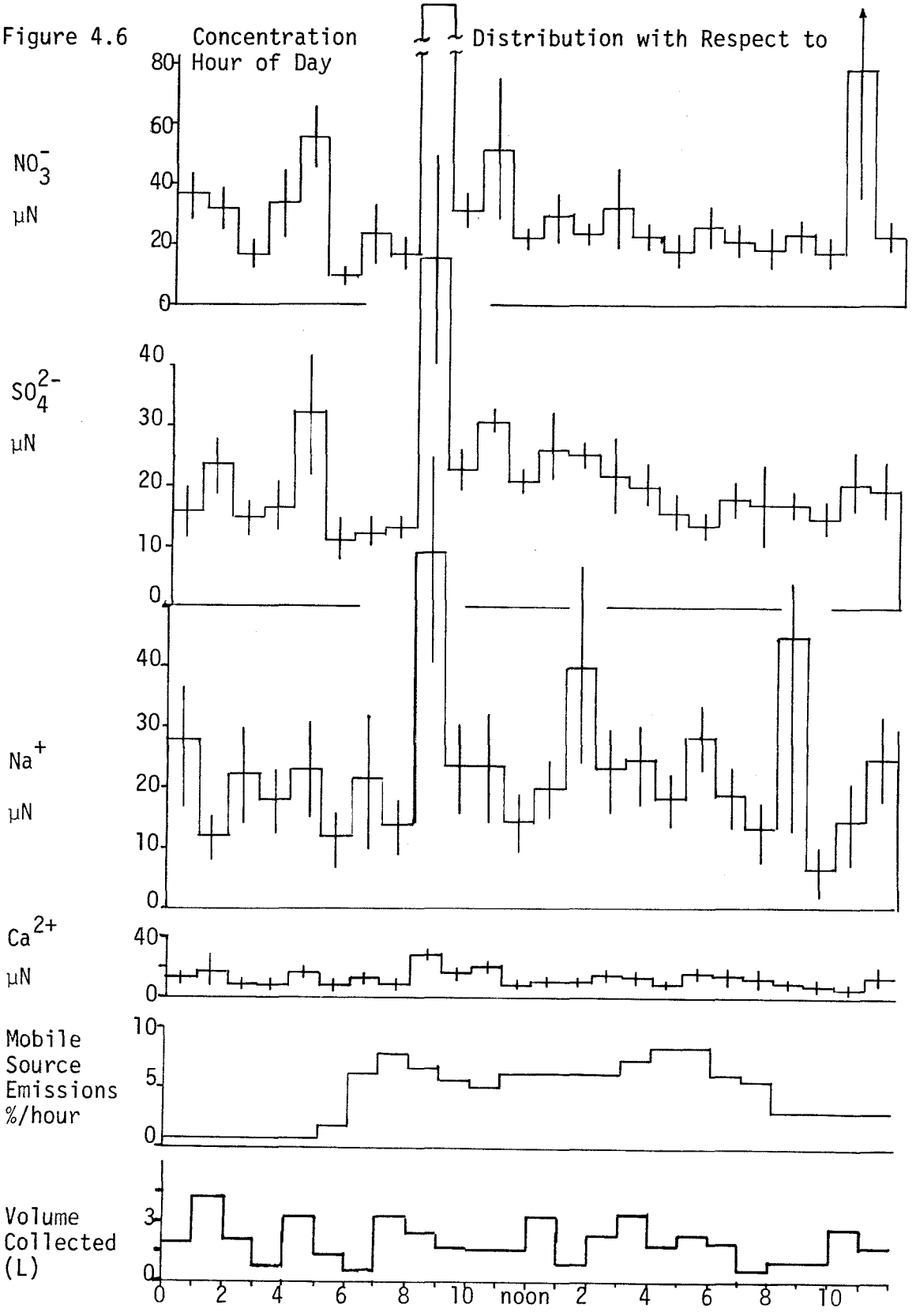

Figure 4.7 Concentration Distribution with Respect to Month of Year

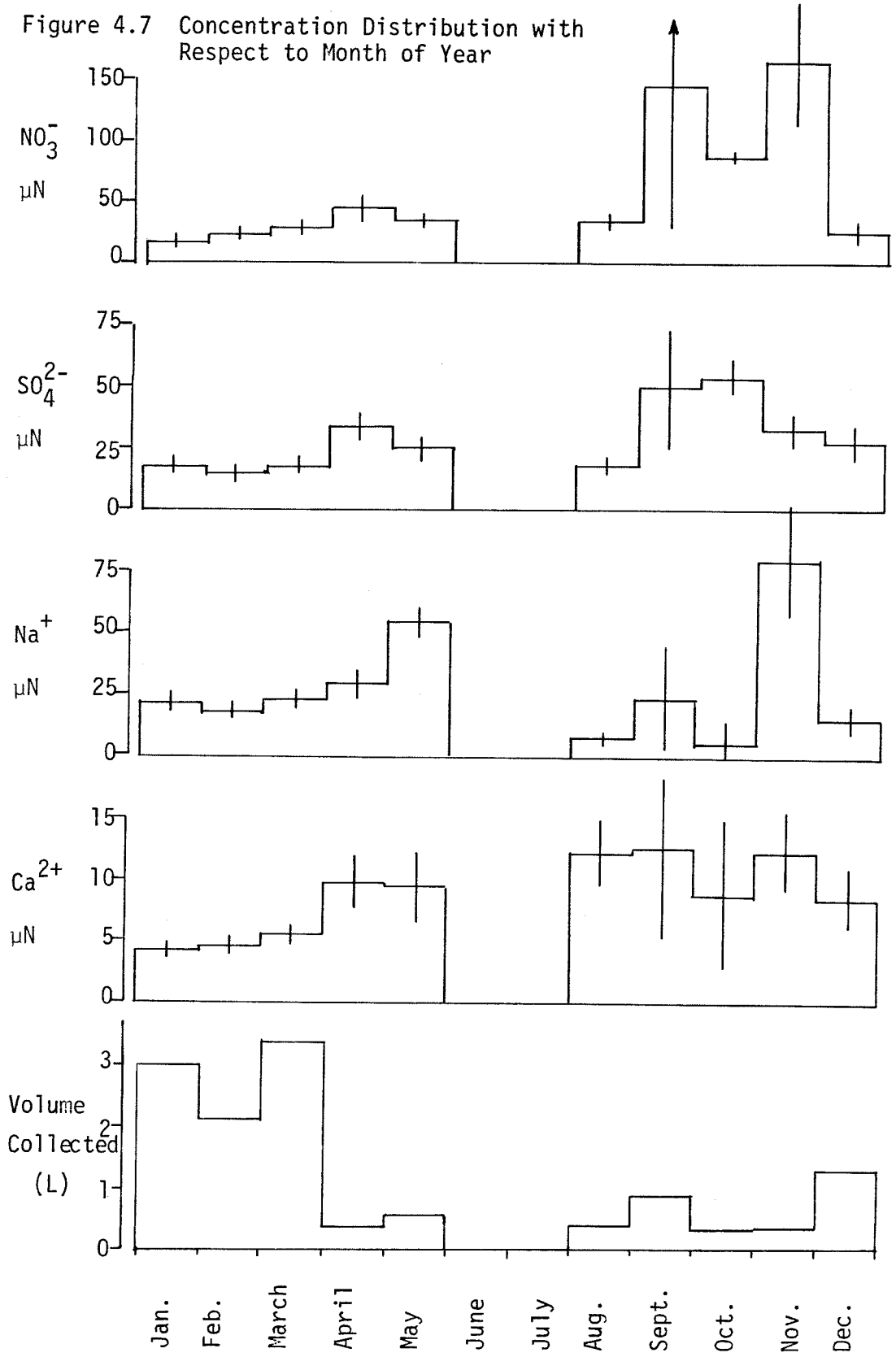

is too small or the precipitation process has a diurnal trend. To correct for the "dilution effect" in precipitation scavenging, the average concentrations of sodium and calcium are given. These chemical species offer control groups to indicate the effects of some of the physical scavenging processes.

The sulfate diurnal variation is only qualitatively similar to the emission pattern. The 8:00 AM spike is due to morning mists/dews, and sodium, calcium, nitrate and sulfate concentrations are all high. The high concentrations represent efficient scavenging by and perhaps evaporation-concentration of the small droplets. The higher daylight hour concentrations could also represent thermal and photochemical catalysis of sulfur oxidation during precipitation scavenging.

4.5 Statistical Models

The previous analyses have been partly based on the use of averages. By averaging over a large number of samples, variations due to many factors will tend to normalize around mean values. Extrapolating average results to individual events is quite tenuous. In biological systems, extreme values may be more important than average ones. Statistical models are useful in describing sample variations due to all the physical, chemical, and biological factors.

4.5.1 Log-Normal Distribution

Because air quality standards are often couched in terms of

frequency of violation or exceeding a standard concentration, air quality frequency distributions have been studied for a variety of pollutants. Larson (1971) concluded that the two parameter log-normal frequency distribution, as often represented by a straight line on log-probability paper, represented the frequency distribution for seven pollutants studies in eight cities during the Continuous Air Monitoring Program (1962-1968). The log-normal distribution fit the data regardless of average time (10 minutes to a year). Bencala and Seinfeld (1976) have shown that other three-parameter distributions, including the three-parameter log-normal, often provide a better fit of the data. The near log-normal air pollutant distributions may be a consequence of wind speed distributions and the correlated mixing depth, although other effects are influential.

Rainwater concentrations can also be shown empirically to be log-normally distributed. Several factors contribute to the frequency distributions including air pollutant frequency distributions, exponential washout of pollutants (discussed in Sections 4.52 and 4.6), choice of averaging time, and evaporation-condensation concentration-dilution processes. Figure 4.8 shows typical ion concentration frequency distributions for 0.25 inch precipitation samples. The linearity is quite good up to the 95% confidence limits.

The predictive capabilities of this simple approach are limited.

Figure 4.8A Log-Normal Distribution of H^+

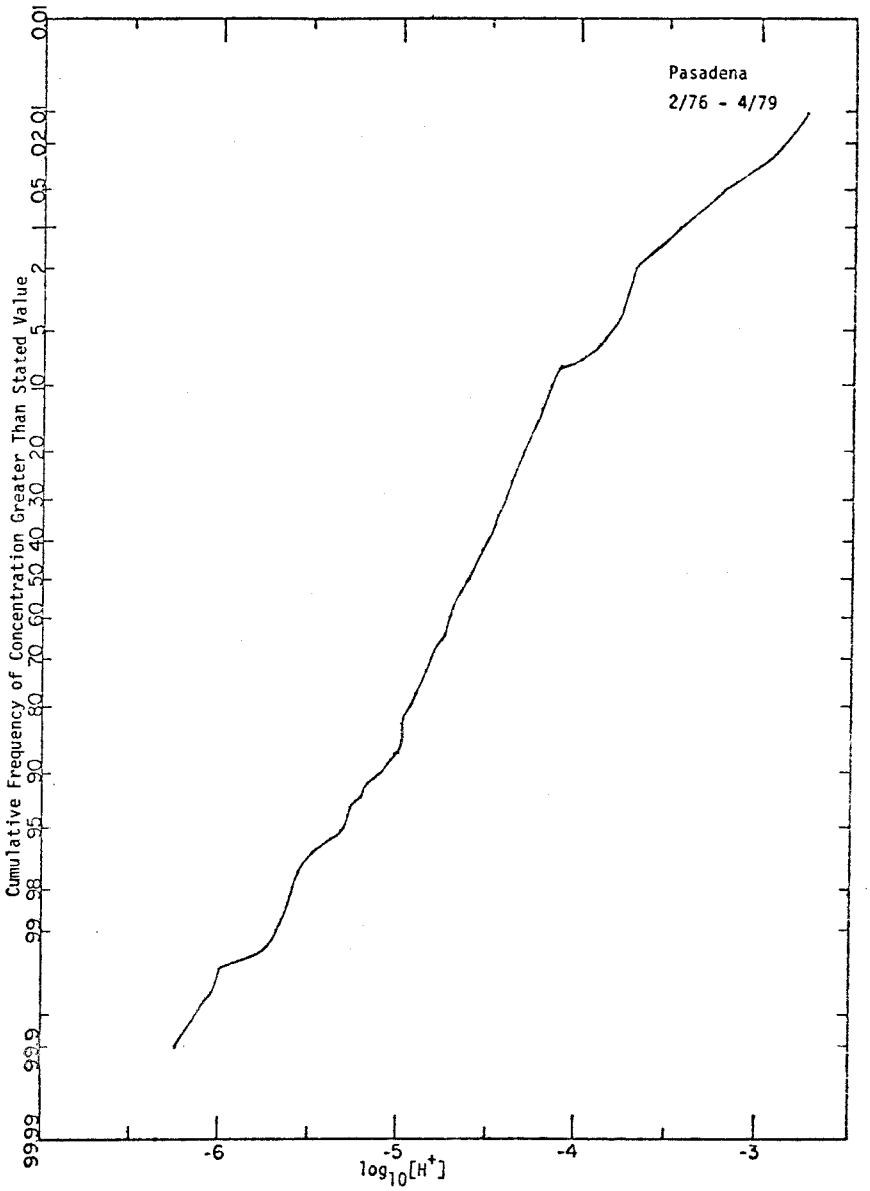

Figure 4.8B Log-Normal Distribution of NO_3^-

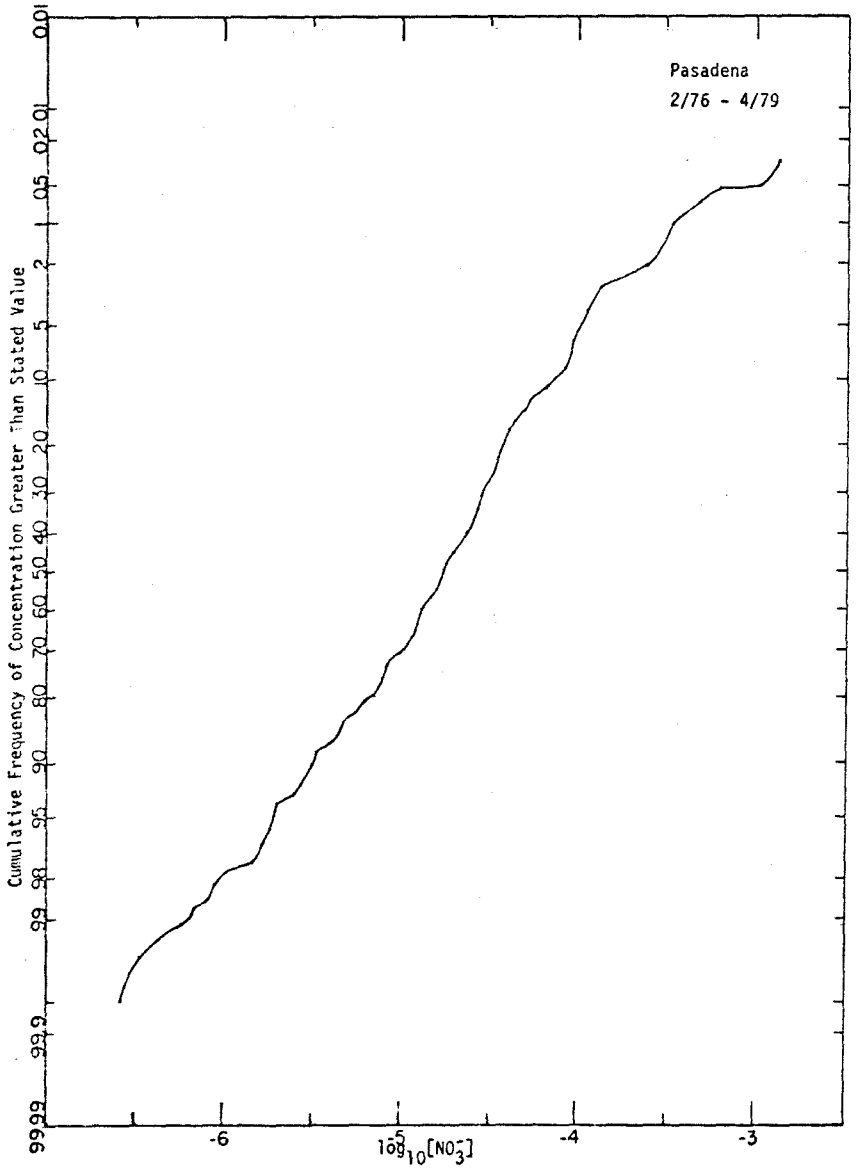

Figure 4.8C Log-Normal Distribution of SO_4^{2-}

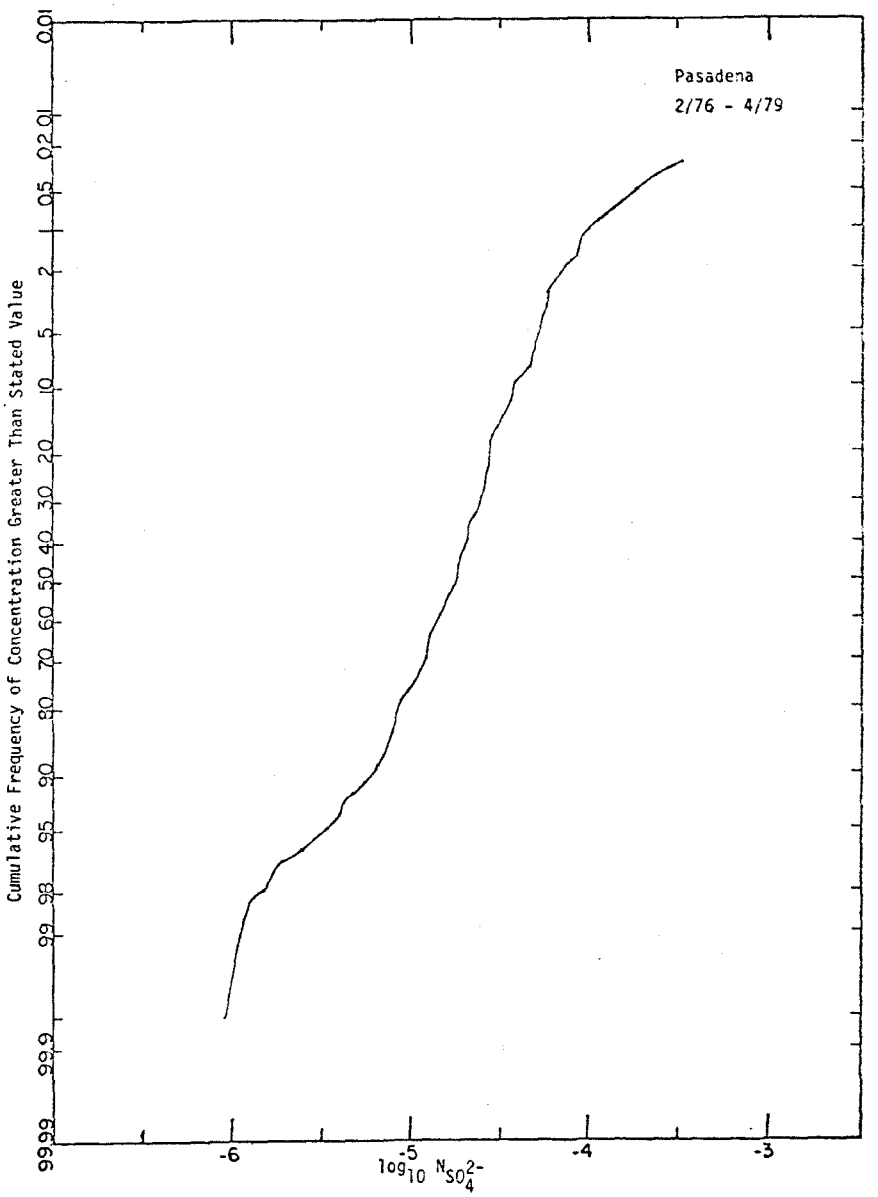

Figure 4.8D Log-Normal Distribution of Na^+

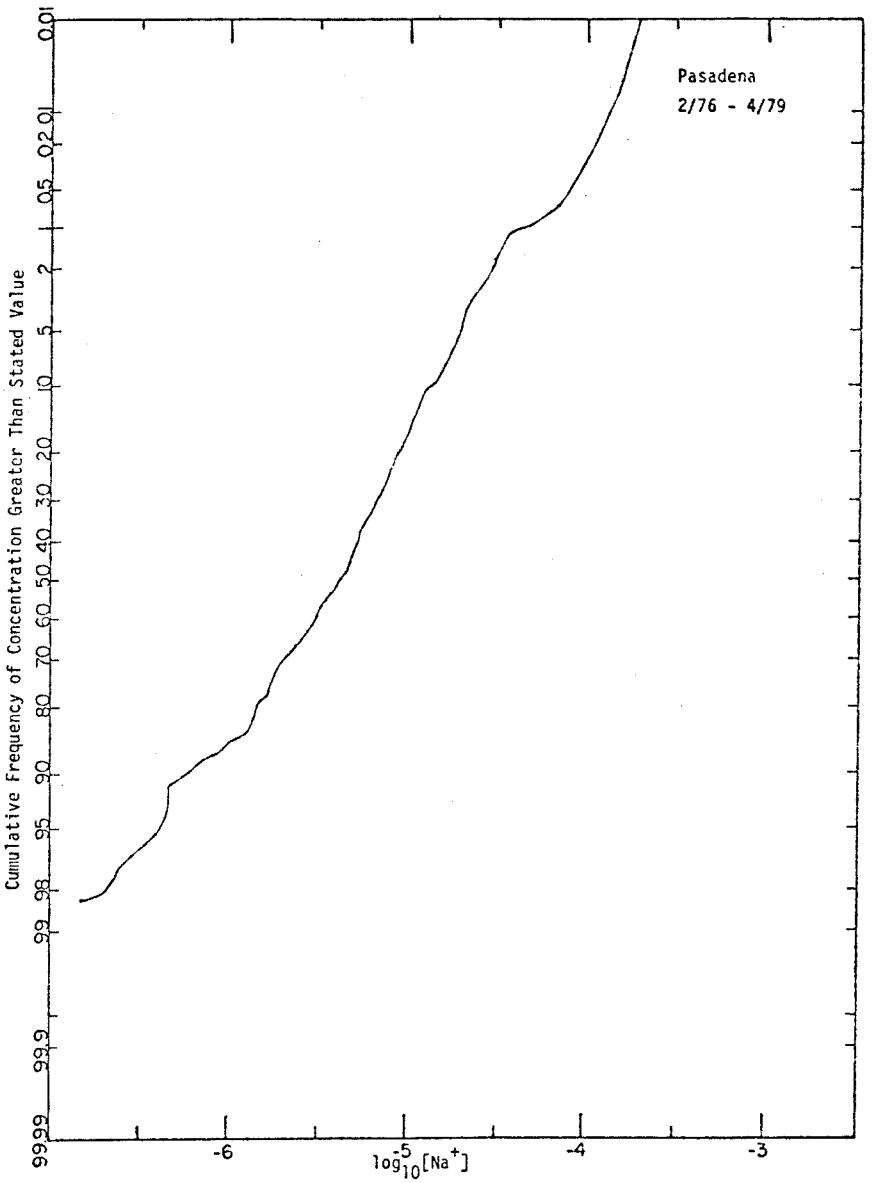

Figure 4.8E Log-Normal Distribution of Ca^{2+}

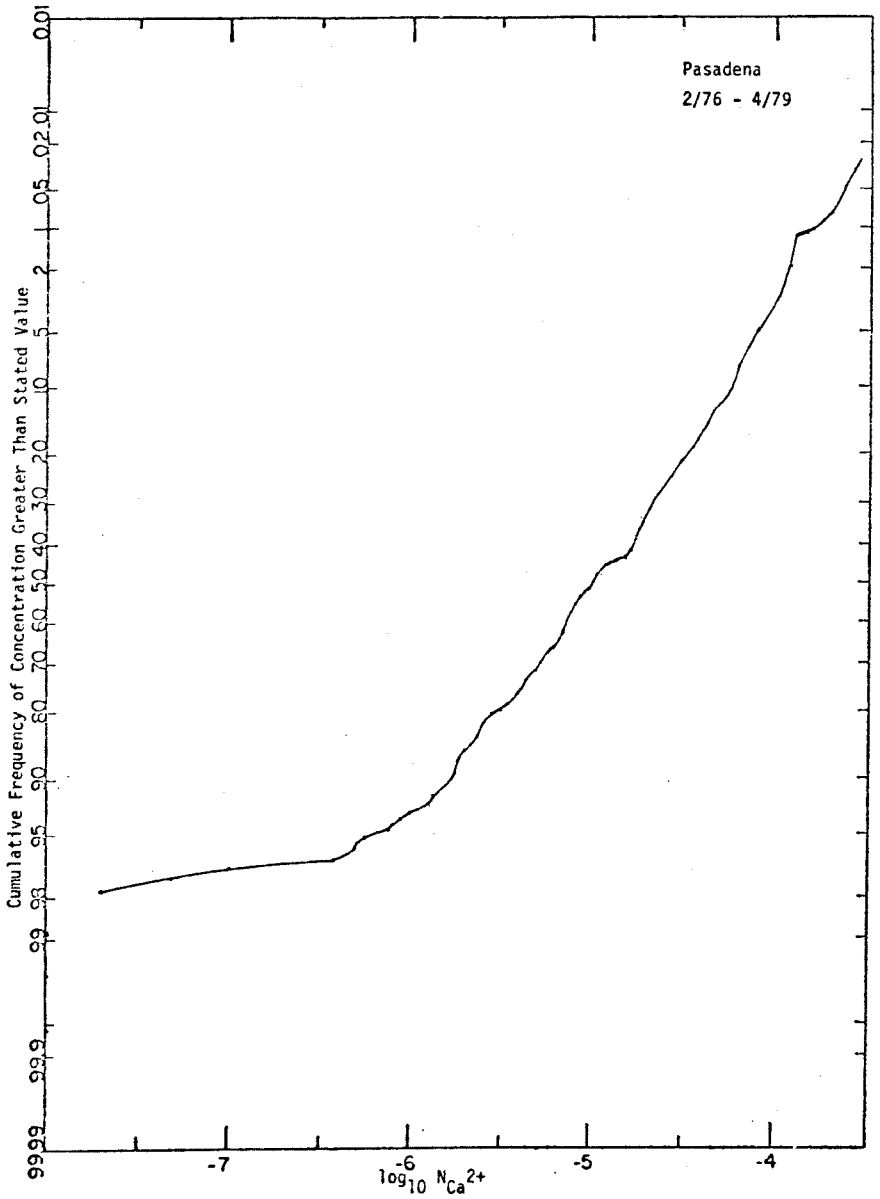

The cumulative frequency plots shown do provide answers to important questions such as how often are plants dosed with a given volume of rain of pH < 4? It does not predict under what conditions or at what time a given acidity will occur. Separate distributions can be determined for each environmental condition, given enough sampling data. Even so, the predictions would be only probabilistic. Physical-chemical models are needed for deterministic predictions.

Certain trends can be determined from monitoring the log-normal probability distribution. As emissions increase, the geometric mean (concentration of 50% cumulative frequency) will increase. Provided the fraction scavenged is constant. u_g will increase linearly with emissions and σ_g, the geometric standard deviation, will be constant (the slope of the log-probability plot will be the same).

4.5.2 Concentration Changes During Storm

Exponential decreases in rainwater concentrations with increasing total precipitation have been noted for the major ionic species. This trend applies to samples taken within a storm (Georgii and Weber, 1960) as well as samples taken for separate storms (Wolaver and Leith, 1972; Erikkson, 1952). An exponential decrease in rainwater concentration is predicted by a simple one-box, linear-scavenging model as has been shown by Halliday and Anderson (1974) for sulfates. If the rainwater concentration of a conservative species, [X], is directly proportional to the ambient air concentration X_{AIR} as

empirically found by washout ratios ([X] = k X_{AIR}, k a constant) then a mass balance of the ambient species is given by Equation 4.1, the semiempirical equation of atmospheric diffusion.

$$\frac{\partial X_{AIR}}{\partial t} + \bar{u} \frac{\partial X_{AIR}}{\partial X} = \frac{\partial}{\partial X}\left(\varepsilon \frac{\partial X_{AIR}}{\partial X}\right) + E \frac{A}{V} - k X_{AIR} \frac{\partial P}{\partial t} \frac{A}{V} \qquad (4.1)$$

See Seinfeld (1975) for an excellent discussion of this Eulerian approach to atmospheric transport and reactions. The mass balance recognizes advection ($\bar{u} \frac{\partial X_{AIR}}{\partial X}$) of species in and out of the control volume where the coordinate system has been chosen with the direction of the wind, eddy diffusion ($\frac{\partial}{\partial X} \varepsilon \frac{\partial X_{AIR}}{\partial X}$), inputs as emissions (E in units mass flux or mass per unit time-ground surface area) times surface area (A) per unit volume (V), and sinks assumed to be the mass per unit volume removed by precipitation scavenging. P is centimeters of precipitation; $\frac{\partial P}{\partial t}$ is the precipitation rate.

For the simplest case of precipitation scavenging much greater than advection, diffusion and emissions, Equation 4.1 reduces to

$$\frac{\partial X_{AIR}}{\partial t} = -k X_{AIR} \frac{\partial P}{\partial t} \left(\frac{A}{V}\right) \qquad (4.2)$$

Integration gives instantaneous concentration in the air (Equation 4.4) and rainwater (Equation 4.5).

$$\log X_{AIR}\Big|_{t=0}^{t=1} = \int \frac{\partial X_{AIR}}{X_{AIR}} = \int -K \frac{A}{V}\, \partial P = -k \frac{A}{V} P\Big|_{P=0}^{P=P} \tag{4.3}$$

or

$$X_{AIR}(t) \doteq X_{AIR}(0)\ 0^{-k\frac{A}{V} P} \tag{4.4}$$

and

$$[X](t) \doteq [X](0)\ e^{-k\frac{A}{V} P} \tag{4.5}$$

The average concentration over a storm is given by

$$\overline{[X]} = \int_0^P [X](0)\ e^{-k\frac{A}{V}P}\ dP \tag{4.6}$$

$$= [X](0)\ \left(\frac{V}{KA}\right)\ e^{-k\frac{A}{V}P}\Big|_0^P \tag{4.7}$$

$$= [X](0)\ \left(-\frac{V}{KA}\right)\left(e^{\frac{-kA_P}{V}} - 1\right) \tag{4.8}$$

$$= [X](0)\ \frac{V}{KA} + [X]\frac{V}{\partial KA}\ e^{-k\frac{AP}{V}} \tag{4.9}$$

As the storm progresses, rainwater concentrations should asymptotically approach those predicted by a steady-state model. For a one box continuously stirred tank reactor model, Equation 4.1 reduces to

$$\frac{\partial X_{AIR_{SS}}}{\partial t} = 0 = \frac{-Q_{AIR_{ENTER}}}{V}\left(X_{AIR_{SS}} - X_{AIR_{ENTER}}\right) + E\frac{A}{V} - k\ X_{AIR_{SS}} \frac{A}{V} \frac{\partial P}{\partial t} \tag{4.10}$$

$$X_{AIR_{SS}} = \frac{Q_{AIR_{ENTER}} X_{AIR_{ENTER}} + EA}{KA\frac{\partial P}{\partial t} + Q_{AIR_{ENTER}}} \qquad (4.11)$$

$$[X]_{SS} = \frac{K(Q_{AIR_{ENTER}} X_{AIR_{ENTER}} + EA)}{KA\frac{\partial P}{\partial t} + Q_{AIR_{ENTER}}} \qquad (4.12)$$

The two models together predict an exponential decrease to an asymptotic value. In practice, variable emission fluxes, mixing volumes, advection and precipitation intensity limit the usefulness of these idealized models. However, the derivations can explain empirical models of concentration changes during storms and changes with total precipitation of storm.

Wolaver and Leith (1973) empirically determined constants to best fit concentration data with equations of the form

$$\overline{[X]} = a \pm b\, e^{\pm c\,(P_{MONTH})} \qquad (4.13)$$

for samples collected by month. P_{MONTH} is the amount of precipitation collected during a month and combined into a monthly sample. A best fit is still qualitative. Predictions are accurate only to a factor of two, at best. This variation could be due to the limitations of the simple models given above as well as to variations in $X_{AIR}(0)$ at the beginning of storms and to averaging over all the storms within a month.

Wolaver and Leith (1972) offer a slightly different interpretation for the cause of the exponential decrease to an asymptotic value Instead of a one box model, in-cloud and below-cloud scavenging processes termed "rainout" and "washout", respectively, are considered separately. High concentrations for the initial precipitation of a storm are primarily attributed to washout of the more polluted air below the cloud. As the storm continues, washout becomes less important as the air below the cloud is cleaned. The asymptotic value is the concentration in the cloud water determined by rainout processes for samples within a storm and by averaging rainout and washout processes for samples by storm or month.

The one box models above (Equations 4.5 and 4.12) are directly applicable to the below cloud washout processes. Washout processes alone would predict the observed behavior. In-cloud processes alone can also give the exponential decrease to low levels. This trend in concentrations is found at the Mt. Wilson site, a sampler in the clouds. Ground level rainwater concentration and total precipitation data by themselves cannot distinguish in-cloud and below-cloud processes.

Since precipitation samples in this study were collected by increment within a storm, the average concentration for an increment at the beginning of the storm is given by

$$[X]_i = [X](0)\left(-\frac{V}{KA}\right)\left(e^{-k\frac{A}{V}P_{i+1}} - e^{-k\frac{A}{V}P_i}\right) \qquad (4.14)$$

P_i is the cumulative precipitation of a storm at the beginning of the collection of the ith sample and P_{i+1} is the cumulative precipitation during the storm at the end of the ith sample. $\overline{[X]}_i$ is the concentration of species X in the ith sample.

Figure 4.9 shows precipitation concentration changes during storms for Pasadena samples. Concentrations are normalized with respect to the initial concentration to reflect initial ambient atmospheric concentration. The extent of precipitation is also corrected for time since prior precipitation during the same storm to allow for the rise in ambient concentrations due to emissions during unsteady rainfall. The results are still qualitative. Concentrations can fluctuate unpredictably during a storm, as has been noted by many investigators (Harrison et al, 1977; Seymour et al, 1978).

4.5.3 Multiple Regression-Correlation Models

The previous model for concentration changes during a storm assumes a linear relationship between air and rainwater concentrations for a species. This approximation is most applicable for species not involved in gas-liquid reactions involving pH and/or oxidation processes. Linear correlations between species should confirm relationships, if they exist.

A number of linear and nonlinear correlations as well as multiple regression techniques have been used to model rainwater concentrations. To a first approximation, all rainwater concen-

Figure 4.9A Concentration Variation within Storms

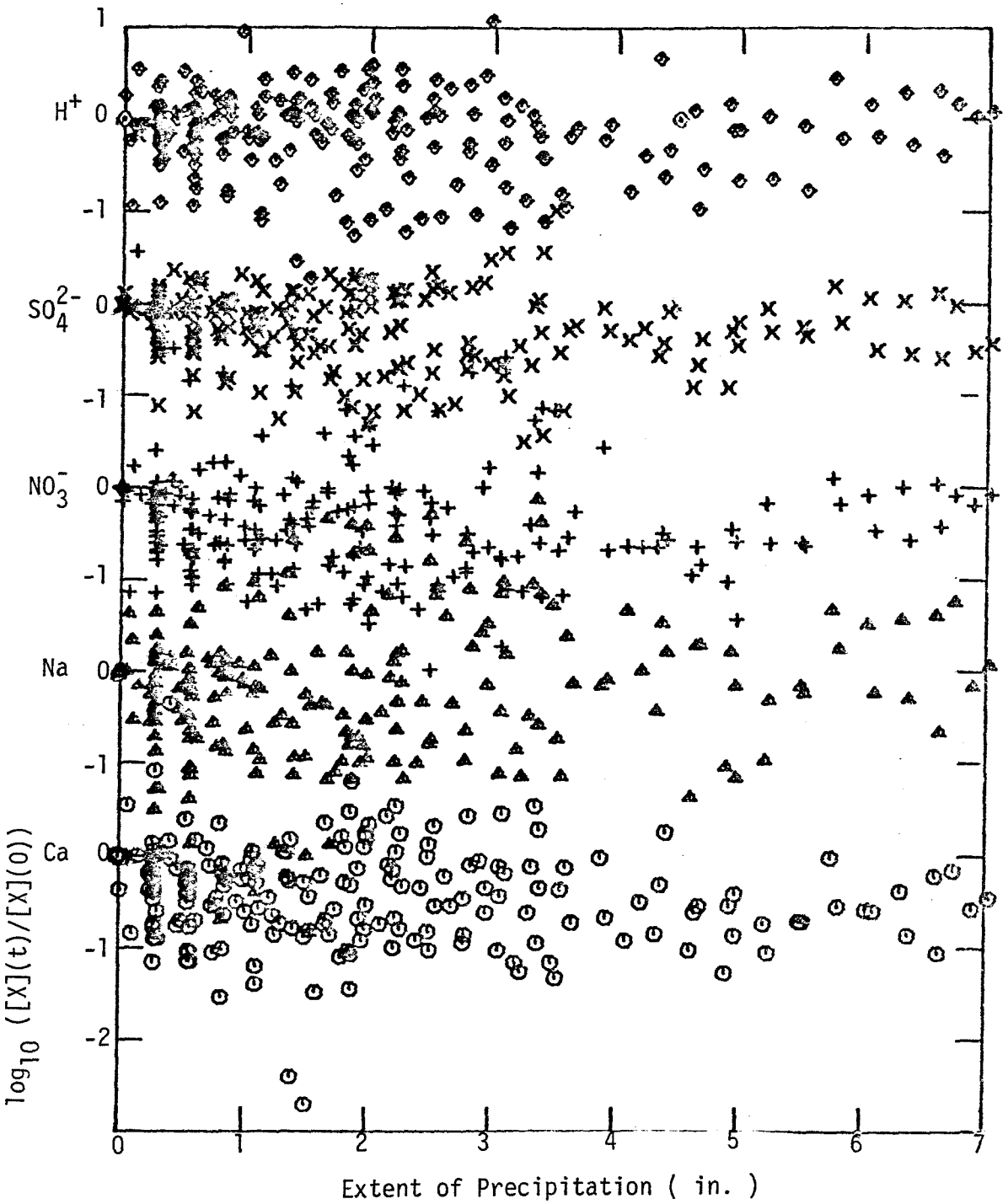

Figure 4.9B Concentration Variation within a Storm (2/28/78-3/1/78)

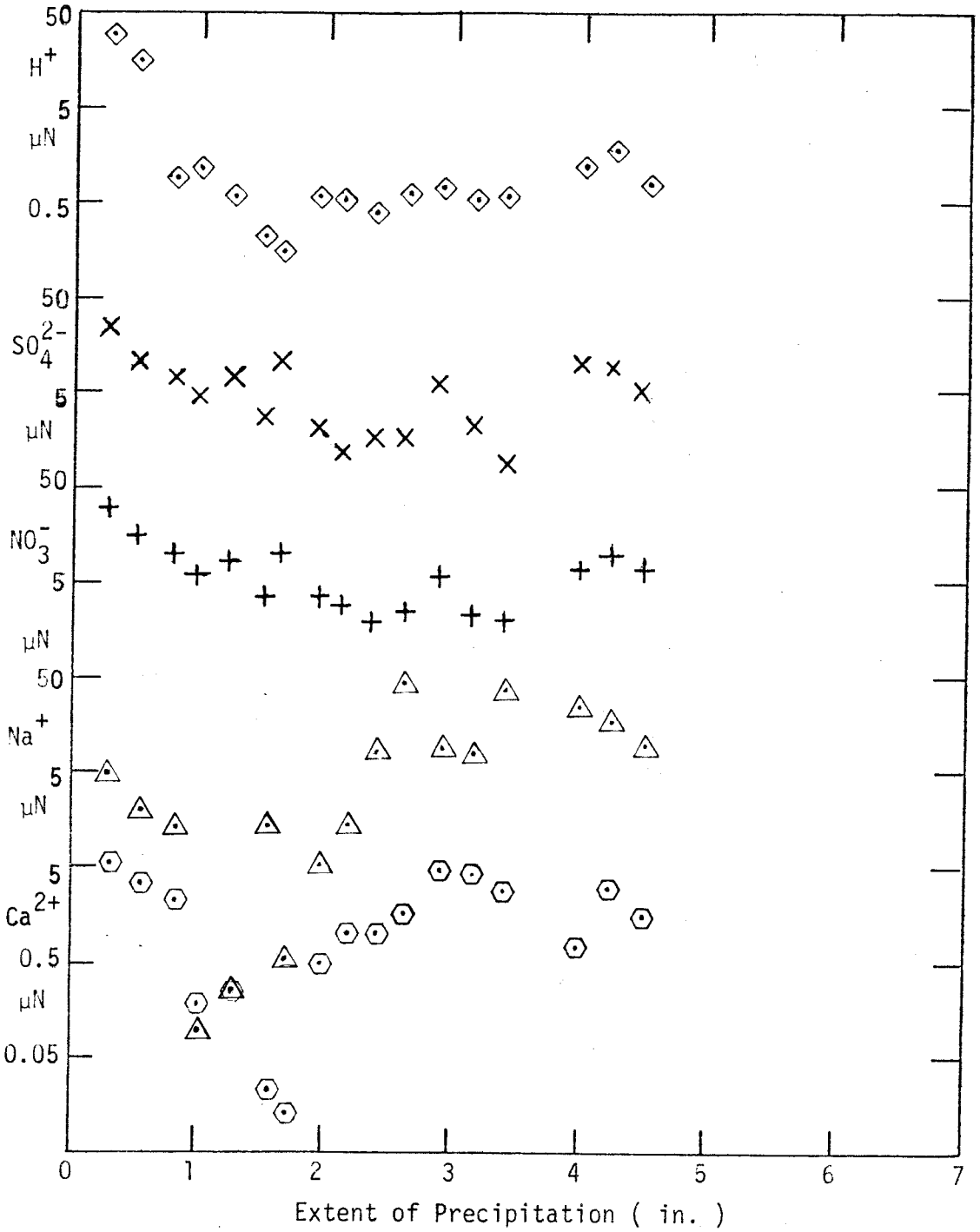

trations tend to be correlated with one another and components tend to be negatively correlated with rainfall rate (Dawson, 1978; Beilke and Georgii, 1968; Kennedy et al, 1979). This dilution effect would be expected from the previous model (Section 4.5.2). Another relationship often found between H^+ and the other major ions is that predicted from the charge balance. The difference in anion and metal ion plus ammonium equivalent concentrations should approximately equal $[H^+]$ for acid precipitation. Significant correlations have been found even when sodium and chloride concentrations (often approximately equal as in seawater) and ions of relatively low concentration (potassium, magnesium and sometimes ammonium) are excluded (Pearson and Fisher, 1971; Fisher, 1968). Correlations between ions from the same source are often found as would be expected from the source strength model (Sections 2.5 and 4.41). Lodge et al (1968) used factor analysis to distinguish soil dust, sea salt and ammonia sources. In northern California, Kennedy et al (1979) found excellent agreement between precipitation ion ratios and those predicted from seawater concentrations. In the Puget Sound area, Knudsen et al (1977) used an elegant method of factor analysis to identify urban and industrial (smelter) plumes above the background chemical composition, which was primarily due to sea salt.

Air and water quality correlations are often found. A linear relationship between emissions and wet fluxes was found for lead

by Lazrus et al (1970) by comparing gasoline consumption with wet lead flux. Vermeulen (1978) found linear correlations of acidity ($[H^+]$) with sulfur dioxide and nitrogen oxides emission for several sites in The Netherlands. At one site, $[H^+]$ and NO_x emissions were inexplicably inversely correlated. There are exceptions to all the generalizations given above.

Multiple stepwise linear regression (Ralston and Wilf, 1960) was performed on air and water quality data for Pasadena. Sulfate as well as nitrate plus nitrite were treated as dependent variables (y) to find the least squares best fit with an equation of the form

$$y = b_o + b_1 X_1 + ... + b_{n-1} X_{n-1} \qquad (4.15)$$

The independent variables were: ground level ambient air concentrations of nonmethane hydrocarbon, ozone, carbon monoxide, sulfur dioxide, nitric oxide, and nitrogen dioxide during the collection of rainwater samples; temperature, relative humidity, and particulate matter. Additional independent variables were precipitation intensity, $[H^+]$, $P_{NO_2}/[H^+]$, and $P_{NO}P_{NO_2}/[H^+]$. The last two variables were chosen as indicators of nitrogen oxide gas-liquid phase equilibrium as discussed in Section 4.6.1.3. Finally, rainwater sulfate was an independent variable for rainwater nitrite and nitrate and vice versa.

The multiple regression examines the variance of the deviations between measured and predicted values of the dependent variable $(y - b_o + \sum_i^n b_i X_i)$. In stepwise regression, the number of independent variables used to predict y is increased from zero in steps of one. The independent variable that causes the largest reduction in the variance is introduced to give the best predictions of y for n independent variables at the nth step. An independent variable "explains" the dependent variable if there is a large reduction in the variance when that independent variable is included in the multiple regression.

For samples collected from January 1978 to April 1979 which were predominantly in winter rains, rainwater nitrate and nitrate were dependent on four variables with variance-ratios significant at the 95% confidence level. The variance-ratio is a test to determine if the variance in the dependent variable explained by the independent variable is greater than that caused by a random variable. Thus, rainwater nitrite and nitrate was more than just randomly dependent on precipitation intensity, ozone, nitric oxide and nitrogen dioxide divided by hydrogen ion concentration.

While multiple regression analysis does not determine the mechanism, these independent variables <u>may</u> represent the following physical-chemical steps in scavenging. Precipitation intensity reflects the "dilution effect" discussed above. Ozone may reflect either the ratio of NO_2 to NO or ambient concentrations of nitric

and nitrous acids in the gas and/or aerosol phase. Higher NO_2/NO would give higher equilibrium rainwater concentrations of nitrite and nitrate, as would higher ambient nitric and nitrous acids, likewise NO and NO_2/H^+ may reflect gas scavenging.

For samples collected from February 1976 to April 1979 (all of the Pasadena samples) which included fall, winter, spring and summer samples, additional variables significantly explained variation in nitrite and nitrate concentration. Temperature and relative humidity were the next most significant variables in the stepwise regression. These variables could reflect evaporation-concentration effects. Alternatively, temperature correlation could reflect effects on chemical kinetics and equilibrium. Sulfur dioxide, carbon monoxide and $[H^+]$were also significant at the 99% confidence level.

Twenty-four hour high volume (HiVol) samples of aerosol are taken every six days in Pasadena by the South Coast Air Quality Management District. While the previous multiple regressions examined 198 and 263 samples, respectively, only 19 samples are available for rainwater-aerosol comparison. As chance would have it, aerosol was collected during only nineteen rainy days over the thirty-seven months during which precipitation was sampled.

Twenty-four hour HiVol lead, sulfate, nitrate and total suspended particulates were also considered as independent variables that may influence rainwater concentrations. Precipitation samples

were collected over periods of one to two hours during the twenty-four hours the HiVol aerosol samples were collected. Because of the different averaging periods, aerosol and rainwater quality would not be expected to be well correlated. Surprisingly, aerosol lead concentration has the highest variance ratio for both rainwater nitrite plus nitrate and sulfate concentrations. Other variables which had significant variance ratios (>99% confidence level) for rainwater nitrite and nitrate in this nineteen sample subset were ozone, one hour averages of particulate matter, temperature, and sulfur dioxide. Rainwater sulfate concentration (perhaps representing the dilution effect), $NO_2/[H^+]$, $\sqrt{NO \cdot NO_2}/[H^+]$, and relative humidity had variance ratios significant at >95% confidence level. Rainwater sulfate in the 19 samples was described by Equation 4.15 with the same independent variables of significant variance-ratio for rainwater nitrite plus nitrate with two exceptions: rainwater nitrate instead of sulfate represented the dilution effect; the variance ratio for $\sqrt{NO \cdot NO_2}/[H^+]$ was not significant at the 95% confidence level.

The similarities between variables influencing rainwater sulfate and nitrite plus nitrate concentrations may be due to similar sources, transport or scavenging processes. Rainwater sulfate for the predominantly winter samples (January 1978 to April 1979) were significantly dependent on three variables: nitric oxide, ozone and precipitation intensity. Rainwater sulfate for all Pasadena samples was also significantly dependent (>95%) on temperature, $[H^+]$,

Table 4.2 Multiple Linear Regression Coefficients for NO_2^- + NO_3^- and SO_4^{2-} in Pasadena Rainwater

2 / 76 - 4 / 79 n=268

$[NO_2^-] + [NO_3^-]$		$[SO_4^{2-}]$	
Independent Variable	Coefficient	Independent Variable	Coefficient
Temp.	0.242±0.053	NO	0.250±0.059
NO_2	0.036±0.058	O_3	0.208±0.049
NO	0.249±0.057	Rain Inten.	-0.095±0.055
Rel. Humid.	-0.199±0.039	H^+	0.185±0.049
NO_2/H^+	0.192±0.042	Temp.	0.202±0.053
CO	0.216±0.056	SO_2	0.182±0.059
H^+	0.149±0.047	Rel. Humid.	-0.094±0.041
SO_2	0.232±0.063		
O_3	0.157±0.047		
SO_4 (rain)	0.018±0.007		

1 / 78 - 4 / 79 n=198

$[NO_2^-] + [NO_3^-]$		$[SO_4^{2-}]$	
Independent Variable	Coefficient	Independent Variable	Coefficient
Rain Inten.	-0.207±0.075	NO	0.247±0.077
O_3	0.320±0.075	O_3	0.286±0.075
NO	0.242±0.077	Rain Inten.	-0.172±0.077
NO_2/H^+	0.151±0.059		

1 / 78 - 4 / 79 n=19

$[NO_2^-] + [NO_3^-]$		$[SO_4^{2-}]$	
Independent Variable	Coefficient	Independent Variable	Coefficient
HiVol Pb	1.061±0.034	HiVol Pb	0.221±0.095
SO_4 (rain)	0.728±0.085	NO_3 (rain)	0.728±0.085
Part. Matter	0.182±0.027	Part. Matter	0.182±0.027
O_3	0.062±0.013	O_3	0.062±0.012
NO_2/H^+	0.221±0.095	NO_2/H^+	0.221±0.095
Temp.	0.309±0.094	Temp.	0.309±0.094
Rel. Humid.	-0.025±0.011	Rel. Humid.	-0.025±0.011

Units					
$[NO_2^-] + [NO_3^-]$	µM	CO	ppm	Rain Intensity	inch/hour
$[SO_4^{2-}]$	µM	O_3	pphm	Relative Humidity	per cent
NO_2	pphm	SO_2	pphm	Temperature	°F
NO	pphm	H^+	µM	24 Hour HiVol Pb	$\mu g/m^3$

relative humidity, and sulfur dioxide.

The predictive capability of results of the multiple linear regression (Equation 4.15) is still qualitative. The best fit often calculates rainwater concentrations which are high or low by a factor of two from the actual concentrations. This error could be due to the exclusion of important independent variables as well as to the limitations of using ground level measurements to describe air quality.

4.6 Physical-Chemical Scavenging Models

The previous statistical models considered the combined effects of all physical-chemical interactions. If all of the atmospheric transport and scavenging processes as well as emissions were well characterized, precipitation concentrations could be predicted from first principles (mechanistic approach). There are still uncertainties in the physical scavenging mechanisms. Slinn (1977) made an excellent review of precipitation scavenging of aerosols and proposed a semi-empirical model for scavenging efficiency accurate within about a factor of two to three. Hales (1972) outlines the relative importance of chemical kinetics and transport in gas scavenging. This section will apply these models to the limited data available.

4.6.1 Equilibrium Models

4.6.1.1 Ammonia-Ammonium

The dissolution of ammonia gas to form amommium in acid rain-

drops is kinetically fast enough to be close to equilibrium. Unfortunately, an equilibrium model cannot be used to predict rainwater ammonium concentrations since the partial pressure of ammonia is poorly characterized. Measurements on smoggy days have shown 0-20 ppb at Riverside (Tauzon et al, 1978) and 0-15 ppb at Los Angeles (ACHEX, 1974). These results are not applicable to winter rain conditions because of higher relative humidity which affects gas-aerosol equilibrium, lower temperature (and lower emissions from biological sources), and larger mixing volume in the atmosphere.

P_{NH_3} during precipitation can be calculated from pH and ammonium concentrations in the rain, assuming the following equilibrium relationships:

$$K_{H_{NH_3}} = \frac{[NH_4OH]\gamma_{NH_4OH}}{P_{NH_3}} \tag{4.16}$$

$$K_{1_{NH^+}} = \frac{\gamma_{NH_4OH}[NH_4OH][H^+]\gamma_{H^+}}{[NH_4^+]\,\gamma_{NH_4^+}} \tag{4.17}$$

$$P_{NH_3(ATM)} = K_{1_{NH_4^+}} \frac{[NH_4^+]}{[H^+]} \frac{\gamma_{NH_4^+}}{\gamma_{H^+}} \frac{\gamma_{NH_4OH}}{K_{H_{NH_3}}} \tag{4.18}$$

Ground level temperature and relative humidity are used to estimate rainwater temperature, and corrections for barometric pressure are included in the results which are reported as parts per billion

(ppb = $P_{NH_3(ATM)}$ x 10^9/total pressure (ATM)).

Figure 4.10 summarizes the calculated P_{NH_3} results. Average P_{NH_3} (ppb) during precipitation is given for each site. In addition, first samples from each storm are examined to determine P_{NH_3} near the onset of precipitation. The highest ammonia gas concentrations are at Riverside and Azusa, reflecting agricultural and feedlot sources. The low concentrations at the eastern mountain sites may be an artifact of the calculation since snow rather than rain was the predominant form of precipitation at these sites. A comparison of the average P_{NH_3} calculated from initial samples of each storm with P_{NH_3} calculated from all samples shows the initial P_{NH_3} can be an order of magnitude greater than the average P_{NH_3} during a storm. Even the first samples of each storm may be enough precipitation (0.25 in) to remove a significant fraction of the ambient ammonia from the atmosphere. In addition, high relative humidity during the storm will cause ammonia to become ammonium in the aerosol phases (and cloud droplets) which decreases the gaseous ammonia concentration. Thus, the calculated partial pressures are representative only during precipitation events.

The same approach has been used by Lau and Charlson (1977) and Dawson (1978). Lau and Charlson (1977) estimated P_{NH_3} as <0.1 ppb for California based on monthly samples. Dawson (1978) found an average P_{NH_3} of 13 pptv (.013 ppb) in summer convective storms in Tuscon, Arizona. Both of these results are in agreement with the .001 to .0067 ppb calculated from rainwater samples in this study.

Figure 4.10A Partial Pressure of Ammonia During Precipitation
Azusa

Mean P_{NH_3} during precipitation for all samples -
0.0037 ppb

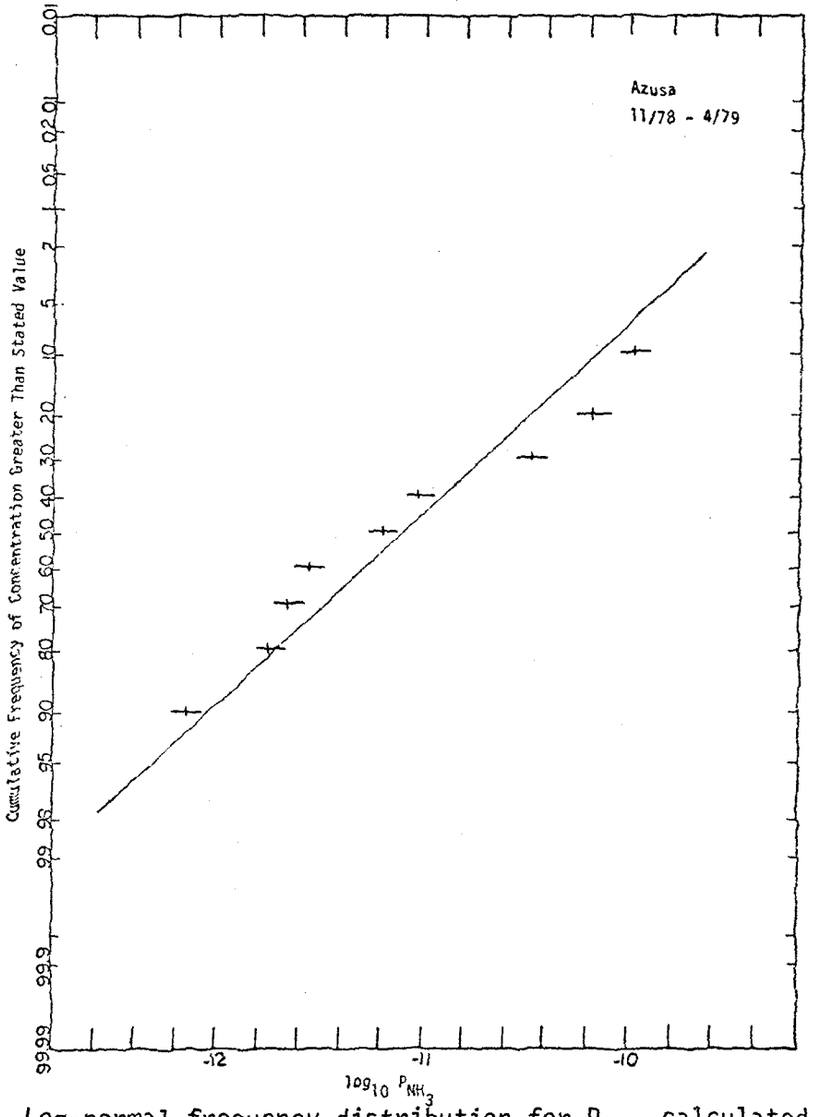

Log-normal frequency distribution for P_{NH_3} calculated from first samples of each storm

Figure 4.10B Partial Pressure of Ammonia During Precipitation
Los Angeles

Mean P_{NH_3} during precipitation for all samples -
0.0025 ppb

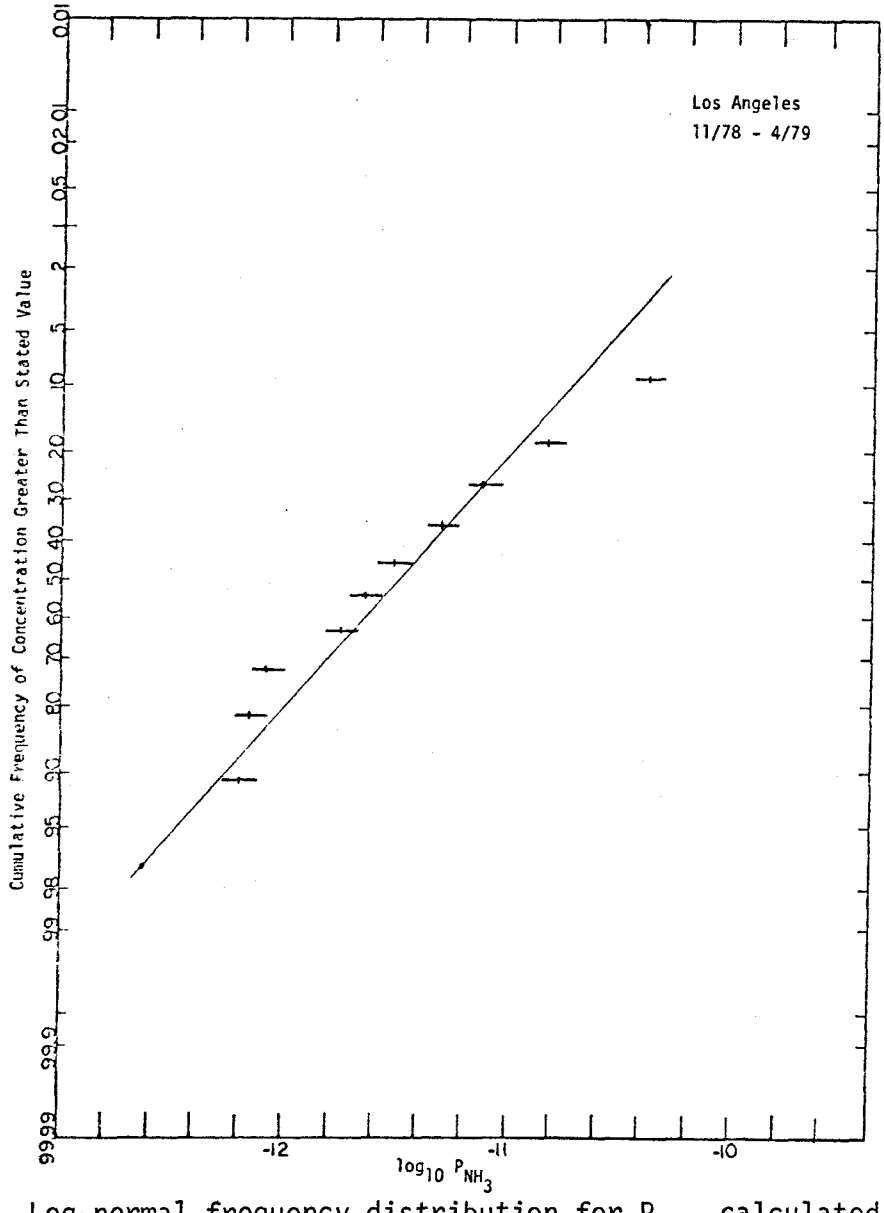

Log-normal frequency distribution for P_{NH_3} calculated from first samples of each storm

Figure 4.10C Partial Pressure of Ammonia During Precipitation
Mt. Wilson

Mean P_{NH_3} during precipitation for all samples -
0.0016 ppb

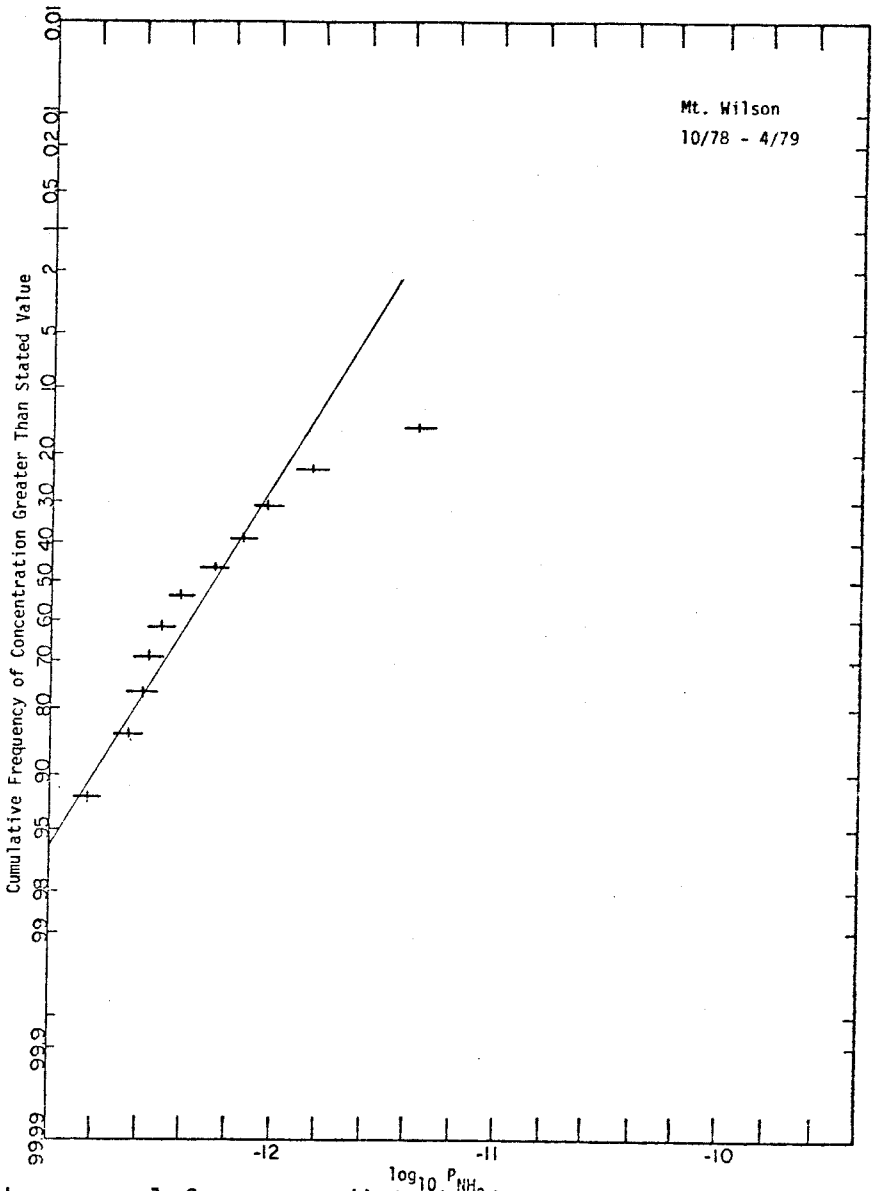

Log-normal frequency distribution for P_{NH_3} calculated from first samples of each storm

Figure 4.10D Partial Pressure of Ammonia During Precipitation
Pasadena

Mean P_{NH_3} during precipitation for all samples -
0.0012 ppb

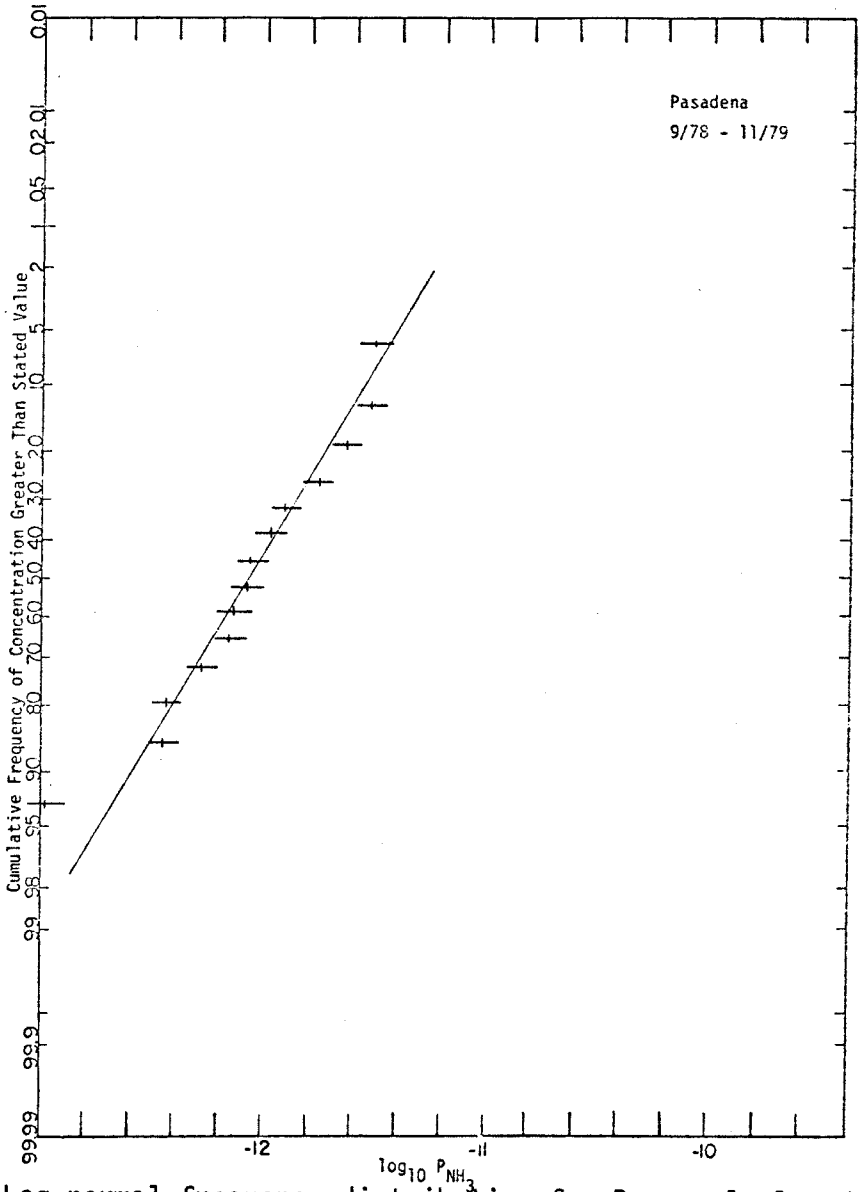

Log-normal frequency distribution for P_{NH_3} calculated from first samples of each storm

Figure 4.10E Partial Pressure of Ammonia During Precipitation
Riverside

Mean P_{NH_3} during precipitation for all samples -
0.007 ppb

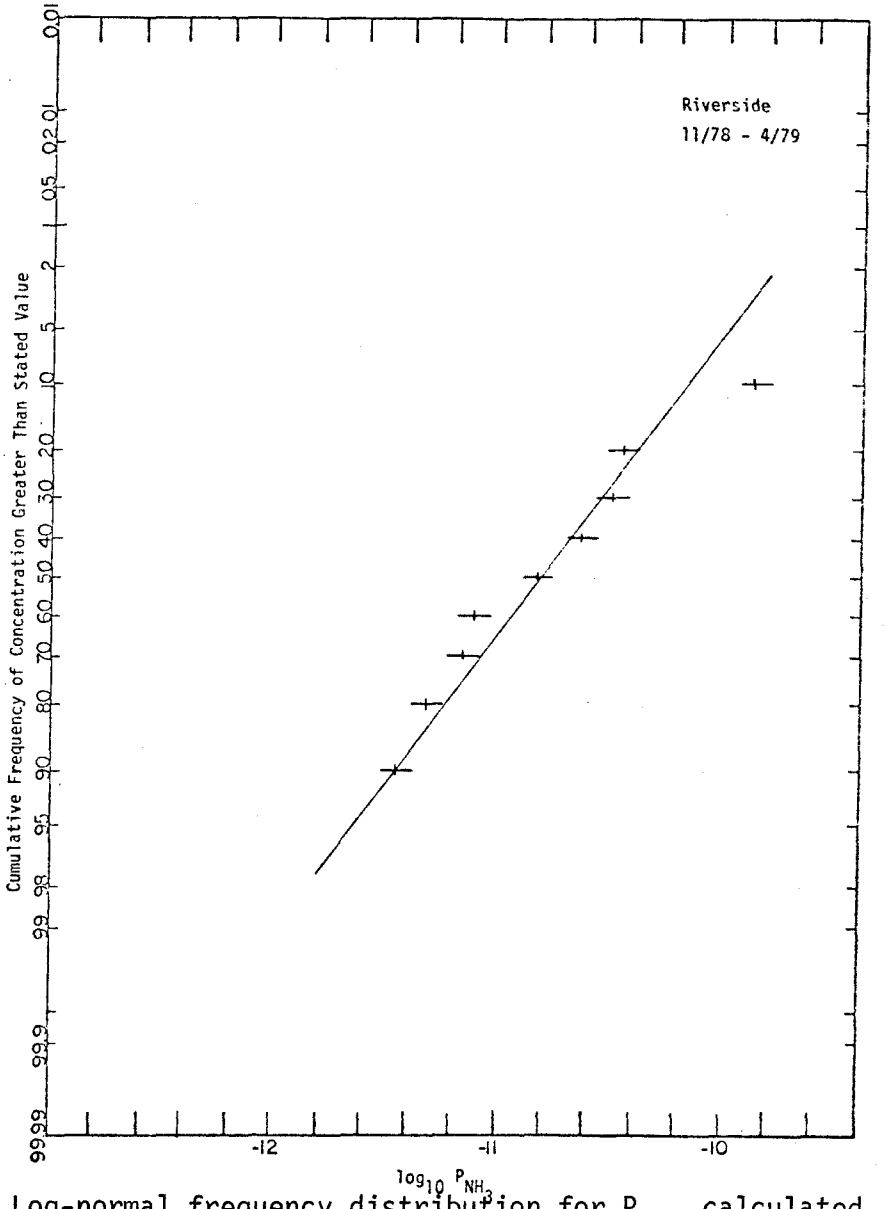

Log-normal frequency distribution for P_{NH_3} calculated from first samples of each storm

Figure 4.10F Partial Pressure of Ammonia During Precipitation
Westwood

Mean P_{NH_3} during precipitation for all samples -
0.0016 ppb

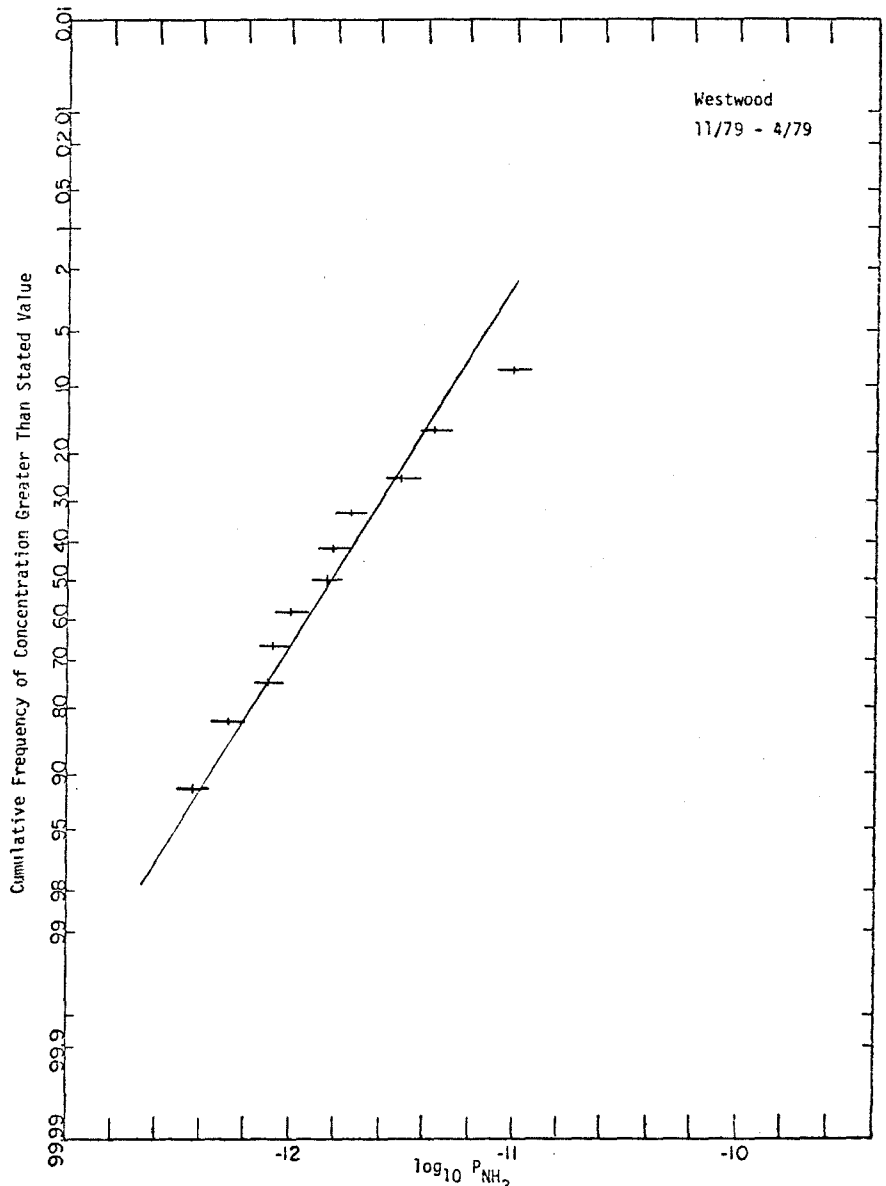

Log-normal frequency distribution for P_{NH_3} calculated from first samples of each storm

4.6.1.2 NO_X - Nitrite - Nitrate

As emphasized in Table 2.1, there are several atmospheric nitrogen oxide species that can lead to the overall production of nitrous and nitric acids in rainwater. The species monitored by the South Coast Air Quality Management District are NO_2, NO or total NO_X, and aerosol nitrates (24 hour HiVol samples every 6 days). Kinetic steady state and equilibrium models can often be used to calculate ambient concentrations of other NO_X species.

One approach to avoid estimating unmeasured concentrations of atmospheric species is to assume equilibrium. Rainwater composition can be calculated directly from measured nitric oxide and nitrogen dioxide concentrations. Precipitation concentrations of nitrite and nitrate are fixed by pH, P_{NO}, and P_{NO_2} assuming equilibrium, regardless of the intermediate species concentrations in attaining equilibrium.

Equilibrium nitrite concentrations are determined by

$$NO_{(g)} + NO_{2_{(g)}} + H_2O_{(\ell)} \rightleftarrows 2\ HNO_{2(aq)} \tag{4.19}$$

$$K_{H_{NO,NO_2}} = 122 = \frac{[HNO_2]^2\ \gamma^2_{HNO_2}}{P_{NO}\ P_{NO_2}} \tag{4.20}$$

$$HNO_{2(aq)} \rightleftarrows H^+ + NO_2^- \tag{4.21}$$

$$K_{1_{HNO_2}}\ (25^oC) = 6\times10^{-4} = \frac{[H^+][NO_2^-]}{[HNO_2]}\ \frac{\gamma_{H^+}\ \gamma_{NO_2^-}}{\gamma_{HNO_2}} \qquad (4.22)$$

These reactions are kinetically fast in the overall equilibrium (Yost and Russell, 1944) nitric oxide and nitrogen dioxide concentrations are typically <10 ppb (10^{-8} ATM) before and during storms in southern California. For pH<5, total nitrite ($[NO_2^-] + [HNO_2]$) is less than 7 μM. The precipitation weighted mean total nitrite for Pasadena calculated from measured P_{NO}, P_{NO_2} and pH is 0.5 μM. This agrees well with the average total nitrite measured by ion chromotography of 0.4±0.3 μM.

The equilibrium nitrate concentration can be calculated from Equation (4.24)

$$3\ HNO_{2(aq)} \rightleftarrows H^+ + NO_3^- + 2NO_{(g)} + H_2O_{(\ell)} \qquad (4.23)$$

$$29 = K\ (25^oC) = \frac{\gamma_{H^+}\ \gamma_{NO_3^-}[H^+][NO_3^-]\ P_{NO}^2}{\gamma_{HNO_2}^3\ [HNO_2]^3} \qquad (4.24)$$

For P_{NO} < 10 ppb, $[HNO_2]$ > 0.01 μM and pH < 5, equilibrium nitrate in rainwater is >0.029 M. NO_3^- calculated from equilibrium models is typically three orders of magnitude greater than observed values in southern California.

Reaction (4.23) has slow kinetics as will be discussed in Section 4.6.2. Thus, while nitrate production is thermodynamically

favorable, the kinetics are not favorable. Nitrite production in rainwater is kinetically favorable, but there is a relatively low equilibrium nitrite concentration.

The partial pressure of nitrous acid can be calculated by assuming the following equilibrium (Abel and Neussar, 1929):

$$HNO_{2(g)} \rightleftarrows HNO_{2(aq)} \tag{4.25}$$

$$K_{H_{HNO_2}}(25^oC) = 32.8 = \frac{[HNO_{2(aq)}]\gamma_{HNO_2}}{P_{HNO_2}} \tag{4.26}$$

Assuming equilibrium is attained in Equation 4.19, P_{HNO_2} is about 3 ppb during precipitation. This value is below the limit of detection of long path Fourier-transform infrared spectroscopy (Pitts et al 1977).

4.6.1.3 Sulfur Dioxide - Bisulfite - Sulfite

The dissolution of sulfur dioxide (SO_2) to form bisulfite (HSO_3^-) and sulfite (SO_3^{2-}) as shown in Equations 4.27-4.33 is close to equilibrium in precipitation (Hales 1972; Dana and Hales 1976).

$$SO_{2(g)} + H_2O_{(\ell)} \rightleftarrows SO_2 \cdot H_2O_{(aq)} \tag{4.27}$$

$$K_{H_{SO_2}}(25^oC) = 1.24 = \frac{[SO_2 \cdot H_2O]\gamma_{SO_2 \cdot H_2O}}{P_{SO_2}} \tag{4.28}$$

$$SO_2 \cdot H_2O \rightleftarrows H^+ + HSO_3^- \tag{4.29}$$

$$K_{1_{SO_2}}(25^oC) = 0.0127 = \frac{\gamma_{H^+}[H^+][HSO_3^-]\ \gamma_{HSO_3^-}}{[SO_2 \cdot H_2O]\gamma_{SO_2 \cdot H_2O}} \tag{4.30}$$

$$HSO_3^- \rightleftarrows H^+ + SO_3^{2-} \tag{4.31}$$

$$K_{2_{SO_2}}(25^oC) = 6.24 \times 10^{-8} = \frac{\gamma_{H^+}[H^+][SO_3^{2-}]\gamma_{SO_3^{2-}}}{[HSO_3^-]\ \gamma_{HSO_3^-}} \tag{4.32}$$

$$\text{Total Sulfite} = [SO_2 \cdot H_2O] + [HSO_3^-] + [SO_3^{2-}] \tag{4.33}$$

From P_{SO_2} and pH measurements, total sulfite in rainwater can be calculated assuming equilibrium. Unfortunately, ambient sulfur dioxide concentrations before and during precipitation are close to the limit of detection for monitoring equipment (10 ppb). Measured P_{SO_2} is consistently 10±5 ppb with occasional values of 20±5 and 0±5 ppb.

Figure 4.11 compares calculated precipitation weighted mean total sulfite with mean non-sea salt sulfate for the basin sampling sites. (P_{SO_2} is not monitored near the mountain sampling sites since it is below the limit of detection). While the uncertainties are high, total sulfite could account for a significant fraction of the excess sulfate. This comparison assumes sulfite species are

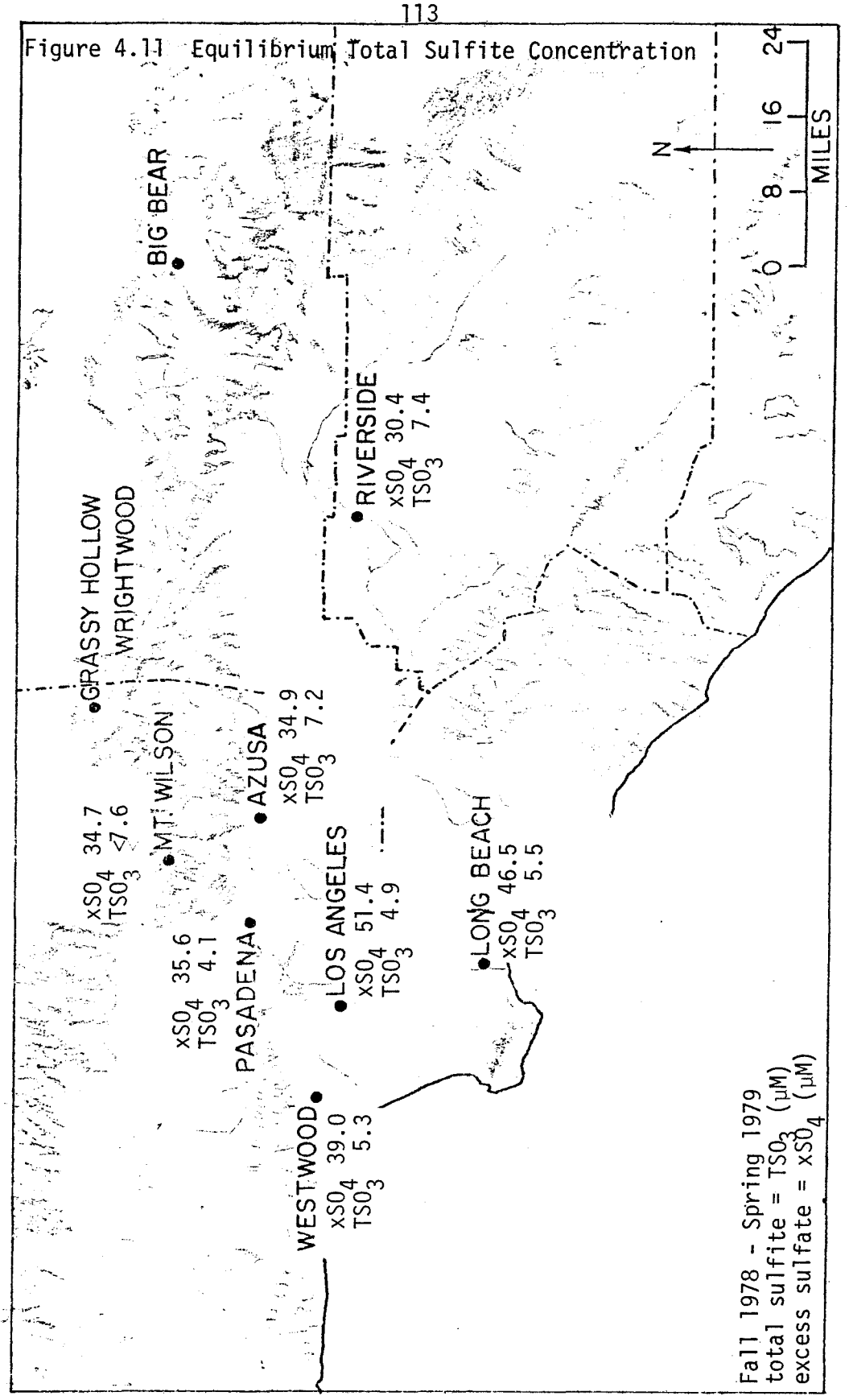

Figure 4.11 Equilibrium Total Sulfite Concentration

oxidized to sulfate before or during analysis for sulfate. The sulfite peak was not detected by ion chromatography with the column and eluent used (see Section 3.4 for analytical procedure). The limit of detection for total sulfite under these conditions was $\sim$0.3 μM. The importance of oxidation of total sulfite to sulfate during precipitation scavenging and prior to analysis is discussed in Section 4.62.

4.6.1.4 Solid Dissolution

The previous models considered gas-liquid equilibria. Precipitation is also influenced by solid phases from aerosol scavenging and cloud condensation nuclei. Solid dissolution kinetics are relatively slow and thus equilibrium is not expected to be achieved over the lifetime of a falling raindrop (O(3 min)). Moreover, the equilibrium constants are poorly characterized for many dissolution reactions, and the choice of equilibrium constant requires identification of the solid phase.

In the context of these large uncertainties, aluminum and silicate concentrations are qualitatively close to those predicted by dissolution of kaolinite clay (Equation 4.34)

$$2\tfrac{1}{2}H_2O + \tfrac{1}{2}Al_2\,Si_2O_5(OH)_{4(s)} \rightleftarrows Al^{3+} + Si(OH)_4 + 3OH^- \qquad (4.34)$$

$$10^{-38.7} = K_{SO} = [Al^{3+}][Si(OH)_4][OH^-]^3 \qquad (4.35)$$

Figure 4.12 Conditional Aluminosilicate Solubility Product

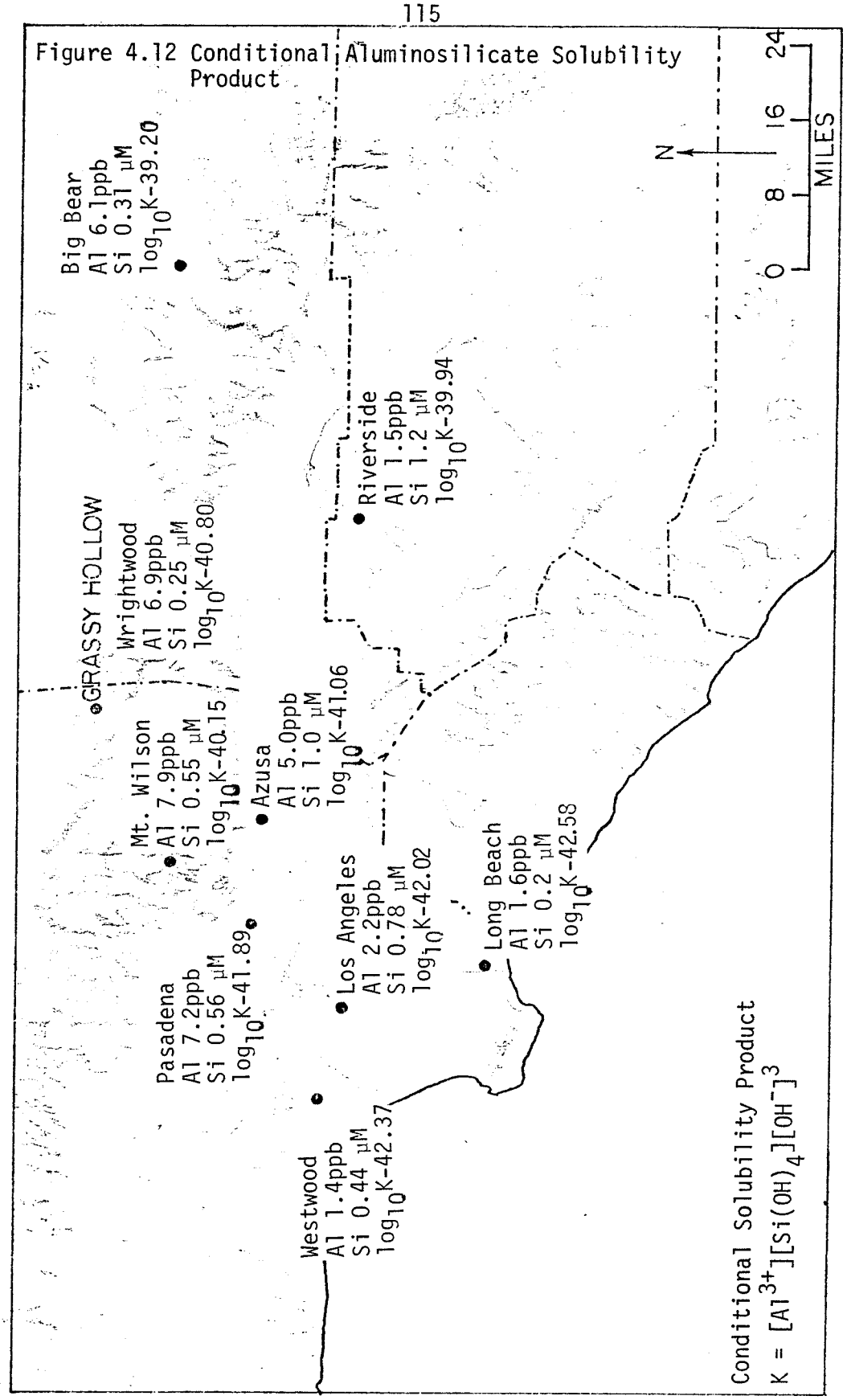

Figure 4.12 shows the areal distribution of dissolved aluminum and silicate and the concentration product corresponding to the right-hand side of Equation 4.35. At all sites, precipitation appears to be in a state of undersaturation with respect to kaolinite dissolution although the less acidic sites (Riverside and mountain sites) are close to equilibrium. These results may be fortuitous. The lower concentration products for the western basin sites may be due to slow kinetics or represent equilibrium with a more insoluble alumino silicate clay.

4.6.2 Kinetic Models of Precipitation Scavenging

4.6.2.1 Nitrate Scavenging

$$3\ HNO_{2(aq)} \rightleftarrows H^+ + NO_3^- + 2NO_{(g)} + H_2O_{(\ell)} \qquad (4.36)$$

The kinetics of Equation (4.23) have been characterized by Abel and Schmid (1928). The forward reaction has the following rate law

$$-\frac{d[HNO_2]}{dt} = 46\ \frac{ATM^2}{min \cdot \left(\frac{moles}{L}\right)^3}\ \frac{[HNO_2]^4}{P_{NO}^2} = 3\ \frac{-d[NO_3^-]}{dt} \qquad (4.37)$$

and the reverse reaction has the following rate law

$$+\frac{d[HNO_2]}{dt} = 1.6\ \frac{}{min \cdot \left(\frac{moles}{L}\right)^2}\ [HNO_2][H^+][NO_3^-] = \frac{d[NO_3^-]}{dt} \qquad (4.38)$$

At equilibrium $d[HNO_2]/dt = 0$ and $K = k_f/k_b = 46/1.6 = 29$ as given in Equation(4.37).

Assuming $[HNO_2]$ is constant (0.1 μM) due to the fast kinetics of Equation (4.19), P_{NO} = 10 ppb (10^{-8} ATM) and pH = 5, the rate of nitrate production is 1.5×10^{-11} mole/liter-minute at 25°C and 1.2×10^{-12} mole/liter-minute at 10°C. This homogeneous liquid-phase reaction is too slow to account for observed nitrate levels within the lifetime of a raindrop.

Abel and Schmid (1928) proposed the following mechanism to explain the observed rate law.

Forward reaction

$$4\ HNO_2 \underset{\text{reversible}}{\rightleftarrows} N_2O_4 + 2NO + 2H_2O \qquad \text{Rapid} \qquad (4.39)$$

$$N_2O_4 + H_2O \xrightarrow[K(25^oC)=1\times10^{+7}]{} HNO_2 + H^+ + NO_3^- \qquad \text{Rate-Determining Step} \qquad (4.40)$$

Reverse reaction

$$HNO_2 + H^+ + NO_3^- \rightarrow N_2O_4 + H_2O \qquad \text{Rate-Determining Step} \qquad (4.41)$$

$$N_2O_4 + 2NO + 2H_2O \underset{\text{reversible}}{\rightleftarrows} 4HNO_2 \qquad \text{Rapid} \qquad (4.42)$$

The kinetics of Equation 4.42 have been described only as "rapid". If the kinetics are fast, nitrate formation is probably due to nitrogen oxide species of higher oxidation state than N_2O_4 or the oxidation of aqueous N(II-IV) species to N(V). Oxidation kinetics are poorly known for aqueous nitrogen species.

The direct route to form nitrate in rainwater is to scavenge gaseous nitric acid, nitrogen pentoxide (N_2O_5) or aerosol nitrate. Ambient gaseous nitrate concentrations have not been measured during precipitation. P_{HNO_3} can be calculated from homogeneous gas phase reaction rates as described by Falls and Seinfeld (1978) and Miller et al (1978). A steady state model (gas phase nitric acid production = nitric acid scavenged) gives rainwater nitrate concentrations of 1-10 μM. Higher concentrations would be expected for intermittent precipitation as gas and aerosol nitrate concentrations increase.

Nitrate and acidity was significantly higher in samples collected during electrical discharges than the immediately previous and succeeding samples collected during no lightning. Lightning produces NO_2 and nitrogen species of higher oxidation state in the cloud. The correlation between electrical activity and precipitation nitrate has been noted by several investigators (Georgii, 1963). Lightning was not the main cause of nitric acid acidity in precipitation in southern California.

4.6.2.2 Sulfate Scavenging

The oxidation of dissolved sulfite to sulfate has been observed for several oxidants. Total sulfite oxidation by oxygen is favored at alkaline pH (Fuller and Christ, 1941) and is catalyzed by trace metal ions (Barron and O'Hearn, 1966).

$$SO_3^{2-} + \frac{1}{2}O_2 \rightarrow SO_4^{2-} \qquad (4.43)$$

Oxidation of total sulfite by ozone is approximately first order with respect to the bisulfite ion and ozone concentrations (Penkett, 1972).

$$HSO_3^- + O_3 \rightarrow H^+ + SO_4^{2-} + O_2 \qquad (4.44)$$

Oxidation of total sulfite by hydrogen peroxide shows general acid catalysis of the reaction which is first order with respect to bisulfite ion and hydrogen peroxide concentrations (Penkett, et al, 1979)

$$HSO_3^- + H_2O_2 \rightarrow \begin{matrix} O^- \\ \diagdown \\ \quad SOOH \\ \diagup \\ O \end{matrix} + H_2O \qquad (4.45)$$

$$\begin{matrix} O^- \\ \diagdown \\ \quad SOOH \\ \diagup \\ O \end{matrix} + HA \rightarrow H_2SO_4 + A^- \qquad (4.46)$$

HA is a proton donating species in the solution, including H_3O^+.

None of these reaction mechanisms can account for the observed sulfate concentrations. Assuming in-cloud concentrations of trace metals and acidity are approximated by the Mt. Wilson and Wrightwood mountain site sample concentrations, trace metal and alkalinity concentrations are too low for air oxidation to produce 1 μM sulfate in the raindrop. Ozone oxidation may be a more important mechanism of sulfate production than oxygen oxidation. Assuming ground level ozone concentrations are in equilibrium with raindrops both in and below the clouds, sulfate concentrations predicted by this overestimate of $[O_3]$ are below observed sulfate values. Hydrogen perioxide concentrations must be above those found in winter rain (2-8 ppb (W/W)) (Bufalini et al, 1979) and must be above that predicted from equilibrium with assumed $P_{H_2O_2}$ (O(1 ppbv)) to account for observed values. $P_{H_2O_2}$ has been detected at concentrations of 10-20 ppbv during moderate photochemical smog in southern California (Kok et al 1978). Perhaps evaporation-concentration in-cloud processes could raise trace metal concentrations in cloud droplets and increase the importance of oxidation by oxygen.

Overall, the kinetics of scavenging and production of nitrates and sulfates are not well known. Scavenging processes are often approximated by overall first order rate constants (Slinn et al, 1979). This approach is exemplified above in the one-box model (Section 4.5.2) and can be expanded to two-box models to consider

in-cloud and below-cloud processes separately. The overall oxidation and scavenging rate constant includes physical-chemical transport processes, aqueous phase reaction kinetics as discussed above as well as gas and aerosol phase reaction kinetics.

Chapter V

DRY FLUX OF ACIDITY

5.1 Introduction

The dry flux of acidity involves the same acids and bases considered in the wet flux. Precipitation scavenging can be viewed as a catalyst for the transport of pollutants to the earth's surface. For the same ambient concentrations, the flux of chemical species due to precipitation processes is 10^{2-4} times the dry flux (Lerman, (1979). The transport steps are scavenging of gas and aerosol by the raindrops and the rapid deposition of the raindrops.

The dry flux is the cumulative effect of transport of the chemical species to the surface and sorption at the surface. For the simple case of an aqueous phase at the surface, the absorption is a dissolution to form acids and bases which may react with the surface. Just as raindrops can reach gas-liquid equilibrium, surfaces can attain saturation with respect to sorption processes, reducing the dry flux to zero. The atmospheric transport to the surface is controlled by an aerodynamic resistance (r_a) and a boundary layer resistance (r_b). The dry flux (F_x) of a species X is given by

$$F_x = v_d \cdot C_x \tag{5.1}$$

$$\frac{1}{v_d} = r_a + r_b + r_s \tag{5.2}$$

where r_s is the surface resistance, C_x is the atmospheric concentration of species X and v_d is the "deposition velocity", a mass transfer coefficient relating the flux to the ambient concentration. The deposition velocity is experimentally defined by $v_d = C_x/F_x$.

5.2 Calculated Dry Flux

Since atmospheric and surface conditions are variable both temporally and spatially, average values of the deposition velocity are often used to calculate average dry deposition fluxes. The following are typical deposition velocities: sulfur dioxide gas, 0.7 cm/sec as reviewed by Roberts (1975) and Cass (1978); nitrate and sulfate aerosol, 0.03 cm/sec based on model of Davidson (1977) and the sulfate mass distribution with respect to particle size; nitrogen dioxide, 0.5 cm/sec; nitric oxide, 0.1 cm/sec (Judeikis and Wren, 1978); and ammonia, 0.5 cm/sec (Hutchinson et al 1972). Sulfur dioxide fluxes have been studied by a number of investigators and reviewed by McMahon and Denison (1979). The deposition velocities for the other species are based on only a few studies and agree with theoretical calculations (Dell et al, 1977).

Ambient concentrations of SO_2, NO, NO_2 and aerosol nitrate and sulfate are monitored by the South Coast Air Quality Management District. The partial pressure of ammonia is poorly known. The ACHEX study (1974) found average ammonia concentrations to be $\sim$15 ppb in Los Angeles, $\sim$30 ppb at Riverside and $\sim$40 ppb at Pomona.

These values determined during smog episodes may be higher than the annual averages. Ammonium to nitrate plus sulfate equivalent ratios in aerosol range from 0.5 to 1 (Orel and Seinfeld (1977), ACHEX (1979), Hicks (1979)). The nitrate and sulfate is balanced by ammonium and hydrogen ions and, to a lesser degree, metal ions.

Table 5.1 shows the net annual dry flux of acidity due to SO_2, NO, NO_2, NH_3, and aerosol acidity. Ambient concentrations are based on annual data for 1976 and 1977 (SCAQMD; 1976, 1977). Assumed deposition velocities and ammonia concentrations are as given above. Due to uncertainties in v_d and assumed ammonia concentrations and aerosol acidities, calculated fluxes are accurate only within a factor of two. While the assumed ammonia concentration may be high, ammonia flux keeps the surface resistance low for the acid gases (Judeikis and Wren, 1978; Judeikis and Stewart, 1976). A lower ammonia flux would be balanced by lower NO_x and SO_2 fluxes. The net acid flux is unchanged if the ammonia, sulfur dioxide and nitrogen oxide fluxes are lower than given in Table 5.1.

Aerosol acid flux is much less than the gaseous flux for three reasons. First, the concentrations of aerosol sulfate and nitrate are much less than the ambient SO_2 and NO_x concentrations on an equivalent basis. Second, the deposition velocity is lower for aerosols by a factor of 3 - 20. Finally, sulfuric and nitric acid acidity is neutralized by ammonia to give weak acid ammonium salts. The environmental impact of acidic aerosols should not be discounted by this equivalent flux calculation. The deposition of acidic aerosol

Table 5.1 Calculated Annual Dry Flux of Acidity 1976-1977

Site	P_{SO_2}*	P_{NO_2}	P_{NO}	P_{NH_3}[1]	Aerosol SO_4^{2-}	Aerosol NO_3^-
Azusa	10	59	28	40	10.5	16.2
Los Angeles	19.5	80	97	15	12.1	15.2
Long Beach	14.5	73	79	10		
Pasadena	15	83.5	82	15	10.7	13.1
Riverside	8.5	40.5	43	30	8.7	11.6
Westwood	8.5	75.5	79	10	7.9	8.3

Site	Corresponding acid flux (equivalents/HA-YR)						Net
Azusa	1970	4156	390	-2820		8.8	3699
Los Angeles	3840	5630	1370	-1060		8.8	9789
Long Beach	2560	5140	1110	- 700			8110
Pasadena	2960	5880	1150	-1060		7.6	8938
Riverside	1680	2850	600	-2110		6.6	3027
Westwood	1680	5310	1110	- 700		5.1	7405

Assumed V_d cm/sec	0.7	0.5	0.1	0.5	0.03	0.03	
Acidity/mole	2	1	1	-1	0.50	0.25	

* ppb

1 Assumed P_{NH_3}

to plant surfaces and resulting necrotic spots may increase host susceptibility to parasite invasion (Tamm and Cowling, 1977).

The deposition of gaseous pollutants to plants is controlled by the stomatal resistance. During photosynthesis, the stomata open to allow carbon dioxide to diffuse into the leaf. Gaseous air pollutants also diffuse into the stomatal pores and are absorbed by fluid in the spongy parenchyma cells. The dissolution products may then be oxidized or reduced by the plant.

In areas of sulfur deficient soil, the wet and dry fluxes of sulfur dioxide and sulfates may be important nutrient sources (Noggle, 1979). Plants reduce these sulfur species to the S(-II) state in the form of amino acids. As shown in Table 2.1 for the cysteine example, this reduction forms a weak acid from relatively strong acids.

Ammonia absorbed by plants and utilized in the synthesis of amino acids would contribute little alkalinity to the dry flux calculation. Equation 5.3 shows the overall formation of the neutral amino acid glycine from ammonia and

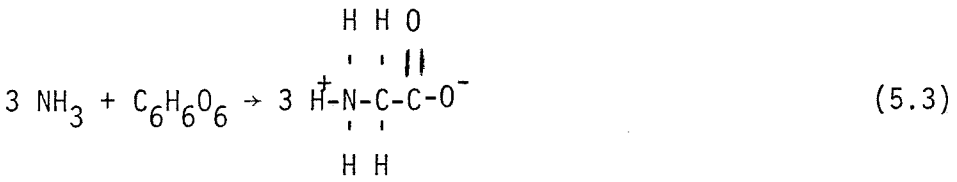

$$3\ NH_3 + C_6H_6O_6 \rightarrow 3\ H\overset{H}{\underset{H}{\overset{|}{\underset{|}{-}}}}N\overset{H}{\underset{H}{\overset{|}{\underset{|}{-}}}}C\overset{O}{\overset{\|}{-}}C-O^- \qquad (5.3)$$

The ammonia utilized to form basic functional groups in amino acids would neutralize an equivalent amount of strong acidity as shown in Equation 5.4 for the synthesis of lysine.

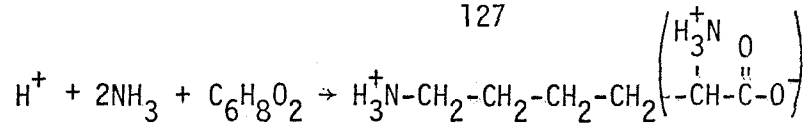

lysine

Basic amino acids are a small percentage of amino acids produced. Most of the ammonia would be utilized in reactions on the type 5.3 rather than 5.4 and thus contribute little alkalinity.

The calculations in Table 5.1 have not included estimates of biological activity in determining the endpoint speciation f_1, as discussed in Section 2. The extent of biological catalysis of redox reactions that change acid and base speciation beyond the initial dissolution products needs to be studied in more detail. The endpoint speciation in the soil and ground-water would be different from that at the land-air interface.

The validity of the dry flux calculation using average deposition velocities was checked by estimating v_d from measurements of wind velocity and atmospheric stability.

$$(\overline{v_d})\ (\overline{C_x}) \simeq (\overline{v_d\ C_x}) = \overline{F_x} \qquad (5.5)$$

Equation 5.5 shows the mean flux ($\overline{F_x}$) is an average of the instantaneous flux ($\overline{v_d\ C_x}$) which is assumed equal to the product of the average velocity ($\overline{v_d}$) and average ambient concentration ($\overline{C_x}$). The instantaneous deposition velocity is calculated from latent heat flux, surface roughness, wind velocity and surface resistance by the model of Wesely and Hicks (1977). The basin surface has been characterized by Davidson (1976). Stomatal surface resistance is modeled by Dell et al (1977). Surface resistance for

nonvegative surfaces is assumed low because of simultaneous acid and base deposition, as discussed above for ammonia. Net flux agrees with the values given in Table 5.1. Assuming lower ammonia concentrations (giving an annual mean of 0-6 ppb) and higher surface resistances yields a net flux in agreement with Table 5.1. The uncertainty is large due to uncertainty in the surface resistance as well as uncertainty in ambient concentrations near the limits of instrument detection. It should be emphasized, the net dry flux is estimated only within a factor of two. Monitoring of ammonia concentrations and gaseous dry flux are needed to provide accurate values.

5.3 Field Studies of Dry Deposition of Acids/Bases

5.3.1 Deposition of Aerosols to Flat Rates

The deposition of aerosol to flat plates is described by Davidson (1977). For aerosol particles greater than 0.3 μM, inertial deposition and sedimentation are more important than diffusion (Eddy and Brownian) to a smooth surface during low wind speed (2m/sec). Sedimentation is the dominant process for large aerosol. For aerosol of aerodynamic diameter <0.3 μm, convective diffusion controls the deposition. By comparing deposition to upward facing plates to deposition to downward facing plates, the importance of sedimentation, and therefore of aerosols >0.3 μm, can be distinguished. The upward facing horizon plate accumulates both large and small aerosol while the downward facing plate accumulates

Figure 5.1 Dry Acidity Flux to Flat Plates (equivalents/HA-YR)

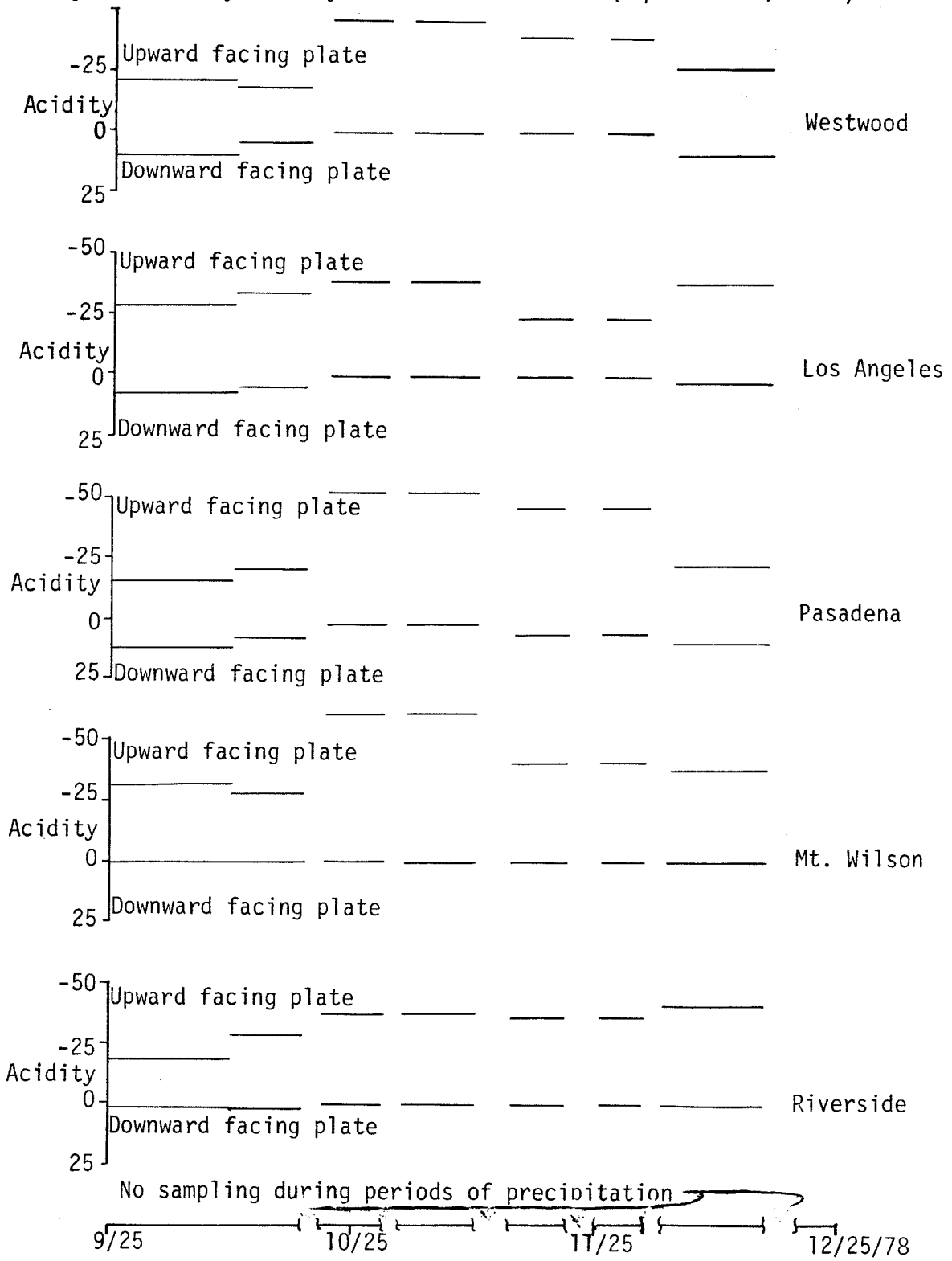

predominantly small aerosol.

Figure 5.1 demonstrates the importance of alkalinity in the larger fraction of the aerosol (soil dust). Upward facing plates accumulate significantly less net acidity than downward facing plates. The higher alkalinity flux noted in the third set of samples is due to ash from brush fires. The acid flux to the downward facing plates average 5 equivalents acidity/HA-YR. The upward facing plates average 30 equivalents alkalinity/HA-YR. Averages are for Azusa, Mt. Wilson, Pasadena, Riverside, central Los Angeles and Westwood.

While the average equivalent flux of aerosol is alkaline, the impact of the smaller size fraction should not be ignored. Material and plant damage results from the deposition of the acidic fraction.

5.3.2 Dry Deposition to Snow

A comparison of the wet and dry fluxes of acidity at the Wrightwood site is shown in Figure 5.2. The dry deposition is low due to low ambient concentrations of pollutants and low deposition velocities (Dovland and Eliassen 1976; Whelpdale and Shaw 1976). Due to the low acidity to low alkalinity of the snow samples, the accumulation of dry deposition of acids/bases may be important in the net acidity of snow melt. During the 1978 sampling period, the dry flux of net acidity was approximately 60% of the wet flux. For the 1979 samples, the dry flux was approximately 20% of the wet flux. The wet flux increased between 1978 and 1979.

Figure 5.2 Dry Acidity Flux to Snow

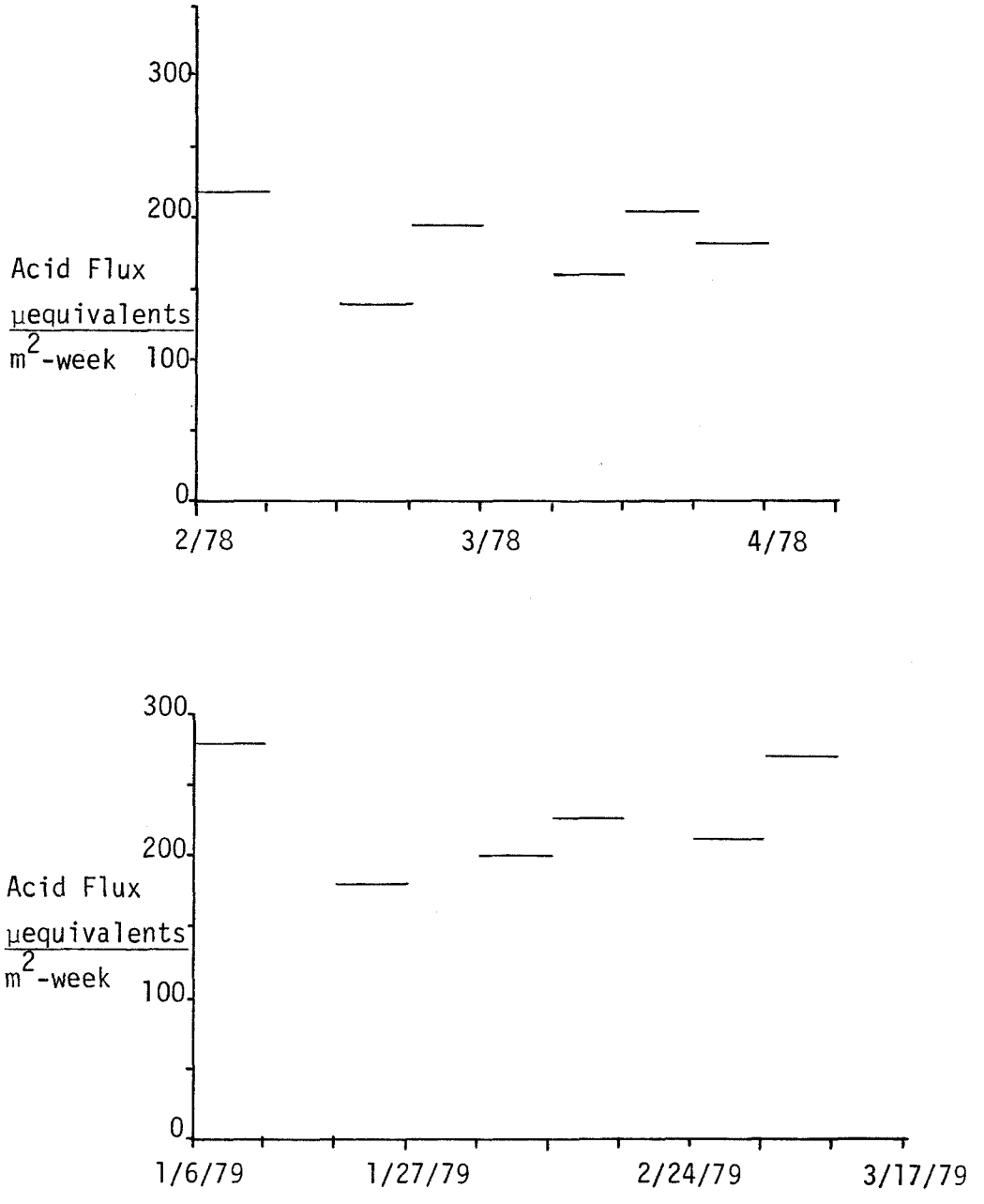

Chapter 6

SUMMARY AND CONCLUSIONS

The semiarid climate of southern California and relatively high air pollutant concentrations during the dry season lead to a higher dry flux than wet flux of acidity. Additional research is needed to measure the dry flux as well as ambient ammonia concentrations. The relative importances of the dry flux, wet flux and advection for the Los Angeles Basin are summarized in Table 6.1. The wet flux is about an order of magnitude less than the total dry flux, although it is greater than the dry flux due to aerosol deposition. Of the acids and bases released in the basin, more than half are exported out of the basin by advection.

Modeling the wet flux is of interest because of unique environmental conditions in the Los Angeles Basin.

1. Wind trajectories show that southern California is not immediately downwind of any major pollutant sources. The wet deposition is due to local sources rather than long range transport.

2. Equivalent emissions of NO_x are more than twice the equivalent emissions of SO_x in the Los Angeles air shed. Consequently, nitric to sulfuric acid equivalent ratios in precipitation are higher than those reported in the northeastern United States and in northern Europe.

3. The high photochemical activity in the Los Angeles air shed catalyzes the precipitation scavenging of nitrates relative to sulfates. The nitric acid contribution was greater in Pasadena from February 1976

Table 6.1 Acid and Base Balance for the Los Angeles Basin

	Emissions [1]	Measured Wet Flux [2]	Calculated Dry Flux [3]	Advection and Chemical Oxidation/Reduction of Acids/Bases to Neutral Species
SO_2 - SO_4^{2-}	9400	210	2400	6790
NO-NO_2-NO_2^--NO_3^-	22000	160	5600	16240
NH_3 - NH_4^+		130	<1450 [5]	

1. Based on 1975-1976 data
2. Based on 1978-1979 data
3. Based on 1976-1977 data
4. Calculated by difference (emissions - wet - dry = advection)
5. Based on assumed P_{NH_3}

All values given in units equivalents/HA-YR.

to November 1977 than from December 1977 to April 1979, the earlier period being characterized by light precipitation and high photochemical activity before each storm and the latter period by heavy winter storms.

The wet flux of acidity has been characterized several ways.

1. Monitoring has described the temporal distributions of acidity. Temporal variations of precipitation concentrations by hour of day, day of week and month of year reflect precipitation characteristics (precipitation intensity, strength of frontal system or amount of advection, precipitation type, etc.) rather than temporal variations of emissions.

2. Spatial distributions of acidity reflect spatial distributions of acids and bases and precipitation amount. In general, ammonium concentrations increase from the coast to inland areas, non-sea salt sulfate decreases from the coastal to inland sites, and nitrate to sulfate ratios increase from coastal to eastern basin and mountain sites. Higher precipitation in the mountains results in lower concentrations than at basin sites, but the acid fluxes are comparable between the mountain and eastern basin sites.

3. Surface and upper air wind trajectory models for Pasadena reflect precipitation characteristics rather than spatial variations of sources.

4. A source strength model has used chemical tracers to identify the contributions of natural and anthropogenic sources to rainwater quality. The major sources are sea salt, soil dust and ammonia alkalinity plus sulfate (primarily due to stationary sources) and nitrate (primarily due to mobile sources) acidity. To confirm the contributions

of stationary and mobile sources to rainwater sulfates and nitrates, stable isotope ratios of precipitation sulfur and nitrogen should be characterized and used as tracers.

5. The mean and extreme values of rainwater quality are described by the log-normal distribution.

Models used in this study to predict rainwater quality are only semi-quantitative.

1. Linear regression models of nitrite plus nitrate and sulfate concentrations based on ground level air quality measurements account for less than 60% of the variance in rainwater concentrations. Nitrite plus nitrate and sulfate concentrations in rainwater show dependences on NO, O_3, and aerosol Pb concentrations measured at ground level as well as precipitation intensity. Other independent variables showed variance ratios significant at the 95% confidence level for Pasadena samples including temperature and relative humidity.

2. Equilibrium models fail to predict rainwater sulfate and nitrate concentrations. Equilibrium models are useful in predicting nitrite concentrations (<1 μM) and the partial pressure of ammonia during precipitation (~ 0.003 ppb). Equilibrium models also estimate the total sulfite contribution to total sulfur in precipitation (10-25%) and provide a clay dissolution relationship between aluminum and silicate concentrations.

3. Aqueous kinetic models of nitrate and sulfate concentrations underestimate measured values. Research into the kinetics of oxidation processes during gas scavenging is needed to determine the mechanisms

of nitrate and sulfate formation in rainwater.

4. Models of concentration changes during a storm work for some species in individual storms but offer no general predictive capability.

The concept of atmospheric acidity is developed to allow acidity balances and to emphasize the acid-base character of gaseous and aerosol species. Atmospheric acidity encompasses strong acid plus base systems, strong and weak acid plus base systems, acid/base systems involved in oxidation-reduction reactions as well as acid-base speciation in the gas, aerosol and precipitation phases. The importance of redox reactions in changing acid-base speciation should be quantified to model the impact of acid fluxes in the terrestrial environment. The average dry fluxes calculated by this investigation should be refined with emphasis on the probability of extreme values which are needed to model biological impacts.

APPENDIX A

PRECIPITATION WEIGHTED MEAN CONCENTRATIONS

Analytical methods are discussed in Chapter 3. Suspended solids correspond to nonfilterable residue as defined by Standard Methods (1975). Reactive silica as defined by Strickland and Parsons (1968) corresponds to silicic acid ($Si(OH)_4$) or total soluble silica for rainwater samples of acidic pH.

The chemical composition of precipitation for each site can be described by linear combinations of the compositions of source emissions. Table A1 gives the source composition matrix used by Miller, Friedlander and Hidy (1975) for the particulate fraction. In addition, there are gaseous emissions of NH_3, NO_x and SO_x for mobile and stationary sources. The fraction emitted as ammonium and acid nitrates and sulfates is considered in the particulated fraction. The amount of particulate nitrate and sulfate emitted depends on combustion characteristics as tabulated by Cass (1978) for Los Angeles sources. The fractionation factors (α_{ij} in equation 2.16) are estimated from empirically determined relative scavenging efficiencies (see Slinn (1979) for a review of washout ratios) and from raindrop collection efficiency, raindrop size distribution and aerosol particle size distribution (Slinn, 1977). Fractionation factors are variable within a storm.

Mean Concentrations in Precipitation at Azusa

November 1978 - March 1979

17 storms, 23 inches of precipitation, 41 samples

Cation	Concentration mg/L	Concentration μ equiv/L	Anion	Concentration mg/L	Concentration μ equiv/L
NH_4^+	0.651	36.2	Cl^-	0.992	28.0
Na^+	0.550	23.9	NO_3^-	2.72	43.9
K^+	0.0667	1.71	SO_4^{2-}	1.81	37.7
Ca^{2+}	0.307	15.3	F^-		< 1
Mg^{2+}	0.0972	8.00	Br^-		0.37
H^+		21.8	$H_2PO_4^-$	<0.005	<0.15
			HCO_3^-		0.23
total cations		106.91	total anions		110.20

Mean pH	4.661	
Organic carbon	6.59	mg/L
Total phosphate	0.274	μg/L
Suspended solids	9.23	mg/L
Reactive silica	1.00	μM

Trace Cations	ppb
Fe	11.6
Al	5.0
Mn	3.66

Mean Concentrations in Precipitation at Big Bear Lake

January 1979 - March 1979

9 storms, 10.7 inches of precipitation, 12 samples

Cation	Concentration mg/L	Concentration μ equiv/L	Anion	Concentration mg/L	Concentration μ equiv/L
NH_4^+	0.134	7.467	Cl^-	0.185	5.21
Na^+	0.0966	4.20	NO_3^-	1.054	17.0
K^+	0.0172	0.440	SO_4^{2-}	0.311	6.47
Ca^{2+}	0.186	9.26	F^-		< 1
Mg^{2+}	0.0916	7.54	Br^-		0.019
H^+		3.78	$H_2PO_4^-$	< 0.005	< 0.15
			HCO_3^-		1.32
total cations		32.69	total anions		30.02

Mean pH 5.422

Reactive silica 0.310 μM

Trace Cations	ppb
Fe	33.46
Al	6.79
Mn	0.793

Mean Concentrations in Precipitation at Long Beach

February 1979 - March 1979

6 storms, 6.3 inches of precipitation, 20 samples

	Concentration	
Cation	mg/L	μ equiv/L
NH_4^+	0.257	14.3
Na^+	0.855	37.2
K^+	0.0376	0.961
Ca^{2+}	0.177	8.82
Mg^{2+}	0.128	11.4
H^+		28.7
total cations		101.4

	Concentration	
Anion	mg/L	μ equiv/L
Cl^-	1.47	41.5
NO_3^-	1.19	19.2
SO_4^{2-}	2.44	50.9
F^-		< 1
Br^-		0.21
$H_2PO_4^-$	< 0.005	< 0.15
HCO_3^-		0.18
total anions		113.0

Mean pH	4.542	
Organic carbon	3.27	mg/L
Total phosphate	0.019	μg/L
Suspended solids	6.04	mg/L
Reactive silica	0.214	μM

Trace Cation	ppb
Fe	23.3
Al	1.60
Mn	1.46

Mean Concentrations in Precipitation at Los Angeles

November 1978 - March 1979

17 storms, 19.4 inches of precipitation, 44 samples

Concentration			Concentration		
Cation	mg/L	μ equiv/L	Anion	mg/L	μ equiv/L
NH_4^+	0.647	35.9	Cl^-	1.42	40.0
Na^+	0.785	34.1	NO_3^-	2.11	34.0
K^+	0.191	4.88	SO_4^{2-}	2.67	55.5
Ca^{2+}	0.292	14.6	F^-		< 1
Mg^{2+}	0.128	10.6	Br^-		0.57
H^+		32.1	$H_2PO_4^-$	< 0.005	< 0.15
			HCO_3^-		0.16
total cations		132.2	total anions		130.2

Mean pH	4.493	
Organic carbon	3.39	mg/L
Total phosphate	0.0923	μg/L
Suspended solids	6.45	mg/L
Reactive silica	0.781	μM

Trace Cations	ppb
Fe	25.8
Al	2.23
Mn	3.12

Mean Concentrations in Precipitation at Mt. Wilson

October 1978 - March 1979

18 storms, 43.7 inches of precipitation, 57 samples

	Concentration			Concentration	
Cation	mg/L	μ equiv/L	Anion	mg/L	μ equiv/L
NH_4^+	0.640	35.5	Cl^-	0.986	27.8
Na^+	0.587	25.5	NO_3^-	1.44	23.2
K^+	0.0668	1.71	SO_4^{2-}	1.90	39.7
CA^{2+}	0.187	9.34	F^-		< 1
Mg^{2+}	0.0804	6.62	Br^-		0.17
H^+		10.35	$H_2PO_4^-$	< 0.005	< 0.15
			HCO_3^-		
total cations		89.0	total anions		91.4

Mean pH	4.985	
Organic carbon	6.3	mg/L
Total phosphate	0.260	μg/L
Suspended solids	9.46	mg/L
Reactive silica	0.548	μM

Trace Cations	ppb
Fe	9.24
Al	7.9
Mn	0.96

Mean Concentrations in Precipitation at Pasadena

February 1976 - August 1977

16 storms, 21.0 inches of precipitation, 43 samples

Concentration			Concentration		
Cation	mg/L	μ equiv/L	Anion	mg/L	μ equiv/L
NH_4^+	0.594	33	Cl^-	1.03	29
Na^+	0.575	25	NO_3^-	4.65	75
K^+	0.082	2.1	SO_4^{2-}	5.76	60
Ca^{2+}	0.385	9.6	F^-		< 1
Mg^{2+}	0.160	6.6	Br^-		0.15
H^+		87	$H_2PO_4^-$	<0.005	< 0.15
			HCO_3^-		0.06
total cations		163.3	total anions		164.2

Mean pH	4.06	
Organic carbon	0.65	mg/L
Suspended solids	2.3	mg/L
Reactive silica	0.90	μM

Trace cations	ppb
Fe	20
Al	7.6
Mn	1.9

Mean Concentrations in Precipitation at Pasadena

September 1977 - December 1977

5 storms, 6.49 inches of precipitation, 22 samples

Concentration			Concentration		
Cation	mg/L	μ equiv/L	Anion	mg/L	μ equiv/L
NH_4^+	0.340	20.5	Cl^-	0.479	13.5
Na^+	0.264	11.5	NO_3^-	1.02	16.4
K^+	0.0363	0.929	SO_4^{2-}	2.25	40.8
Ca^{2+}	0.200	9.99	F^-		< 1
Mg^{2+}	0.0446	3.67	Br^-		0.22
H^+		24.0	$H_2PO_4^-$	< 0.005	< 0.15
			HCO_3^-		0.23
total cations		70.59	total anions		71.15

Mean pH	4.62	
Organic carbon	3.73	mg/L
Suspended solids	0.33	mg/L
Reactive silica	0.663	μM

Trace cations	ppb
Fe	23.90
Al	1.94
Mn	0.866

Mean Concentrations in Precipitation at Pasadena

January - August 1978

20 storms, 34.8 inches of precipitation, 119 samples

Cation	Concentration mg/L	Concentration μ equiv/L	Anion	Concentration mg/L	Concentration μ equiv/L
NH_4^+	0.292	16.2	Cl^-	0.843	23.8
Na^+	0.467	20.3	NO_3^-	1.41	22.7
K^+	0.0537	1.37	SO_4^{2-}	1.78	37.2
Ca^{2+}	0.142	7.08	F^-		< 1
Mg^{2+}	0.0744	6.12	Br^-		0.28
H^+		33.8	$H_2PO_4^-$	< 0.005	< 0.15
			HCO_3^-		0.148
total cations		84.87	total anions		84.13

Mean pH	4.471
Organic carbon	1.69 mg/L
Total phosphate	1.10 μg/L
Suspended solids	1.44 mg/L
Reactive silica	0.522 μM

Trace cations	ppb
Fe	20.7
Al	10.5
Mn	1.09

Mean Concentrations in Precipitation at Pasadena

September 1978 - March 1979

18 storms, 23.2 inches of precipitation, 79 samples

Cation	Concentration mg/L	Concentration μ equiv/L
NH_4^+	0.379	21.1
Na^+	0.553	24.0
K^+	0.0657	1.68
Ca^{2+}	0.133	6.66
Mg^{2+}	0.0869	7.15
H^+		38.5
total cations		99.09

Anion	Concentration mg/L	Concentration μ equiv/L
Cl^-	0.998	28.1
NO_3^-	1.94	31.4
SO_4^{2-}	1.85	38.5
F^-		< 1
Br^-		0.25
$H_2PO_4^-$	< 0.005	< 0.15
HCO_3^-		0.13
total anions		98.38

Mean pH	4.414	
Organic carbon	3.09	mg/L
Total phosphate	0.671	μg/L
Suspended solids	2.80	mg/L
Reactive silica	0.564	μM

Trace cations	ppb
Fe	40.8
Al	1.94
Mn	1.39

Mean Concentrations in Precipitation at Riverside

November 1978 - March 1979

17 storms, 13.6 inches of precipitation, 42 samples

Cation	Concentration mg/L	Concentration μ equiv/L	Anion	Concentration mg/L	Concentration μ equiv/L
NH_4^+	0.601	33.7	Cl^-	1.06	30.0
Na^+	0.578	25.1	NO_3^-	2.02	32.6
K^+	0.0943	2.41	SO_4^{2-}	1.60	33.4
Ca^{2+}	0.345	17.2	F^-		< 1
Mg^{2+}	0.102	8.37	Br^-		0.17
H^+		10.74	$H_2PO_4^-$	< 0.005	< 0.15
			HCO_3^-		0.467
total cations		97.5	total anions		96.6

Mean pH	4.969	
Organic carbon	4.25	mg/L
Total phosphate	0.189	μg/L
Suspended solids	6.13	mg/L
Reactive silica	1.206	μM

Trace Cation	ppg
Fe	172.
Al	1.53
Mn	2.73

Mean Concentrations in Precipitation at Westwood

January 1978 - August 1978

18 storms, 33.5 inches of precipitation, 18 samples

Cation	Concentration mg/L	Concentration μ equiv/L	Anion	Concentration mg/L	Concentration μ equiv/L
NH_4^+	0.227	12.6	Cl^-	1.37	42.1
Na^+	0.789	34.3	NO_3^-	0.599	9.66
K^+	0.0250	0.764	SO_4^{2-}	1.21	25.2
Ca^{2+}	0.0912	4.55	F^-		< 1
Mg^{2+}	0.114	9.40	Br^-		0.22
H^+		16.0	$H_2PO_4^-$	< 0.005	< 0.15
			HCO_3^-		0.31
total cations		77.5	total anions		77.5

Mean pH 4.796
Reactive silica 0.457 μM

Trace Cations ppb

Fe	6.37
Al	1.03
Mn	0.575

Mean Concentrations in Precipitation at Wrightwood

January 1978 - August 1978

18 storms, 55 inches of precipitation, 27 samples

Concentration			Concentration		
Cation	mg/L	μ equiv/L	Anion	mg/L	μ equiv/L
NH_4^+	0.00156	0.086	Cl^-	0.0597	1.68
Na^+	0.0314	1.37	NO_3^-	0.0487	0.786
K^+	0.00313	0.080	SO_4^{2-}	0.0722	1.50
Ca^{2+}	0.078	3.90	F^-		< 1
Mg^{2+}	0.0193	1.58	Br^-		0.024
H^+		1.24	$H_2PO_4^+$	< 0.005	< 0.15
			HCO_3^-		4.03
total cations		8.26	total anions		8.03
		Mean pH	5.905		
		Reactive silica	0.212 μM		

Trace Cations	ppb
Fe	12.75
Al	1.89
Mn	7.2

Mean Concentrations in Precipitation at Westwood

September 1978 - March 1979

20 storms, 20.5 inches of precipitation, 50 samples

Cation	Concentration mg/L	Concentration μ equiv/L	Anion	Concentration mg/L	Concentration μ equiv/L
NH_4^+	0.375	20.8	Cl^-	1.16	32.6
Na^+	0.664	28.9	NO_3^-	1.68	27.0
K^+	0.595	1.52	SO_4^{2-}	2.04	42.4
Ca^{2+}	0.205	10.2	F^-		< 1
Mg^{2+}	0.106	8.75	Br^-		0.42
H^+		29.65	$H_2PO_4^-$	< 0.005	< 0.15
			HCO_3^-		0.17
total cations		99.8	total anions		102.6

Mean pH	4.528	
Organic carbon	4.243	mg/L
Total phosphate	0.294	μg/L
Suspended solids	4.347	mg/L
Reactive silica	0.444	μM

Trace Cations	ppb
Fe	9.08
Al	1.37
Mn	2.25

Mean Concentrations in Precipitation at Wrightwood

December 1978 - March 1979

16 storms, 48 inches of precipitation, 24 samples

Cation	Concentration mg/L	Concentration μ equiv/L
NH_4^+	0.0156	0.864
Na^+	0.0935	4.07
K^+	0.00939	0.240
Ca^{2+}	0.0782	3.90
Mg^{2+}	0.0204	1.68
H^+		12.56
total cations		23.31

Anion	Concentration mg/L	Concentration μ equiv/L
Cl^-	0.179	5.05
NO_3^-	0.657	10.6
SO_4^{2-}	0.345	7.18
F^-		< 1
Br^-		0.032
$H_2PO_4^-$	< 0.005	< 0.015
HCO_3^-		0.399
total anions		23.26

Mean pH 4.901

Reactive Silica 0.251 μM

Trace Cations	ppb
Fe	4.14
Al	6.87
Mn	2.75

Table A1 Source Composition Matrix

(Mass Fractions)

(Miller, Friedlander and Hidy, 1975)

Species	Sea salt	Soil dust	Mobile sources	Stationary sources	Tire dust
Al	2.9×10^{-7}	8.2×10^{-2}		8.0×10^{-3}	
Br	1.9×10^{-3}		7.9×10^{-2}		
C	1.4×10^{-5}		4.0×10^{-1}		2.9×10^{-1}
Ca	1.1×10^{-2}	1.5×10^{-2}		1.3×10^{-2}	
Cl	5.4×10^{-1}		6.8×10^{-2}		
Fe	2.9×10^{-7}	3.2×10^{-2}	4.0×10^{-3}	6.9×10^{-2}	
K	1.1×10^{-2}	1.5×10^{-2}		2.0×10^{-3}	
Mg	3.9×10^{-2}	1.4×10^{-2}		6.0×10^{-4}	
Mn	5.7×10^{-8}	1.1×10^{-3}		6.0×10^{-4}	
Na	3.1×10^{-1}	2.5×10^{-2}		5.0×10^{-2}	
Ni	5.7×10^{-8}	4.0×10^{-5}		2.0×10^{-2}	
NO_3	1.4×10^{-5}				
Pb	1.3×10^{-7}	2.0×10^{-4}	4.0×10^{-1}	7.0×10^{-4}	
Si	8.5×10^{-5}	2.0×10^{-1}		1.0×10^{-1}	
SO_4	7.7×10^{-2}				
Zn	2.9×10^{-7}		1.4×10^{-3}	2.0×10^{-4}	1.5×10^{-2}

APPENDIX B

PRECIPITATION CONCENTRATIONS OF ORGANIC CARBON/ORGANIC ACIDS

The precipitation concentrations of organic carbon and organic acids are poorly characterized. Jordan and Likens (1975) found annual precipitation weighted mean organic carbon concentrations of 1 to 2.4 mg C/L in the Hubbard Brook Valley, New Hampshire. The wet flux of organic carbon to Mirror Lake represented about 5% of the annual gross phytoplankton production. Galloway et al (1976) reported organic acid concentrations for Ithaca, New York and Hubbard Brook, New Hampshire. Of twenty samples from fifteen storm events, eight showed no organic acids of concentration greater than 1 μeq/L. The remaining twelve samples had total organic acid concentrations of 1.1 to 15.6 μeq/L and the acids were C_1 to C_3. Isocitric acid, a C_6 acid, was found in two additional samples at concentrations of 17 and 37 μeq/L. Schindler et al (1976) report average values of 3.75 mg/L dissolved organic carbon and of 1.73 mg/L particulate carbon for bulk precipitation in western Ontario. Brezonik (1976) reported preliminary results of around 1 mg/L dissolved organic carbon in rain near Gainesville, Florida.

Lunde et al (1977) reported organic compounds in snow in Norway. Absolute concentrations of individual organic acids were not given but were less than a few hundred ng/L. Even numbered fatty

acids, C_8 to C_{30}, as well as even numbered straight chain dicarboxylic acids were identified and presumed to originate from biological sources. Odd numbered and branched chain fatty acids as well as phthalic and benzoic acids were identified at lower concentrations and showed a similar spatial distribution to that of polycyclic aromatic hydrocarbons. These compounds were probably from anthropogenic sources.

Table B1 shows the weighted mean concentrations of organic compounds at Hubbard Brook (Galloway and Cowling, 1978). Concentrations of organic carbon species determined for southern California are given for comparison. Total carbon and particulate carbon concentrations and particulate to total carbon ratios are similar in southern California and Hubbard Brook. Organic acid concentrations are higher at Hubbard Brook. The organic acid to total carbon ratio at Hubbard Brook is similar to that found for aerosol in southern California (Tabor et al, 1958; Grosjean and Friedlander, 1975).

Figure B1 and B2 show temporal and spatial distributions of organic carbon concentrations characterized in this study. Organic acid concentrations are all less than 1 μeq/L. The sources of the organic acids could be biological or anthropogenic. Since samples over several storms were aggregated to have detectable organic acid concentrations, it is hard to assess the contribution to rainwater of organic acids formed by the photochemical oxidation of reactive hydrocarbons.

Table B1 Precipitation Weighted Mean Concentrations of Organic Substances (mg/L)

	Hubbard Brook Experimental Forest	Pasadena 2/76 - 4/79
Total organic carbon	1.31	1.82
Particulate carbon (>0.54μ)	0.16	0.24
Carbon in compounds >1000 MW	0.47	
Carbon in organic acids	0.25	
Carbon in aldehydes	0.14	
Carbon in carbohydrates	0.10	
Carbon in tannins	0.09	
Carbon in amines	0.01	
Carbon in phenols	0.01	
Carbon in hydrocarbons	0.01	
Undefined	0.07	

Figure B1 Organic Species Distribution, 11/78 - 4/79

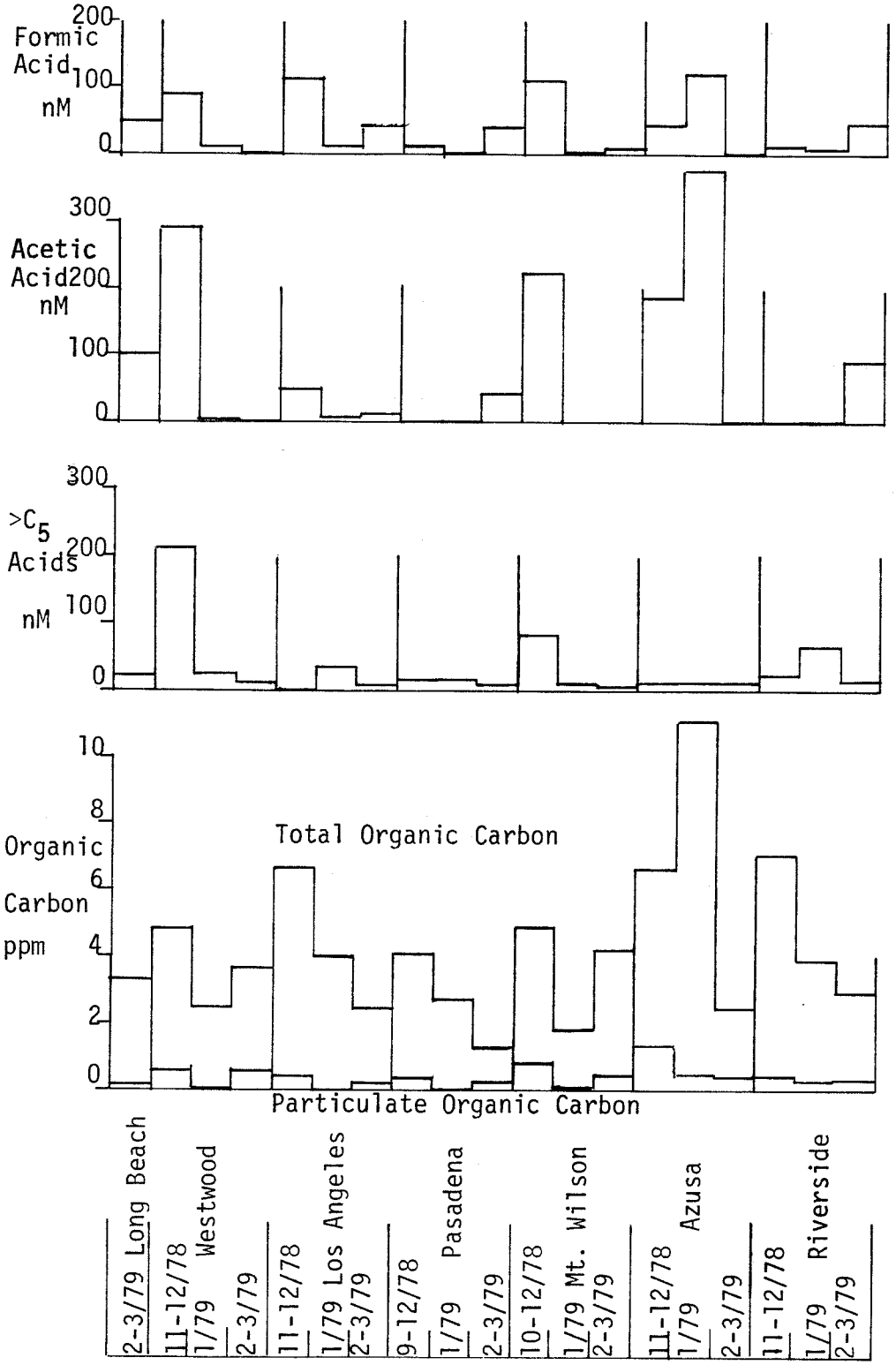

Figure B2 Organic Species Concentrations in Pasadena

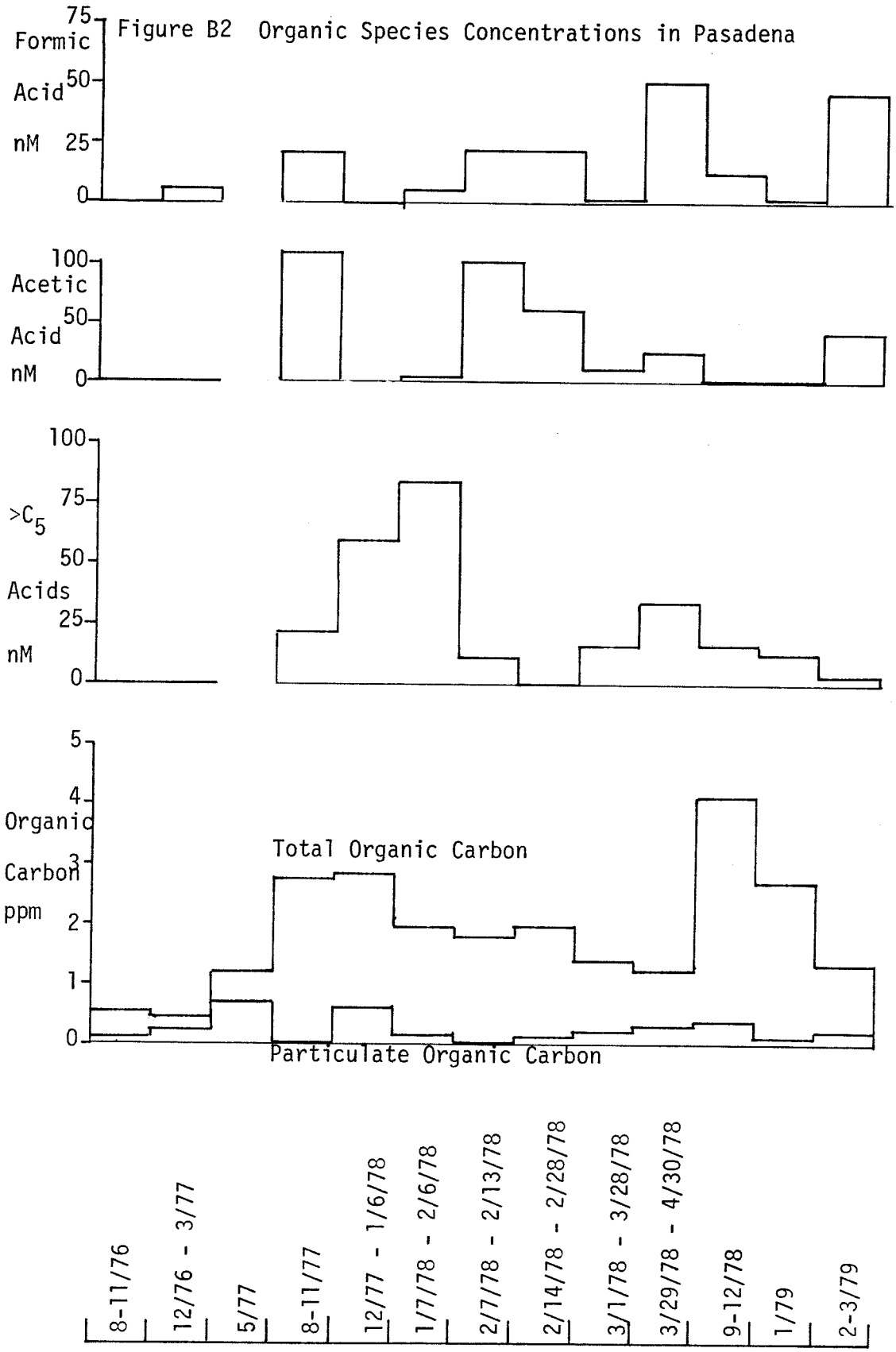

REFERENCES

Abel, E., and E. Neussar, 1929, Monatshefte für Chemie, 54;855-873.

Abel, E., and H. Schmid, 1928, Z. Physikal. Chem., 136:430-436.

ACHEX, 1974, Characterization of Aerosols in California (ACHEX), California Air Resources Board.

Anderson, L. J., 1948, Bul. Am. Meteor, Soc., 29:362-366.

Andren, A. W., and S. E. Lindberg, 1977, Water Air Soil Pollut., 8:199-215.

Barron, C. H., and H. A. O'Hearn, 1966, Chem. Eng. Sci., 21:397-404.

Bass-Becking, L. G. M., et al, 1960, J. Geol., 68:243-284.

Beilke, S., and H. W., Georgii, 1968, Tellus, 20:435-442.

Bencala, K. E., and J. H. Seinfeld, 1976, Atmos. Environ. 10:941-950.

Bethge, P.O., and K. Lindström, 1974, Analyst, 99:137-142.

Brezonik, P. L., 1976, J. Great Lakes Res., 2 (Supplement 1):166-186.

Brosset, C., 1976, Water Air Soil Pollut., 6:259-275.

Bufalini, J. J., et al, 1979, J. Environ. Sci. Health, A14:135-149.

Burden, S. L., and D. E. Euler, 1975, Anal. Chem., 47:793-797.

Butler, F. E., et al, 1978, in Ion Chromatographic Analysis of Environmental Pollutants, ed., E. Sawicki et al, Ann Arbor, Science, Ann Arbor, Mich.

Carroll, D., 1962, U. S. Geol. Surv. Water Supply Pap. 1535-g, 1-18.

Cass, G. R., 1978, Ph. D. Thesis C.I.T.

Cheng, L., 1977, Environ. Sci. Tech., 11:192-193.

Cochran, W. G., 1964, Biometrics, 20:191.

Cogbill, C. V., 1974, M.S. Thesis, Cornell U.

Cogbill, C. V., 1976, Water Air Soil Pollut., 6:407-413.

Cogbill, C. V., and G. E. Likens, 1974, Water Resour. Res., 10:1133-1137.

Commission on Natural Resources, 1975, Air Quality and Stationary Source Emission Control, prepared for U. S. Senate, 94th Congress, 94-9.

Council on Environmental Quality, 1979, Chem. Eng. News, 57:6.

Dana, M. T., et al, 1975, J. Geophys. Res., 80:4119-4129.

Davidson, C. I., 1976, in Atmosphere-Surface Exchange of Particulate and Gaseous Pollutants (1974), ERDA Conf-740921.

Davidson, C. I., 1977, Ph. D. Thesis, C.I.T.

Dawson, G. A., 1978, Atmos. Environ., 12:1991-1999.

Demarrais, G. A., et al, 1965, U. S. Weather Bureau, Tech. Pap. 54.

Dickson, W., 1975, Report Institute Freshwater Res., Drottningholm, Sweden, 54:8-20.

Dovland, H., and A. Eliasson, 1976, Atmos. Environ., 10:783-785.

Ekdahl, C. A., and C. D. Keeling, 1973, in Carbon and the Biosphere, ed. G. M. Woodwell and E. V. Pecan, AEC Conf-720510, 51-85.

Erikkson, E., 1952, Tellus, 4:214-232.

Falls, A. H., and J. H. Seinfeld, 1978, Env. Sci. Technol., 12:1398-1410.

Feth, J. H., et al, 1964, U. S. Geol. Surv. Water Supply Pap. 1535-J, 1-39.

Fisher, D. W., 1968, U. S. Geol. Surv. Water Supply Pap. 1535-M.

Florence, T. M., 1971, Anal. Chim. Acta, 54:373-377.

Flückiber-Keller, H., et al, 1979, Water Air Soil Pollut., 11:153-157.

Forland, E. J., and Y. T. Gjessing, 1975, Atmos. Environ.,9:339-352.

Fox, D. G., 1976, Water Air Soil Pollut., 6:173-198.

Fuller, E. C., and R. H. Crist, 1941, J. Amer. Chem. Soc., 63:1644-1650.

Galloway, J. N., et al, 1976a, Science, 194:722-724.

Galloway, J. N., et al, 1976b, Water Air Soil Pollut., 6:423-433.

Galloway, J. N., and E. B. Cowling, 1978, J. Air Pollut. Cont. Assoc., 28:229-235.

Galloway, J. N., and G. E. Likens, 1976, Water Air Soil Pollut., 6:241-258.

Galloway, J. N., and G. E. Likens, 1978, Tellus, 30:71-82.

Gartrell, G., Jr., and S. K. Friedlander, 1975, Atmos. Environ., 9:279-299.

Gauri, K. L., 1978, Scien. Amer., 238:126-136.

Georgii, H. W., 1963, J. Geophys. Res., 68:3963-3970.

Georgii, H. W., and E. Weber, 1960, Tech. Note 1, Contract AF 61 (052)-249, Frankfurt am Main.

Gran, G., 1952, Analyst, 77:661-671.

Granat, L., 1972, Tellus. 24:550-560.

Granat, L., 1974, in Precipitation Scavenging (1974), ERDA Conf.-741003, 531-551.

Granat, L., 1975, J. Great Lakes Res., 2 (Supplement 1):42-55.

Grosjean, D., and S. K. Friedlander, 1975, J. Air Pollut. Con. Assoc. 25:1038-1044.

Hales, J. M., 1972, Atmos. Environ., 6:635-659.

Halliday, L. A., and J. M. Anderson, 1974, Environ. Lett., 6:55-75.

Hansen, L. D., et al, 1979, Anal. Chem., 51:633-637.

Hanst, P. L., et al, 1975, EPA 650/4-75-006.

Harrison, H., et al, 1977, in Precipitation Scavenging (1974), ERDA Conf-741003, 602-610.

Hicks, B. B., 1979, Proceedings, 12th Annual Rochester International Conference on Environmental Toxicity, Plenum Press, New York.

Huntzicker, J. J., S. K. Friedlander, and C. I. Davidson, 1975, Environ. Sci. Tech., 9:448-457.

Hutchinson, G. L., et al, 1972, Science, 175:771-772.

Jacobson, J. S., et al, 1976, Water Air Soil Pollut., 6:339-349.

Jernelöv, A., 1974, in The Sea, Vol. 5, Marine Chemistry, ed. E. D. Goldberg, John Wiley and Sons, New York, p. 799-815.

Jordan, M. J., and G. E. Likens, 1975, Verh. Internat. Verein. Limnol., 19:994-1003.

Judeikis, H. S., and A. G. Wren, 1978, Atmos. Environ., 12:2315-2319.

Judeikis, H. S., and T. B. Stewart, 1976, Atmos. Environ., 10: 769-776.

Junge, C. E., 1958, Eos Trans. AGU, 39:241-248.

Junge, C. E., and R. T. Werby, 1958, J. Meteorol., 15:417-425.

Kennedy, V. C., et al, 1976, U. S. Geol. Surv. Open File Report 76-852, Menlo Park, CA, 1-7.

Kennedy, V. C., et al, 1979, Water Resour. Res., 15:687-701.

Knudson, E. J., et al, 1977, ACS Symp. Series, 52:80-116.

Kok, G. L., et al, 1978, Environ. Sci. Tech., 12:1077-1080.

Krupa, S., M. R. Casio, and F. A. Wood, 1976, J. Air Pollut. Control Assoc. 26:221-223.

Lathouse, J., and R. W. Coutant, 1978, in Ion Chromatographic Analysis of Environmental Pollutants, ed. E. Sawicki, et al, Ann Arbor Science, Ann Arbor, Mich.

Lau, N. C., and G. A. Charlson, 1977, Atmos. Environ., 11:475-478.

Lazrus, A. L., et al, 1970, Environ. Sci. Tech., 4:55-58.

Lerman, A., 1979, Geophysical Processes, Wiley-Interscience, New York.

Lewis, W. M., Jr., and M. C. Grant, 1978, Water Resour. Res., 14: 1098-1104.

Likens, G. E., 1976, Chem. Eng. News, 54:29-44.

Liljestrand, H. M., and J. J. Morgan, 1978, Environ. Sci. Tech., 12:1271-1273.

Liljestrand, H. M., and J. J. Morgan, 1979, Tellus, in press.

Liljestrand, H. M., and J. J. Morgan, 1979, Proceedings, 12th Annual Rochester International Conference on Environmental Toxicity, Plenum Press, New York.

Lodge, J. P., Jr., et al, 1968, Chemistry of United States Precipitation, NCAR, Boulder, CO.

Lunde, G., et al, 1977, Atmos. Environ., 11:1007-1014

McMahon, T. A., and P. J. Denison, 1979, Atmos. Environ., 13:571-585.

McColl, J. G., and D. S. Bush, 1978, J. Environ. Qual., 7:352-357.

Miller, D. F., et al, 1978, Science, 202:1186-1188.

Miller, J. M., 1977, in Precipitation Scavenging (1974), ERDA Conf-741003, 639-659.

Miller, J. M., et al, 1978, Geophys. Res. Let., 5:757-760.

Miller, M. S., S. K. Friedlander and G. M. Hidy, 1972, J. Colloid Interface Sci., 39:165-176.

Morel, F., R. E. McDuff, and J. J. Morgan, 1976, Marine Chem., 4:1-28.

Morel, F., and J. J. Morgan, 1972, Env. Sci. Tech., 6:59-67.

Noggle, J. L., 1979, Science, 205-383.

Nordo, J., 1976, Water Air Soil Pollut., 6:199-217.

O'Dell, R. A., et al, J. Air Pollut. Con. Assoc., 27:1104-1109.

Odén, S., 1968, Statens Naturvetenskapliga Forskningsrad Stockholm Bull., 1:1-86.

Odén, S., 1976, Water Air Soil Pollut., 6:137-66.

O'Neal, H. E., and C. Blumstein, 1973, Int. J. Chem. Kinetics, 5:397-413.

Orel, A. E., and J. H. Seinfeld, 1977, Environ. Sci. Tech., 11: 1000-1007.

Pack, D. H., et al, 1978, Atmos. Environ., 12:425-444.

Patterson, C. C., and D. M. Settle, 1976, NBS Special Publication 422.

Pearson, F. J., and D. W. Fisher, 1971, U. S. Geol. Surv. Water Supply Paper 1535-P.

Penkett, S. A., 1972, Nature, 240:105-106.

Penkett, S. A., et al, 1979, Atmos. Environ., 13:123-137.

Pitts, J. N., Jr., et al, 1977, Environ. Sci. Tech., 11:568-573.

Ralston, A., and H. S. Wilf, 1960, Mathematical Methods for Digital Computers, John Wiley and Sons, New York.

Reuss, J. O., 1977, Water Air Soil Pollut., 7:461-478.

Roberts, P. T., 1975, Ph. D. Thesis, C.I.T.

Schindler, D. W., et al, 1976, J. Great Lakes Res. 2 (Supplement 1): 167.

Seinfeld, J. H., 1975, Air Pollution, McGraw Hill, New York.

Semonin, R. G., D. F. Gatz, M. E. Peden, G. J. Stensland, 1978, Study of Atmospheric Pollution Scavenging, Ill. State Water Survey, COO-1199-59.

Seymour, M. D., et al, 1978, Water Air Soil Pollut., 10:147-161.

SCAQMD, 1976, Air Quality and Meteorology 1976 Annual Report, South Coast Air Quality Management District, El Monte, CA.

SCAQMD, 1977, Air Quality and Meteorology, South Coast Air Quality Management District, El Monte, CA.

Scott, B. C., and N. S. Laulainen, 1979, J. Applied Meteor., 18: 138-147.

Sillén, L. G., and A. E. Martell, 1964, Stability Constants of Metal-Ion Complexes, Spec. Pub. 17, Chemical Society, London.

Sillén, L. G., and A. E. Martell, 1971, Stability Constants of Metal Ion Complexes, Spec. Pub. 25, Chemical Society, London.

Slinn, W. G. N., 1977, Water Air Soil Pollut., 7:513-543.

Slinn, W. G. N., 1979, "Precipitation Scavenging", Chapter 11 of Atmospheric Sciences and Power Production-1979, in press.

Slinn, W. G. N., et al, 1979, Atmos. Environ. 12:2055-2087.

Smith, D. K., 1976, J. Great Lakes Res., 2 (Supplement 1):78-81.

Söderlund, R., 1977, Ambio, 6:118-122.

Standard Methods for the Examination of Water and Wastewater, 14th ed, 1975, APHA, AWWA, WPCF, American Public Health Association, Washington, D. C.

Strickland, J. D. H., and E. Parsons, 1968, A Practical Handbook of Seawater Analysis, Fisheries Research Board of Canada.

Stumm, W., and J. J. Morgan, 1970, Aquatic Chemistry, Wiley Interscience, New York.

Tabor, E. C., et al, 1958, A. M. A. Archives Industrial Health, 17:58-63.

Tamm, C. O., and E. B. Cowling, 1977, Water Air Soil Pollut., 7:503-511.

Tauzon, E. C., et al, 1978, Atmos. Environ., 12:865-875.

Umeh, E. O., 1971, J. Chromatogr., 56:29-36.

Vermeulen, A. J., 1978, Env. Sci. Tech., 12:1016-1021.

Wesely, M. L., and B. B. Hicks, 1977, J. Air Pollut. Con. Assoc. 27:1110-1116.

Whelpdale, D. M., and R. W. Shaw, 1976, Tellus, 26:196-205.

Whitehead, H. C., and J. H. Feth, 1964, J. Geophys. Res., 69:3319-3333.

Wolaver, T. G., and H. Leith, 1973, Edv. Medizin. Biol. (Stuttgart), 4:74-87.

Wolff, G. T., et al, 1979, Env. Sci. Tech., 13:209-212.

Yost, D. M., and H. Russell, Jr., 1944, Systematic Inorganic Chemistry of the Fifth-and-Sixth-Group Nonmetallic Elements, Prentice-Hall, Inc., New York.